TECHNICAL REPORT N-73-8

DYNAMIC STRENGTH STUDY OF SMALL FIXED-EDGE, LONGITUDINALLY RESTRAINED TWO-WAY REINFORCED CONCRETE SLABS

Final Report

by

W. M. Brown, M. S. Black

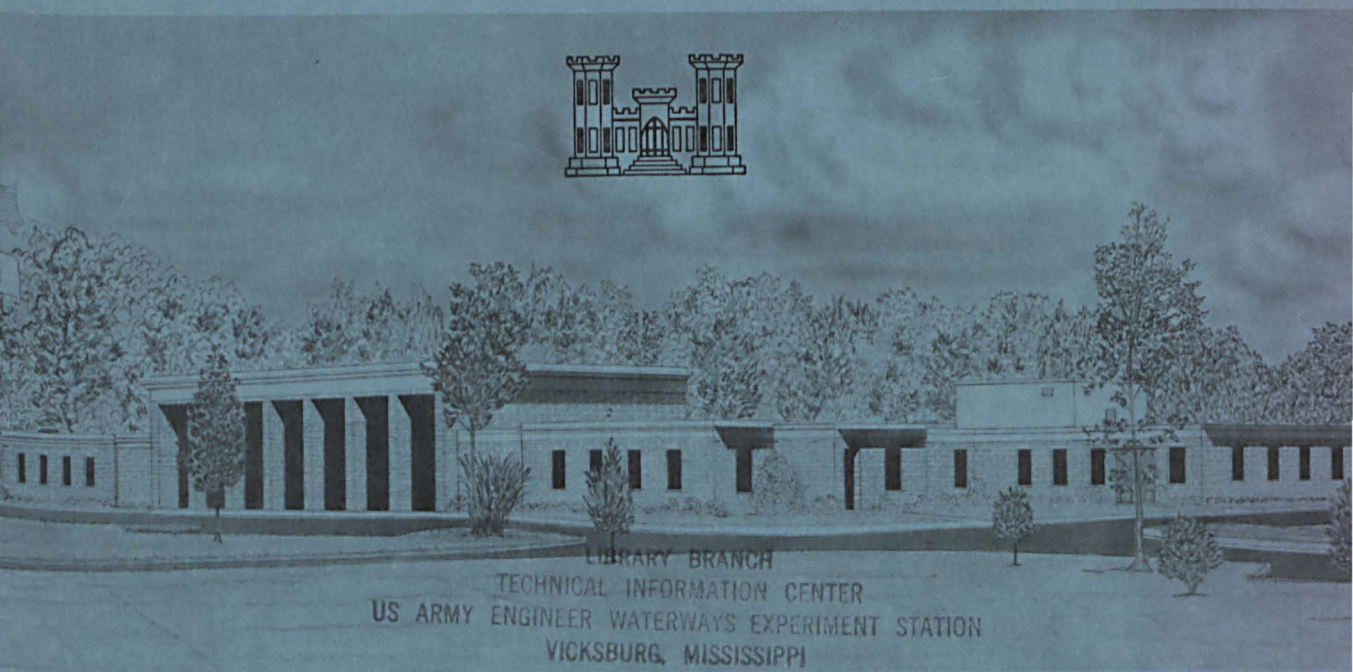

December 1973

Sponsored by Defense Civil Preparedness Agency
Contract No. DAHC 20-68-W-0192, Work Unit 1127E

Conducted by U. S. Army Engineer Waterways Experiment Station
Weapons Effects Laboratory
Vicksburg, Mississippi

TECHNICAL REPORT N-73-8

DYNAMIC STRENGTH STUDY OF SMALL FIXED-EDGE, LONGITUDINALLY RESTRAINED TWO-WAY REINFORCED CONCRETE SLABS

Final Report

by

W. M. Brown, M. S. Black

December 1973

REVIEW NOTICE

This report has been reviewed in the Defense Civil Preparedness Agency and approved for publication. Approval does not signify that the contents necessarily reflect the views and policies of the Defense Civil Preparedness Agency.

Sponsored by Defense Civil Preparedness Agency
Contract No. DAHC 20-68-W-0192, Work Unit 1127E

Conducted by U. S. Army Engineer Waterways Experiment Station
Weapons Effects Laboratory
Vicksburg, Mississippi

ARMY-MRC VICKSBURG, MISS.

THE CONTENTS OF THIS REPORT ARE NOT TO BE USED FOR ADVERTISING OR PROMOTIONAL PURPOSES. CITATION OF TRADE NAMES DOES NOT CONSTITUTE AN OFFICIAL ENDORSEMENT OR APPROVAL OF THE USE OF SUCH COMMERCIAL PRODUCTS.

ABSTRACT

The study reported herein is one phase of an effort to develop criteria that will be helpful in evaluating or predicting the airblast load-carrying capacity of conventional floor slabs in existing Defense Civil Preparedness Agency approved shelters. The general objective of this study was to investigate the static and dynamic behavior of small, fixed-edge, longitudinally restrained, two-way reinforced concrete slabs.

Twelve tests, four static and eight dynamic, were conducted on slabs with a clear span of 29 inches and a thickness of 0.89 inch. Two series of slabs (I and II) corresponding to two different percentages of steel reinforcement (0.78 and 1.17 percent) were used. The slabs were subjected to uniformly distributed static loads up to 36.5 psi using water pressure and to dynamic airblast overpressures ranging from 26.5 to 56.8 psi using explosives.

Measurements of pressure, deflection, and reinforcement strains were made, and results are presented herein.

The average ultimate collapse strengths of the slabs tested under static loading were 23.2 and 36.5 psi for the Series I and II slabs, respectively. The average values of ultimate flexural resistance were 14.1 and 18.2 psi for the Series I and II slabs, respectively. It was noted that the ultimate strength of the slabs was substantially increased by membrane action.

Midspan deflections at the peak of tensile membrane action for the slabs tested statically averaged 4.40 inches for the Series I slabs and 4.10 inches for the Series II slab. The ultimate collapse strengths of the dynamically tested slabs averaged 28.7 and 45.5 psi for the Series I and II slabs, respectively. Midspan deflections at collapse of the slabs tested dynamically averaged 7.25 inches for the Series I slabs and 8.1 inches for the Series II slabs.

A comparison of the ultimate collapse strengths of the slabs tested dynamically with those tested statically shows that increases in ultimate strength of 23.7 and 24.6 percent under dynamic loading were

obtained for the Series I and II slabs, respectively.

Slab strength was determined theoretically through the use of equations for predicting tensile membrane resistance and midspan deflection. After some modification of the equations used, good predictions of tensile membrane resistance of the static slabs were realized. These equations were also used in predicting the peak pressures sustained by the dynamic slabs. Using the equations to predict dynamic slab strength was less successful than using the equations to predict static slab strength.

PREFACE

This study, sponsored by the Defense Civil Preparedness Agency (DCPA) under Contract No. DAHC 20-68-W-0192, Work Unit 1127E, was conducted at the U. S. Army Engineer Waterways Experiment Station (WES) during the period April 1971 through June 1972.

The study was under the general supervision of Mr. G. L. Arbuthnot, Jr., Chief of the Weapons Effects Laboratory, and Mr. W. J. Flathau, Chief of the Protective Structures Branch, and under the direct supervision of Messrs. W. L. Huff and T. E. Kennedy. This report was prepared by SP5 Wayne M. Brown and SP4 Michael S. Black.

BG E. D. Peixotto, CE, and COL G. H. Hilt, CE, were Directors of WES during the preparation and publication of this report. Mr. F. R. Brown was Technical Director.

CONTENTS

FIGURES

NOTATION

A_s	Area of steel
d	Distance from compression edge of slab to the centroid of tension reinforcement (inches)
D	Denotes dynamic test
f'_c	Compressive stress of concrete (psi)
f_r	Tensile stress of reinforcement at rupture (psi)
f_s	Stress in tension reinforcement (psi)
f_t	Tensile stress of concrete (psi)
f_u	Ultimate stress of tension reinforcement (psi)
f_y	Yield stress of tension reinforcement (psi)
k	Constant
L	Clear span of slab (inches)
L_x, L_y	Spans of the slab in the x and y directions with $L_x = L_y$
n	Odd integers
p	A_s/d, ratio of tension reinforcement per unit width of slab
p'	A_s/d, ratio of compression reinforcement per unit width of slab
P_s	Static overpressure during secondary flexural resistance of the slab
P_{so}	Static overpressure
P_t	Static overpressure during tensile membrane resistance of the slab
P_u	Static overpressure during ultimate flexural resistance of the slab
q	Tensile membrane resistance
S	Denotes static test
T_x, T_y	Yield forces, per unit width, of the reinforcement in the x and y directions which is placed over the whole area of the slab
w	Uniformly distributed load per unit area of the slab
x,y	Rectangular coordinates parallel to the slab edges and in the plane of the slab
Z	Midspan deflection
Z_c	Collapse midspan deflection

Z_s Midspan deflection during secondary flexural resistance

Z_t Midspan deflection during tensile membrane resistance

Z_u Midspan deflection during ultimate flexural resistance

Δ Maximum value of deflection of any point of the slab in the direction of the normal to the x-y plane (positive in the direction of loading)

CONVERSION FACTORS, BRITISH TO METRIC UNITS OF MEASUREMENT

British units of measurement used in this report can be converted to metric units as follows:

Multiply	By	To Obtain
mils	0.0254	millimeters
inches	2.54	centimeters
feet	0.3048	meters
cubic feet	0.0283168	cubic meters
pounds	0.45359237	kilograms
kips	453.59237	kilograms
pounds (force) per square inch	0.6894757	newtons per square centimeter
pounds (force) per square foot	47.88026	newtons per square meter
kips (force) per square inch	0.6894757	kilonewtons per square centimeters
Fahrenheit degrees	5/9	Celsius or Kelvin degrees[a]

[a]To obtain Celsius (C) temperature readings from Fahrenheit (F) readings, use the following formula: $C = (5/9)(F - 32)$. To obtain Kelvin (K) readings, use: $K = (5/9)(F - 32) + 273.15$.

CHAPTER 1

INTRODUCTION

1.1 BACKGROUND

The study described in this report is part of an effort to develop criteria that will be helpful in evaluating or predicting the airblast load-carrying capacity of conventional floor slabs in existing Defense Civil Preparedness Agency (DCPA) approved shelters.

Conventional structures provide some degree of inherent protection from the airblast and radiation effects of nuclear weapons (Reference 1). In the past, the DCPA has designated fallout shelters considering only the radiation protection provided. Presently, they are engaged in an all-effects shelter survey in an effort to determine the protection provided by existing shelters. Part of the data collected in this survey consist of the building's structural characteristics, which are obtained from on-site inspections and from construction drawings for the buildings. The information obtained from this survey will be used to predict the airblast protection provided by the shelters. In order to improve the prediction methods, additional information is needed on the collapse modes and strengths of the reinforced concrete floor and roof systems characteristic of those found by the survey.

The nuclear and high-explosive tests of the United States and the data from Hiroshima and Nagasaki have provided information on the dynamic behavior of buildings. Although much information is available, not all of it is applicable to conventional structures. The dynamic responses of individual structural elements such as beams, columns, slabs, and wall panels have been studied theoretically and experimentally. Valuable information for analysis purposes, including the pressure-time loading required to cause collapse, has been obtained. However, the dynamic response of an element of a structure tested independently frequently differs significantly from that of a similar element tested as an integral part of a structure. Because most of the tests to date have been on individual elements, there is insufficient criteria on

which to base damage predictions for conventional buildings. Data and criteria exist for elastic and small deflection response, but they are not sufficient if large deflections are part of the design or analysis problem.

Population density and shelter distribution are the primary factors involved in determination of destruction of life resulting from a nuclear explosion. However, it is not economically feasible to design structures to provide complete protection of life in areas of great population density and close structure distribution. Because of this, limiting overpressure has been adopted as a partial standard against which to evaluate shelters. In this study, a design overpressure level of 15 psi[1] has been selected as the base line overpressure.

Protective structures are designed to resist the dynamic forces of airblast loading and ground shock as well as other effects resulting from a nuclear explosion. Such structures are generally designed to provide protection for specific overpressure levels from a fixed-yield weapon. To provide the required protection, the structures are sometimes isolated from shock, are frequently buried in soil or rock, and are designed to resist lateral forces of appreciable magnitude. In the design of such structures, damage levels, ductility, and ductility ratios are important considerations. In contrast, conventional buildings are usually designed for allowable stresses and then checked for deflections to determine if they are acceptable. This procedure is used because stresses are usually easier to determine than deflections; thus, most design codes are based on allowable or maximum stresses. However, this does not mean that deflections in conventional buildings are unimportant. Excessive deflection may interfere with the intended purpose or serviceability of the building. In contrast, protective structures are designed for permanent deflections, the magnitudes of which are primarily determined by the level, duration, and repetition of loading. Although ultimate strength design in reinforced concrete

---

[1] A table of factors for converting British units of measurement to metric units is given on page 12.

and plastic design in steel are sometimes used in conventional design, protective structure design is primarily based on damage level and ductility ratios. In conventional structures, these are not usually considered as important design parameters.

1.2 OBJECTIVES AND SCOPE

The general objective of this study was to experimentally investigate the static and dynamic behavior of small, fixed-edge, longitudinally restrained, two-way reinforced concrete slabs. Specific objectives were to investigate the following: (1) dynamic and static collapse strengths of the slabs tested, (2) relation between the static and dynamic responses of the slabs, (3) deflection histories for both static and dynamic tests, (4) reinforcing strain distributions and magnitudes, and (5) possible methods of analysis for determining collapse strengths of slabs.

To accomplish the objectives of this study, twelve tests were conducted on small, square, fixed-edge, longitudinally restrained, two-way reinforced concrete slabs with a clear span of 29 inches and a thickness of 0.89 inch.

Four static and eight dynamic slabs were tested. The geometry and materials used were the same for all slabs tested; however, two different percentages of steel reinforcing (0.78 and 1.17 percent) were used. The slabs were subjected to uniformly distributed static loads up to 36.5 psi and dynamic airblast overpressures ranging up to 56.8 psi. On one of the test slabs of the first series, two dynamic tests were conducted since the initial test did little damage.

The slabs were instrumented to measure midspan deflection, reinforcement strains, and the pressure-time history of the loading.

1.3 COMPARISON WITH PREVIOUS STUDIES

This project differs from most previous work in this area in that determination of the total collapse response of the slab is the primary objective. Generally, previous tests have been carried out to only slightly beyond the general yield point. Determination of the total

collapse history of the slab is required because prior to total collapse, only limited casualties occur in shelters having two-way slab roofs, mainly from falling pieces of concrete and from venting. Only at complete collapse does a high precentage of casualties occur.

Collapse of a reinforced concrete slab with a high degree of edge restraint occurs after large deflections result in membrane action. This membrane action is the primary mode of response investigated in this study. During membrane action, the overpressure-induced loads are carried by tensile forces in the steel reinforcing bars, with the concrete acting to distribute the blast loads. Tensile rupture of the individual bars around the periphery of the slab initiates total collapse.

Many tests have been conducted to obtain the static strength of slabs, but relatively few slabs have been tested dynamically. A previous study conducted at WES (Reference 2) investigated the dynamic and static ultimate strength of two-way reinforced concrete slabs. Failure of the test slabs was based on response resulting in the formation of a general yield line pattern. The present study extends the work done in this initial investigation. Test slab scale and edge constraint are the main physical differences between the slabs described in Reference 2 and those of this project.

An investigation conducted by the Naval Civil Engineering Laboratory (NCEL), Reference 3, also dealt with the static and dynamic strength of slabs. This study was similar to the one reported herein except for the edge constraint, slab geometry, and reinforcement. Reference 3 presents a comprehensive analysis of the behavior of slabs. Nine slabs were tested, each with a clear span of 72 inches. The tests and analysis included the effects of tensile membrane action. The work reported herein extends the work in Reference 3 and provides additional information on slab strength.

A considerable amount of previous work has been performed on reinforced concrete slabs, but most of the studies assumed failure as the point at which the slab first yielded. Therefore, a complete picture of slab failure has not been obtained. This study contributes to the determination of the behavior of slabs in the region beyond yield.

CHAPTER 2

EXPERIMENTAL PROGRAM

2.1 DESCRIPTIONS OF TEST SLABS

Selection of the prototype slab was based on several factors. First, it was required that the ultimate collapse strength of floor systems typical of DCPA fallout shelters be investigated. Second, a fully restrained fixed edge was desired to properly simulate a typical interior slab. Third, slabs similar to that selected, but simply supported, had been previously studied at WES. A summary of the experimental program of this study is presented in Table 2.1.

The basic prototype structural system selected for testing in this study is shown in Figure 2.1. The prototype steel reinforcing layout and bar schedule are shown in Figure 2.2. Except for edge restraint, the two prototype slabs (Series I and II) selected for testing in this program were models of the prototype of two-way slabs tested earlier at WES (Reference 2). These slabs were designed for live loads of 105 and 225 psf, respectively, and a dead load of 86 psf in accordance with the provisions of the Building Code Requirement for Reinforced Concrete (ACI 318-56), Method 2 (Reference 4). Half of the positive moment steel in the prototype was bent up near the edges similar to that of an interior panel of a two-way reinforced floor slab system.

For the test slabs, the primary criterion for selection of the clear span size were the inner dimension of the Small Blast Load Generator (SBLG), which was used as the loading device. The maximum slab clear span that will fit in the SBLG is 29 inches. Because of the small scale of the test slab, some difficulty was experienced in fabricating the concrete and reinforcing. The test slab thickness was 0.89 inch. The slabs were cast inside 46-3/4-inch-I.D. circular steel rings, which are part of the SBLG. Slab reinforcing consisted of smooth 0.08-inch-diameter steel wire. Concrete was a scaled mixture of Type III portland cement (early strength) with graded sand as aggregate. Geometry and steel layout for the two types of test slabs (Series I and II) are shown in Figures 2.3 and 2.4.

The test slab support structure provided the slab edges with nearly 100 percent fixity. A prototype structure may not have quite this degree of fixity because it would generally be supported on flexible beams. Results of these tests on slabs with a high degree of fixity coupled with previous test results on simply supported slabs of similar design provide a useful comparison of upper- and lower-bound values for the prototype boundary characteristics.

Geometric similarity between the prototype and test slabs was maintained by direct length scaling. The prototype and test slabs were sufficiently similar so the test results would be quantitatively indicative of prototype response and behavior.

2.2 MATERIALS OF THE TEST SLABS

2.2.1 Concrete. The ingredients of the concrete mix used in this study were water, Type III (high early strength) portland cement, and a fine-graded aggregate of natural sand. The proportions by weight of the constituent materials, i.e. cement, fine aggregate, and water, were 1.00:5.37:0.79. Figure 2.5 shows the distribution of particle size in the fine aggregate. The sand was screened to eliminate particles larger than a size 8 sieve and smaller than a size 100 sieve.

Proportioning of the concrete mixture was based on a desired compressive strength, f'_c, of 3,000 psi at an age of 14 days. The concrete was mixed in 8-ft^3 batches in a 14-ft^3-capacity rotary mixer.

2.2.2 Reinforcement. Obtaining steel wire reinforcing for the test slab to properly simulate prototype reinforcing bars was a major problem. Because of the need for simulating the reinforcing up to and including tensile rupture, prototype reinforcing bars and test slab reinforcing wire had to exhibit nearly identical properties. Typically, the prototype steel (#5 reinforcing bars) is hot-rolled AISI 1030 carbon steel. This type of steel exhibits a sharp yield point at approximately 50,000 psi and has an ultimate strength of about 70,000 psi, satisfying ASTM Specification A615 (Reference 5). Elongation is typically between 12 and 25 percent.

In order to maintain the same percentage and spacing of steel as in the prototype, the test slab reinforcing diameter had to be 0.08 inch. This diameter is equal to a standard wire gage #14. Typically, hard-drawn wire is available only with low carbon contents, i.e. AISI 1008. This is necessary so that the wire can be drawn to a small diameter without rupturing due to strain-hardening. A search was conducted for a #14 gage wire of AISI 1030 steel. Finally, through the U. S. Steel Corporation, 100 pounds of galvanized AISI 1039 steel wire were obtained from a larger mill order. The wire was wound in a 2-foot-diameter coil in the hard-drawn condition.

The task of straightening the wire presented difficulties. Mechanical straightening was tried, but results were less than satisfactory. Finally, electrical straightening was tried and was found to be successful and quick. Twenty-foot-long strands of wire were strung from a mounting point, and welding machine electrodes were attached to each end. Due to the high resistance of the wire, the electric current caused a rapid heat rise in the wire. The galvanizing was partially burned off during heating. Strength of the wire after straightening was only slightly reduced.

Because of the high yield of the wire in the hard-drawn condition, heat treatment of the wire was required to obtain a yield strength of about 50,000 psi. For AISI 1039 steel, this meant a fully annealed condition. The wire was placed in a gas furnace for 2 hours at 1400 F and then oven-cooled overnight. This heat treatment resulted in an average yield strength of 43,600 psi and an ultimate strength of 73,500 psi. Average elongation was 12 percent over a 5-inch gage length. Because of the higher carbon content, the strain-hardening ratio was a little higher than that for AISI 1030 steel.

The zinc coating was almost completely burned away in the annealing process. It was noted that in the tensile tests of the annealed wire an apparent brittle exterior layer existed. This may have been some form of embrittlement caused by the zinc coating. The brittle coating did not seem to affect the material properties significantly; however, elongation at rupture may have been slightly reduced because of this

condition. The wire was cleaned with steel wool before use to remove the loose zinc and iron oxide. The wire was used in the smooth condition, i.e. no attempt was made to deform it in any way. It was practically impossible to deform the wire by mechanical means so that it looked like deformed bar. However, it was believed that the deformations would not be required to generate the membrane tensile stresses in the reinforced slabs tested since bar pullout was precluded by the continuous bar lengths.

2.2.3 Material Sampling. The concrete specimens used in determining the strength characteristics of the slab material were standard 6- by 12-inch test cylinders. Six cylinders, three for compression and three for tensile splitting tests, were cast from each batch of concrete. One compression cylinder per batch was instrumented to measure longitudinal and transverse stress and strain. Table 2.2 gives the cylinder strength data for the concrete used in the test slabs. A typical stress-strain diagram is shown in Figure 2.6.

The wire reinforcing was tested for strength using an 8-inch gage length between serrated surface grips in an Instron testing machine. Twenty tests were conducted on samples cut from the centers of 5-ft-long strands. Tests of samples cut from the ends showed that the strands had good consistency of strength along their length. The results of the tension tests are given in Table 2.3. A typical stress-strain diagram for the wire is shown in Figure 2.7.

2.3 CONSTRUCTION OF TEST SLABS

Each test slab was cast monolithically with its side support structure. This provided edge fixity and continuity of reinforcing at the edges of a slab. The side beam structure was designed to support all loads imposed by the slab during testing without failure. A welded reinforcing cage with moment and shear steel reinforcing was fabricated to provide the required side beam strength.

Formwork consisted of a plastic-coated plywood platform on which a 29-inch-square plywood box was attached. The box was designed for ease of removal after curing of the concrete. A 6-inch-deep SBLG steel

spacer ring was used as a side form and as a surface reference for screeding the slab. All joints in the formwork were sealed against leakage of wet concrete with silicone rubber. The concrete slab and support structure were held in the ring after curing by two small angles welded to the bottom of the ring.

Proper location of the wire reinforcing was critical. Spacing between wires was maintained by drawing lines on the top of the box form and aligning the wires over the marks. Proper vertical spacing was accomplished by securing strips of sheet metal cut to the required width to the reinforcing cage and then tying the wire to the strips. The wire mat was supported on short lengths of 3/32-inch-diameter wire and was tied together at every third intersection with 24-gage copper wire. The whole mat was tied down to the box form at four points. Glue was used at some wire intersections and at the edge strips to prevent movement of the wires during casting. Strain gages were bonded to some of the reinforcing wires prior to assembly. The ends of the wire strands were bent up into the side beam area to provide the required restraint. Details of the reinforcement fabrication are shown in Figure 2.8.

Where accessible before casting, the forms around the side beams were coated with form oil. The slabs were cast in an upright (loaded surface up) position. Figure 2.9 shows a slab form ready for casting with all the reinforcing steel in place.

Four slabs were cast at once using two batches of concrete mix. The first batch of approximately 8 ft^3 was mixed in a 14-ft^3-capacity rotary mixer and was used to fill the side beam area. The concrete was vibrated using a 3/4-inch-diameter-head internal vibrator with minimum vibration because of the possibility of damage and displacement of the wire reinforcing. The second batch of approximately the same size was mixed and immediately placed over the first batch and onto the slab area of the forms with a minimum of vibration. This procedure resulted in air pockets along and under the wire reinforcing in the first set of four slabs, as shown in Figure 2.10. The voids probably did not affect slab strength appreciably. The second and third sets of four slabs were vibrated more extensively in the slab area. This eliminated virtually

all air pockets. After the forms had been completely filled with concrete, the surfaces of the slabs were screeded flush with the top of the steel ring with a wooden screed. This was followed with screeding using an aluminum angle. After the concrete had stiffened sufficiently, the surface was finished with a steel trowel to produce a smooth, flat surface. The exposed surface was covered with wet burlap and plastic. The burlap was soaked with water at least once a day for seven days after casting, and then the burlap and plastic were removed. The slabs were then air-cured until the day of testing. Figure 2.11 shows a slab after casting and curing.

A portion of each concrete batch placed in the slab area was used to make the test cylinders for later strength testing. These were cured in the same manner and tested at the same time as the test slabs.

2.4 TEST PROCEDURES

Both the dynamic and static slab tests were conducted in the SBLG. The configuration of the SBLG used in this study is shown in Figure 2.12. The only difference between the SBLG setup for dynamic and static testing was in the bonnet used. The reaction structures used in all tests were identical. Except for strain gages, instrumentation for all tests was similar. Descriptions of the test measurements made and instrumentation equipment used are presented in Section 2.5.

The setup for the static testing, as shown in Figure 2.13a, consisted of placing a 6-inch-deep SBLG ring containing the slab and support structure over a 9-inch-deep SBLG ring, which was filled with reinforced concrete with a 29-inch-square hole in the center. This structure provided support for the slab and clearance under the slab for any large deflections. The 9-inch-deep ring was in turn supported by a base consisting of a flat steel plate with a hole in the center support that was accessible when the base was bolted to the floor. The hole in the center of the plate provided a location for mounting deflection gages. For the static tests, a closed static bonnet was used to cover the top of the slab. All elements of the test structure were bolted securely together to transmit the loads to the foundation and prevent leaks.

For the static tests, a 3/32-inch-thick neoprene rubber diaphragm was placed over the slab's top surface. This prevented loss of pressure when the slab deflected and cracked. The diaphragm extended across the slab and was secured by placing the edge between the bolt flanges of the bonnet and 6-inch-deep ring. An extra strip of neoprene was taped to the edges of the slab where large cracks were expected. Between the neoprene and slab, there was an unsecured 6-mil-thick sheet of polyethylene. It was covered with powder to provide a low-friction surface for the neoprene diaphragm to slide on.

The static bonnet was filled with water to develop the slab overpressure. Water pressure was regulated manually using a line hose feeding into the bonnet through a screw valve. A large-dial pressure gage was mounted on the bonnet to monitor pressure. The load was applied slowly by opening the valve, with the flow rate controlled to produce a pressure increase of approximately 1 psi/min. Water flow was continued until total loss of pressure or diaphragm rupture occurred. Posttest photographs were taken of each test slab with a still camera. The slab and support structure were then removed from the 6-inch-deep rings, and the rings were prepared for another casting.

For the dynamic tests, Figure 2.13b, the bonnet was changed to one that contained firing tubes for producing a dynamic overpressure. No diaphragms were used over the slab during the dynamic tests. The overpressure was produced by electrically detonating primacord explosive in the firing tubes. All measurements were recorded on high-speed analog magnetic tape. After each test, photographs were taken. The slabs were then removed from their rings as in the static tests.

2.5 TEST MEASUREMENTS AND INSTRUMENTATION

Measurements made during the static and dynamic slab tests included pressure, deflection, and reinforcing steel strains. All measurements were recorded on analog magnetic tape. During the static tests, an X-Y plotter was also used to monitor the pressure-deflection history of the test slabs.

The dynamic test data required detailed processing to obtain a

clear picture of the pressure and deflection measurements. These data were digitized and then filtered to reduce periodic noise. The resulting pressure data were then numerically integrated to obtain an impulse-time diagram of the overpressure.

Static pressure levels were measured using strain-gaged diaphragm transducers. Specifically, two 200-psi Norwood pressure transducers were fitted to the static bonnet with a tee fitting, as shown in Figure 2.13a. During the dynamic tests, as many as four gages were used. One Norwood gage was mounted on each side of the dynamic bonnet, and two other gages, either Norwood or CEC, were embedded in the slab support structure flush with the slab's top surface, as shown in Figure 2.14. Pressure ranges of the gages varied from 100 psi for the CEC to 500 psi for the highest pressure Norwood gage. The Norwood gages in the bonnet were mounted on Teflon disks for shock-isolation, and those in the slab structure were surrounded by silicone rubber. The pressure gages and mounts are shown in Figure 2.15.

Midspan deflection was measured during both static and dynamic tests. In the static tests, two gages were used at the same point for redundancy, i.e. a 12-inch, linear-travel, Collins linear variable differential transformer (LVDT) and a rotary potentiometer with a cable-reel pickup and a maximum deflection range of 4 feet. Only the LVDT was used during the dynamic tests because inertial effects would prevent the rotary potentiometer from functioning. The LVDT probe was attached to the slab by means of a universal joint and a rod cast into the slab at the center.

Two static and two dynamic slabs were instrumented with strain gages on the wire reinforcing, shown in Figure 2.16. In the figure, each gage location is numbered for ease of correlation with the appropriate strain curves. Longitudinal strain at various points along the edge and center of the slab were measured. One epoxy-backed strain gage (M-M Type EA-06-125BT-120) was used at each location. The small size of the wire prevented mounting two gages opposite each other. The bridge circuits for the strain gages were completed with dummy gages mounted on a steel block outside the test fixture.

TABLE 2.1 EXPERIMENTAL PROGRAM SUMMARY

Series	Slab Designation[a]	p[b]	Concrete Stress[c]		Steel Stress		Remarks
			Compressive f'_c	Tensile f_t	Yield f_y	Ultimate f_u	
			psi	psi	ksi	ksi	
I	IS1	0.0078	3,683	328	43.6	73.5	--
	IS2	0.0078	3,683	328	43.6	73.5	
	IS3	0.0078	3,683	328	43.6	73.5	Strain-gaged
	ID1	0.0078	3,683	328	43.6	73.5	Two tests
	ID2	0.0078	3,485	332	43.6	73.5	--
	ID3	0.0078	3,485	332	43.6	73.5	--
	ID4	0.0078	3,485	332	43.6	73.5	
	ID5	0.0078	3,485	332	43.6	73.5	--
II	IIS1	0.0117	3,810	275	43.6	73.5	Strain-gaged
	IID1	0.0117	3,810	275	43.6	73.5	Strain-gaged
	IID2	0.0117	3,810	275	43.6	73.5	--
	IID3	0.0117	3,810	275	43.6	73.5	Strain-gaged

[a] S denotes static test; D denotes dynamic test.

[b] $p = A_s/d$, ratio of tension reinforcement per unit width of slab.

[c] Values are averages of three tests after a 14-day cure time.

TABLE 2.2 RESULTS OF TESTS ON CONCRETE CONTROL SPECIMENS

Slab	Specimen	Test Age	Cylinder Strength		Poisson's Ratio at 1,500 psi	Strain at Maximum Load
			Compressive f'_c	Splitting Tensile f_t		
		days	psi	psi		μin/in
IS1, IS2, IS3, ID1	1	15	3,750	--	0.19	2,100
	2	15	3,680	--		
	3	15	3,620	--		
		Average	3,683			
	4	15		345		
	5	15		350		
	6	15		290		
			Average	328		
ID2, ID3, ID4, ID5	1	14	3,520	--	0.20	1,800
	2	14	3,450	--		
	3	14	2,980[a]	--		
		Average	3,485			
	4	14	--	310		
	5	14	--	330		
	6	14	--	355		
			Average	332		
IIS1, IID1, IID2, IID3	1	14	3,790	--	0.17	2,600
	2	14	3,770	--		
	3	14	3,870	--		
		Average	3,810			
	4	14	--	265		
	5	14	--	290		
	6	14	--	270		
			Average	275		

[a] Value not used in figuring average because of diagonal tension-type failure.

TABLE 2.3 RESULTS OF STATIC TESTS OF REINFORCING STEEL

Specimen	Average Diameter	Distance Between Grips	Strain Rate		Tensile Stress			Elongation Over 5-inch Gage Length	Remarks
			Yield	Ultimate	Yield f_y	Ultimate f_u	Rupture f_r		
	inches	inches	in/min	in/min	ksi	ksi	ksi	percent	
1	0.079	8.0	0.02	0.10	46.5	78.4	68.5	16.3	Broke near grip
2	0.080	8.0	0.02	0.10	46.0	77.5	68.1	16.8	Broke near grip
3	0.080	8.0	0.02	0.10	46.4	77.0	68.0	17.8	Broke near grip
4	0.079	8.0	0.02	0.10	44.8	78.7	68.5	17.2	Broke near grip
5	0.079	8.0	0.02	0.10	47.0	79.5	69.4	17.2	Broke near middle
6	0.079	8.0	0.02	0.10	45.9	76.4	68.0	16.4	Broke near grip
7	0.079	8.0	0.02	0.10	46.4	78.7	68.7	16.2	Broke near grip
8	0.079	8.0	0.02	0.10	46.2	77.2	68.5	16.6	Broke near grip
9	0.079	8.0	0.02	0.10	44.4	78.5	73.5	14.8	Broke near grip
10	0.081	8.0	0.02	0.10	43.8	73.0	63.6	8.1	Broke near grip
11	0.079	8.0	0.02	0.10	47.4	79.4	69.5	14.0	Broke near middle
12	0.079	8.0	0.02	0.10	47.4	80.0	69.4	15.6	Broke near grip
13	0.084	8.0	0.02	0.10	37.9	65.5	56.5	6.6	Broke near grip
14	0.084	8.0	0.02	0.05	39.3	64.5	55.9	5.2	Broke near grip
15	0.081	8.0	0.02	0.10	44.0	72.5	63.5	6.5	Broke near grip
16	0.084	8.0	0.02	0.10	39.1	65.4	57.3	5.1	Broke near grip
17	0.080	8.0	0.02	0.10	45.6	76.6	66.6	15.8	Broke near grip
18	0.084	8.0	0.02	0.05	38.6	63.5	54.0	5.3	Broke near grip
19	0.085	8.0	0.02	0.05	36.2	60.0	53.1	5.8	Broke near middle
20	0.083	8.0	0.02	0.05	40.2	67.0	57.5	6.2	Broke near middle
				Average	43.6	73.5	64.4	12.2	

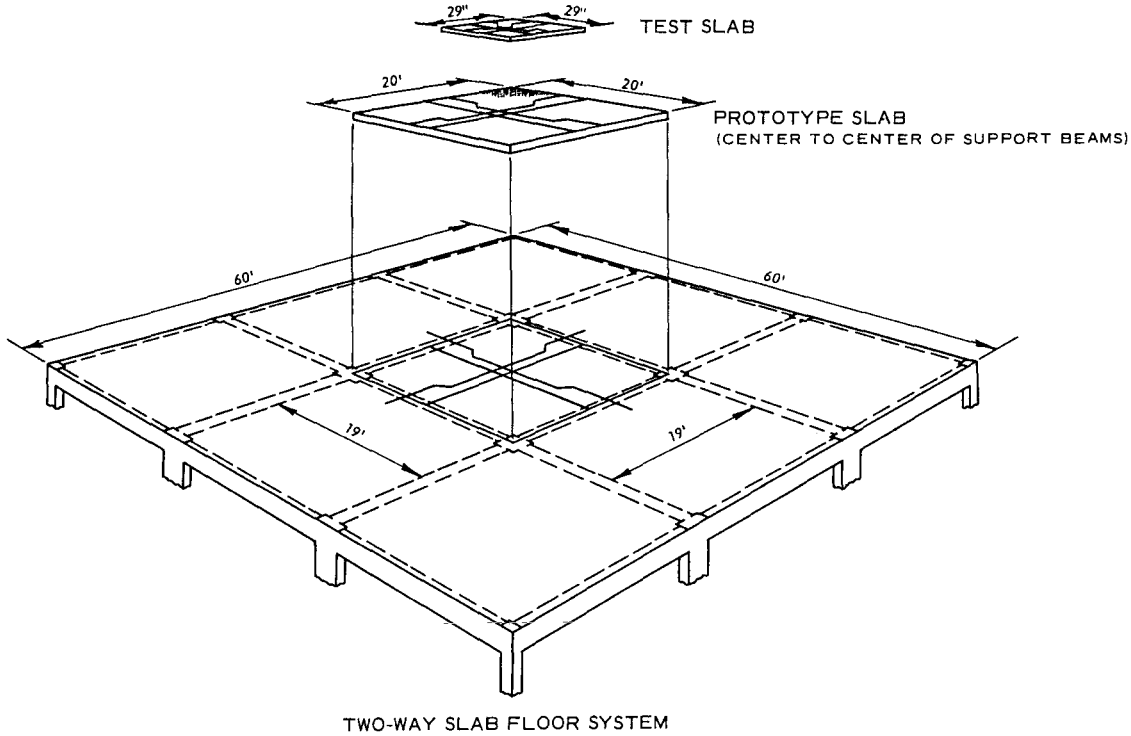

Figure 2.1 Prototype structural system.

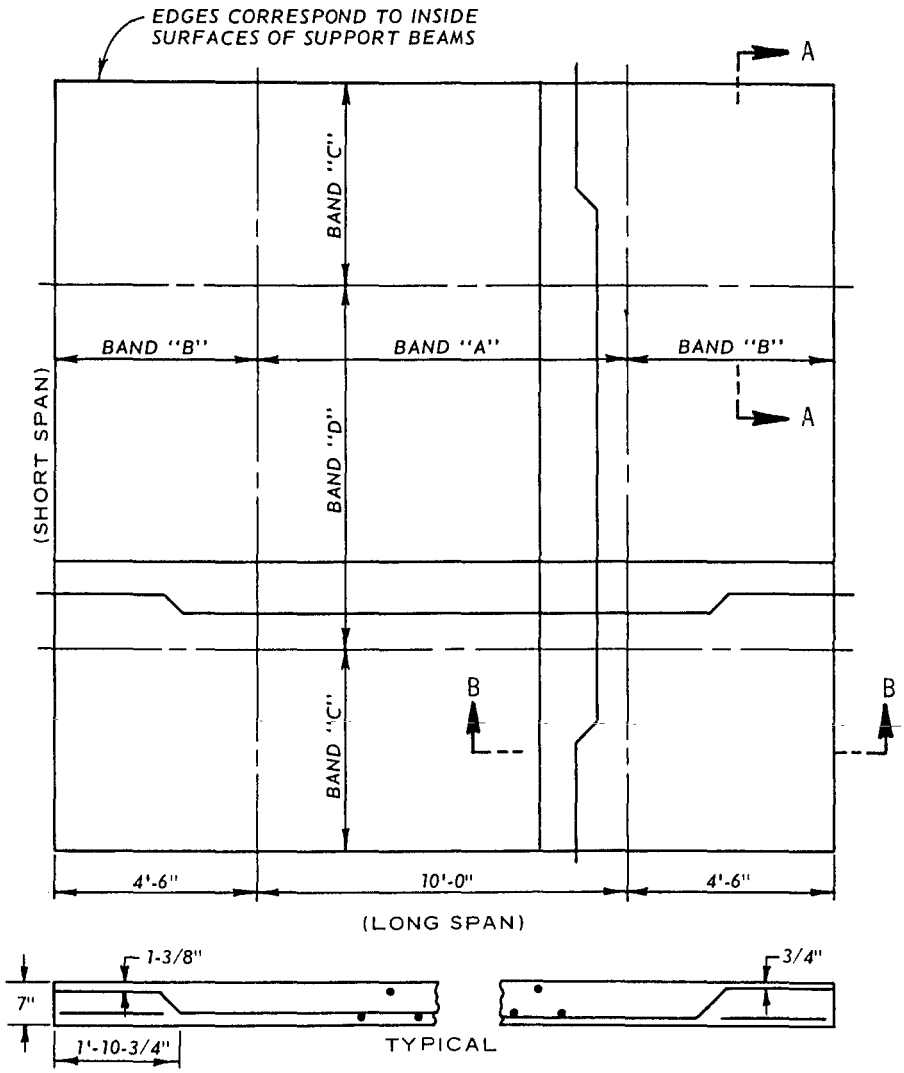

BAR SPACING

	SERIES I	SERIES II
BAND A	#5 @ 7-1/2"	#5 @ 5"
BAND B	#5 @ 10-1/2"	#5 @ 7-1/2"
BAND C	#5 @ 9"	#5 @ 6"
BAND D	#5 @ 6-3/4"	#5 @ 4-1/2"

NOTE: ALTERNATE BARS ARE BENT UP.

Figure 2.2 Steel layout and bar schedule for prototype slab.

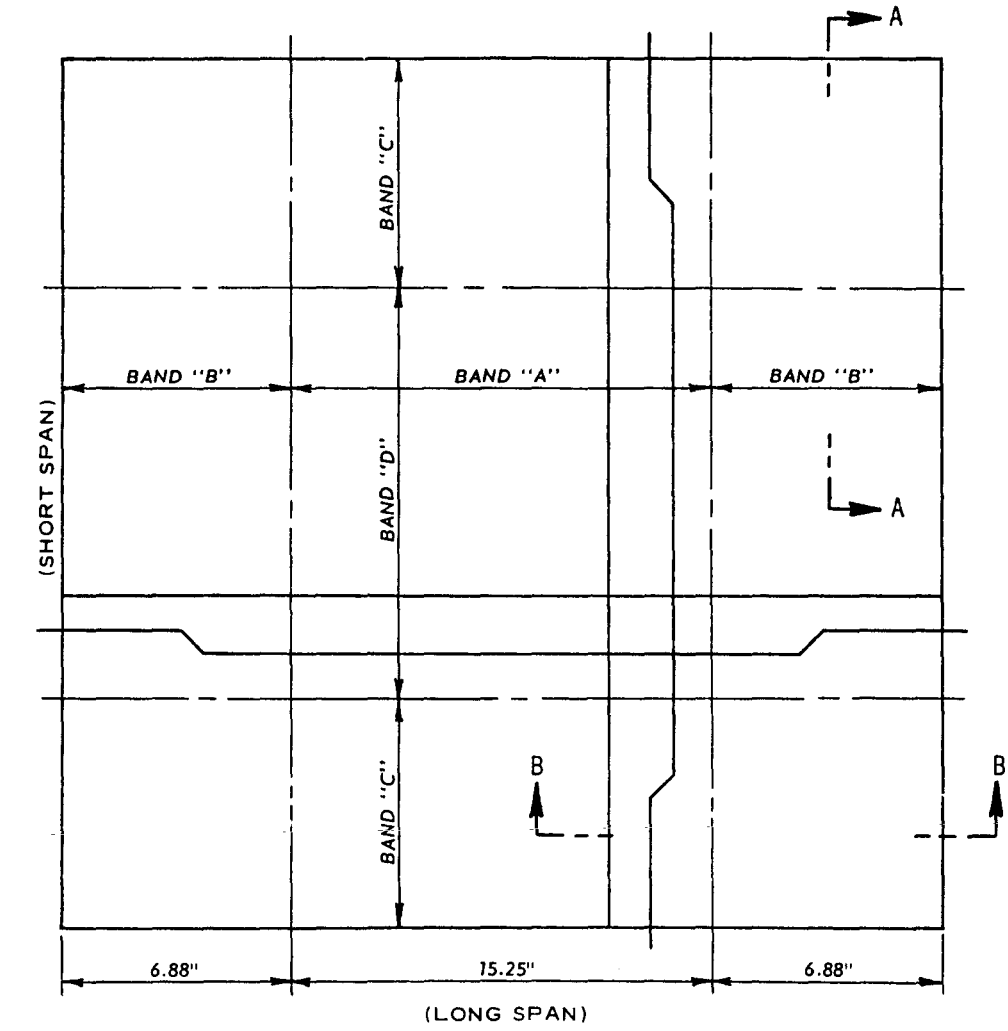

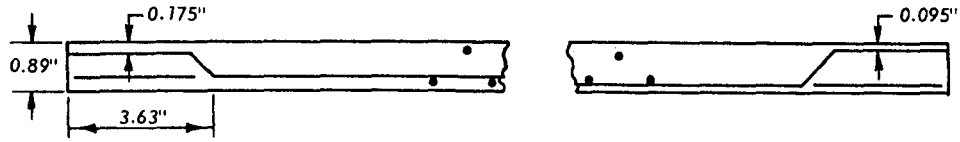

SECTION A-A

SECTION B-B

BAR SPACING

BAND A	@ 0.955"
BAND B	@ 1.34"
BAND C	@ 1.15"
BAND D	@ 0.86"

NOTE: ALL REINFORCING IS 0.080-IN.-DIAMETER STEEL WIRE.

ALTERNATE BARS ARE BENT UP.

Figure 2.3 Series I test slab geometry and steel layout.

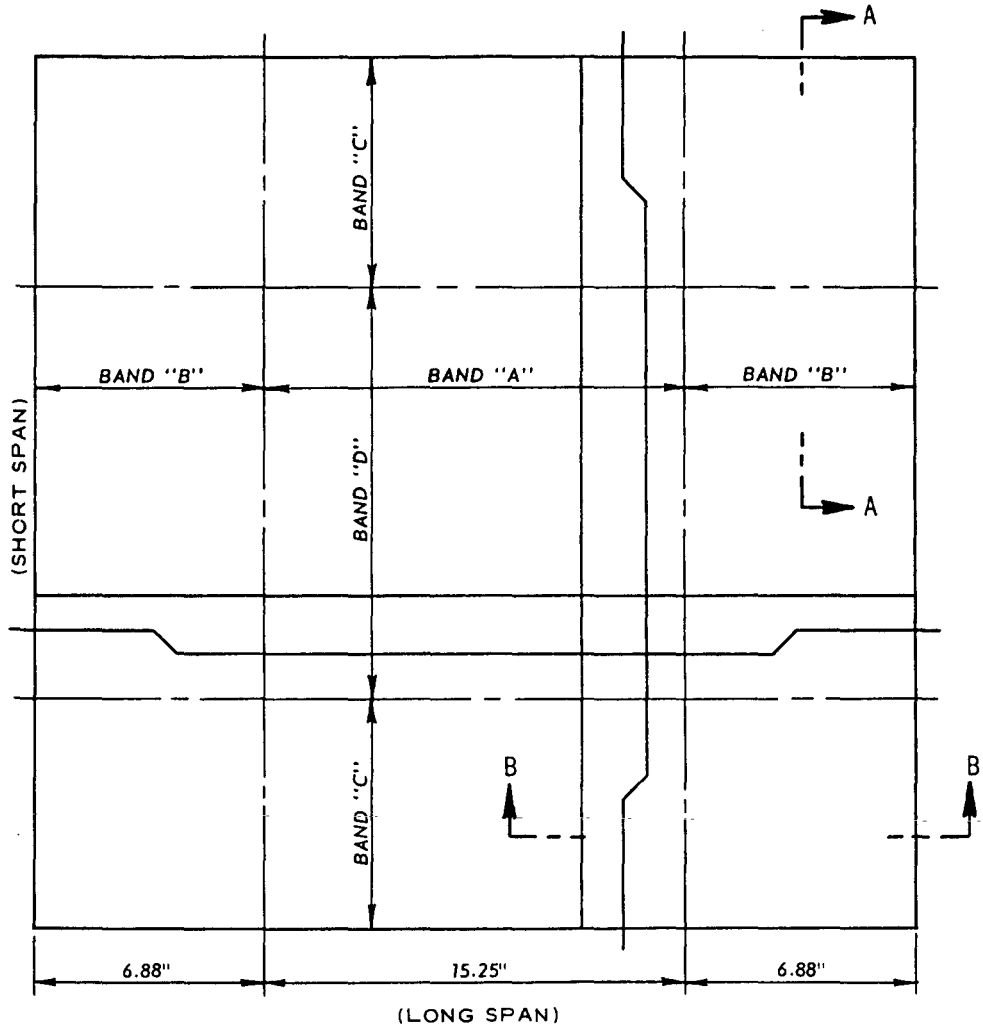

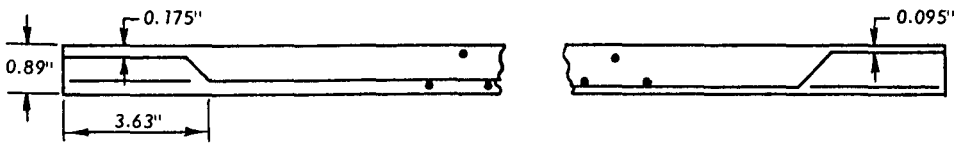

SECTION A-A

SECTION B-B

BAR SPACING

BAND A	@ 0.621"
BAND B	@ 0.954"
BAND C	@ 0.763"
BAND D	@ 0.555"

NOTE: ALL REINFORCING IS 0.080-IN.-DIAMETER STEEL WIRE.

ALTERNATE BARS ARE BENT UP.

Figure 2.4 Series II test slab geometry and steel layout.

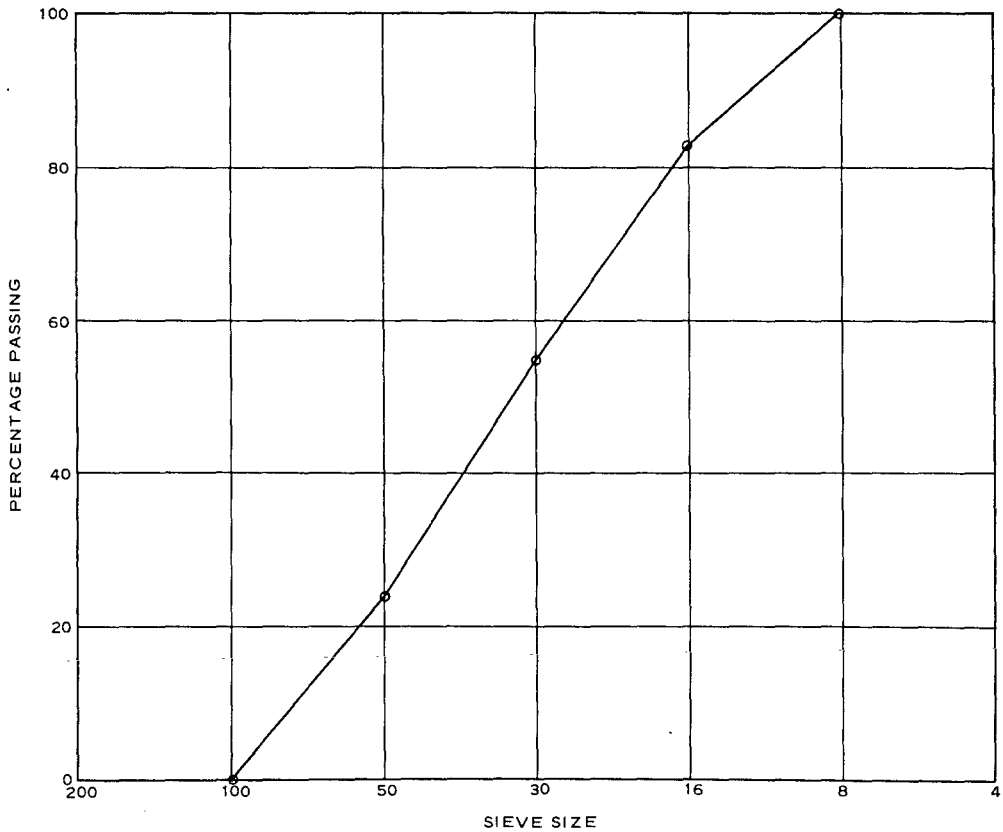

Figure 2.5 Gradation curve for sand aggregate used in concrete mixture.

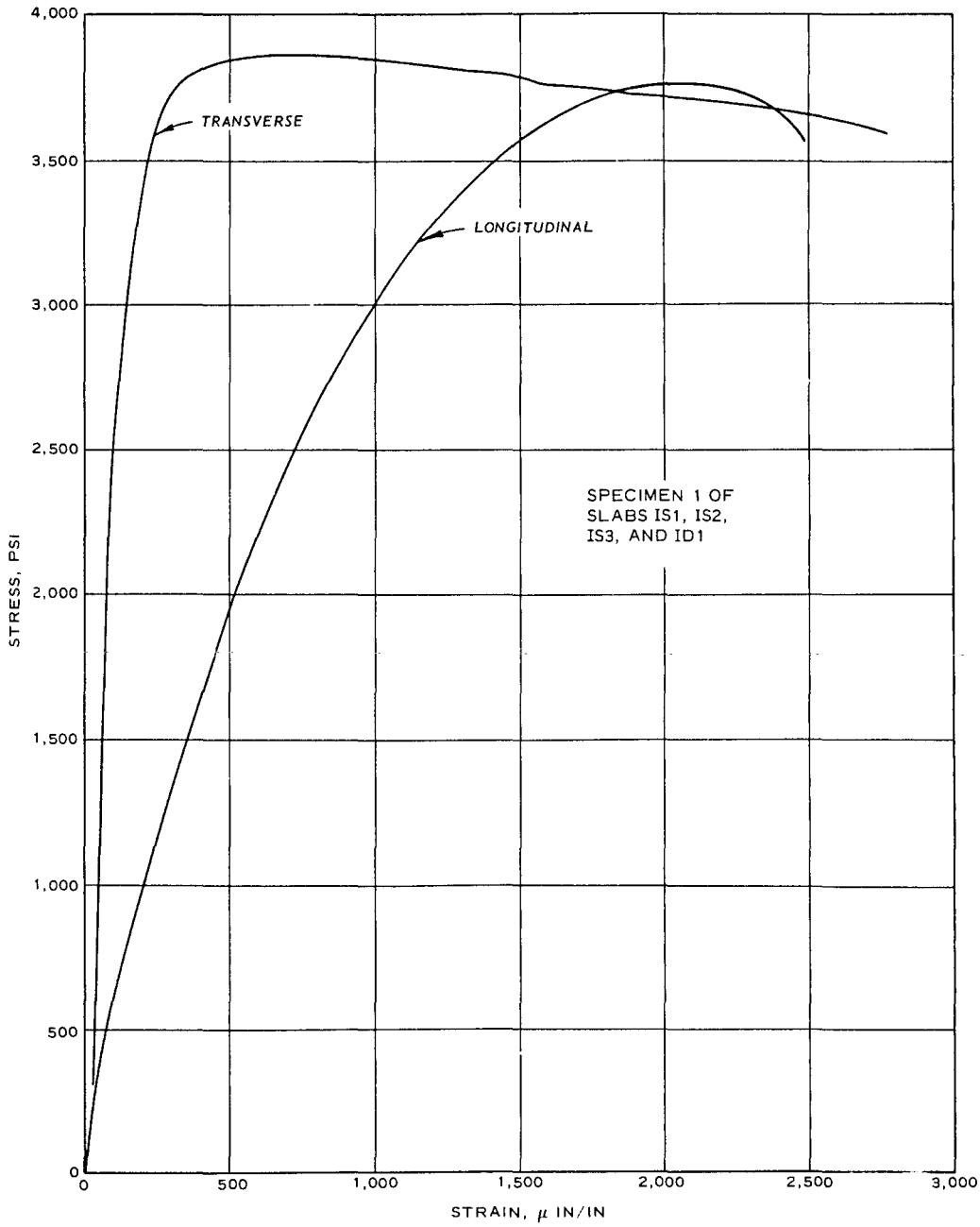

Figure 2.6 Typical static stress-strain curve for 6- by 12-inch concrete cylinder.

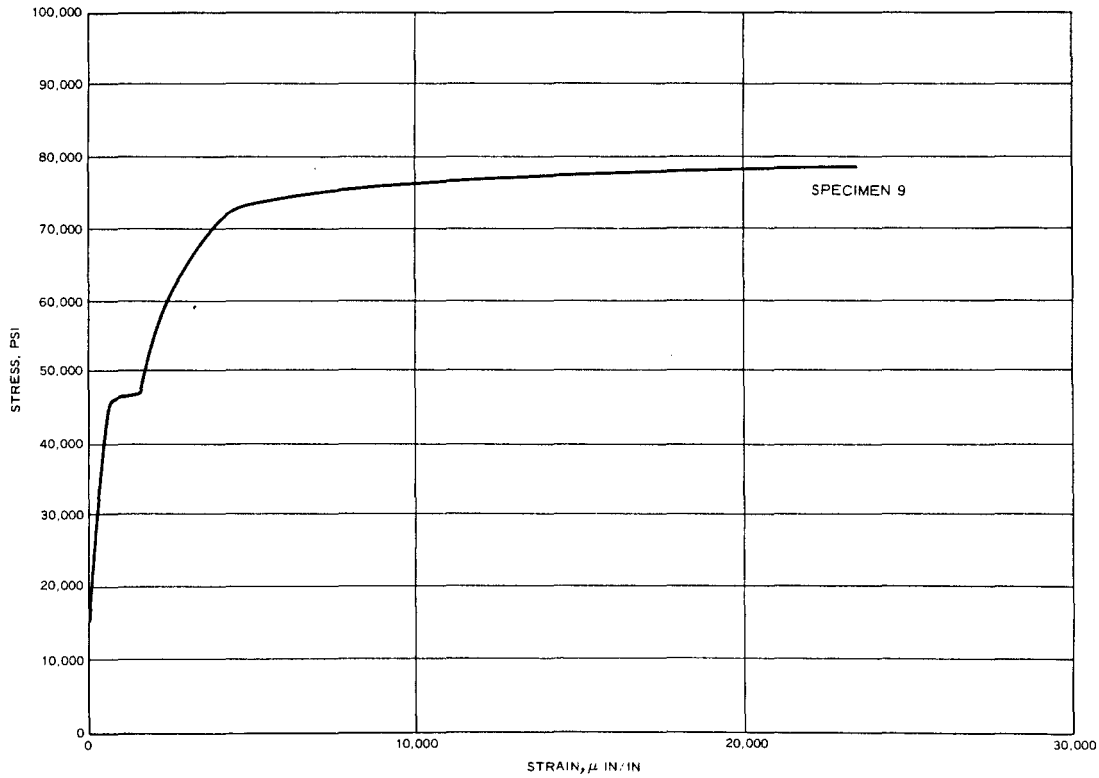

Figure 2.7 Typical static stress-strain curve for wire reinforcing.

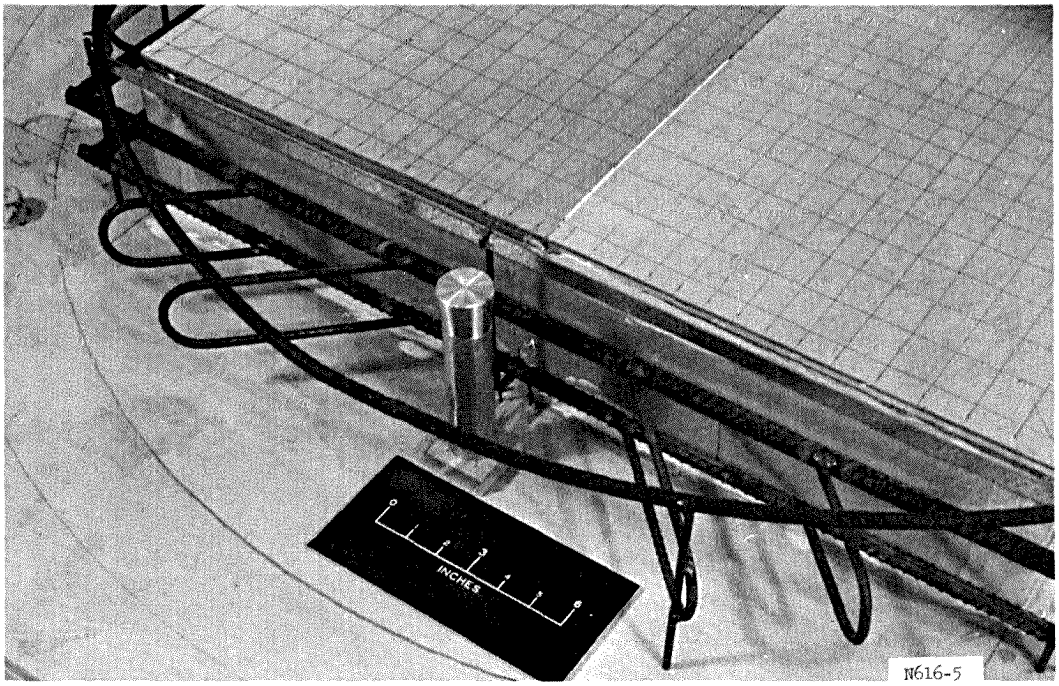

a. Slab form showing lines drawn for reinforcement spacing.

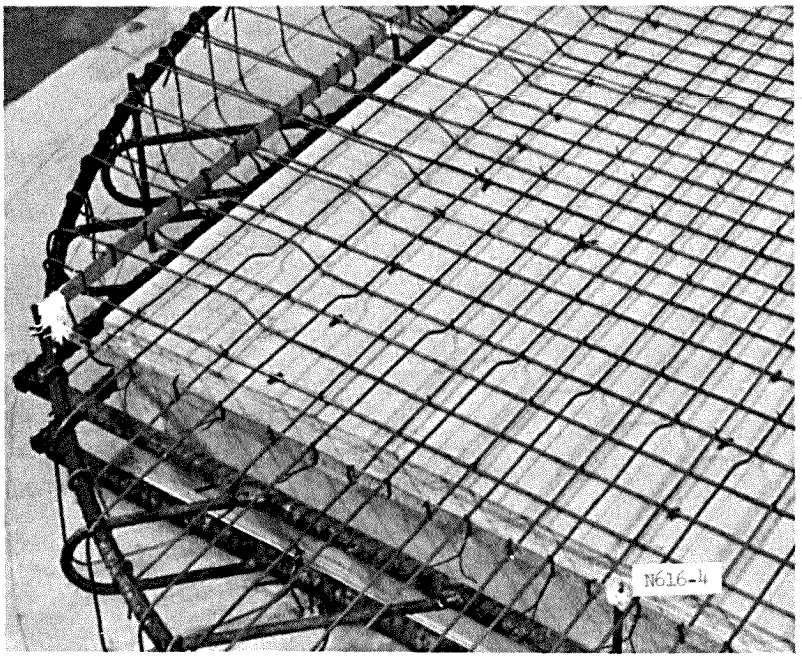

b. Wire mat showing tie-down points and metal strips for vertical spacing.

Figure 2.8 Reinforcement fabrication (sheet 1 of 2).

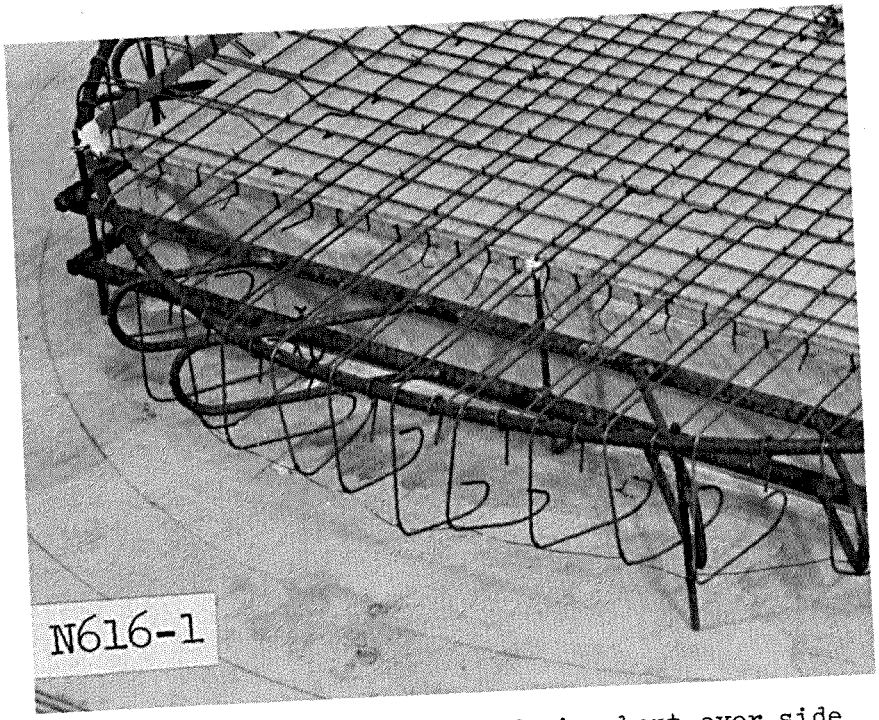

c. Wire mat showing ends of wire bent over side support structure.

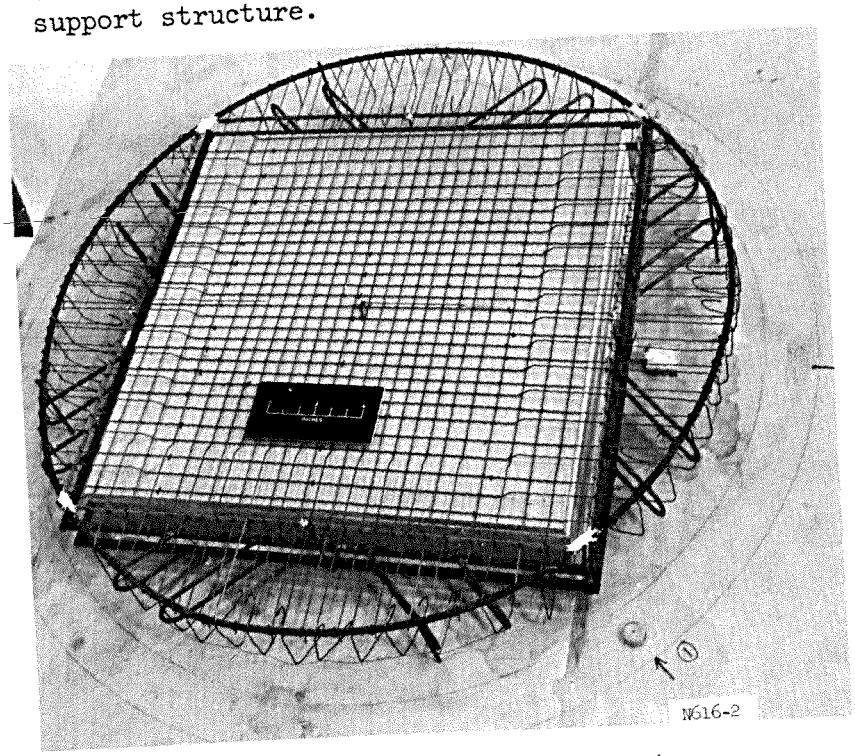

d. Completed reinforcement mat.

Figure 2.8 (sheet 2 of 2).

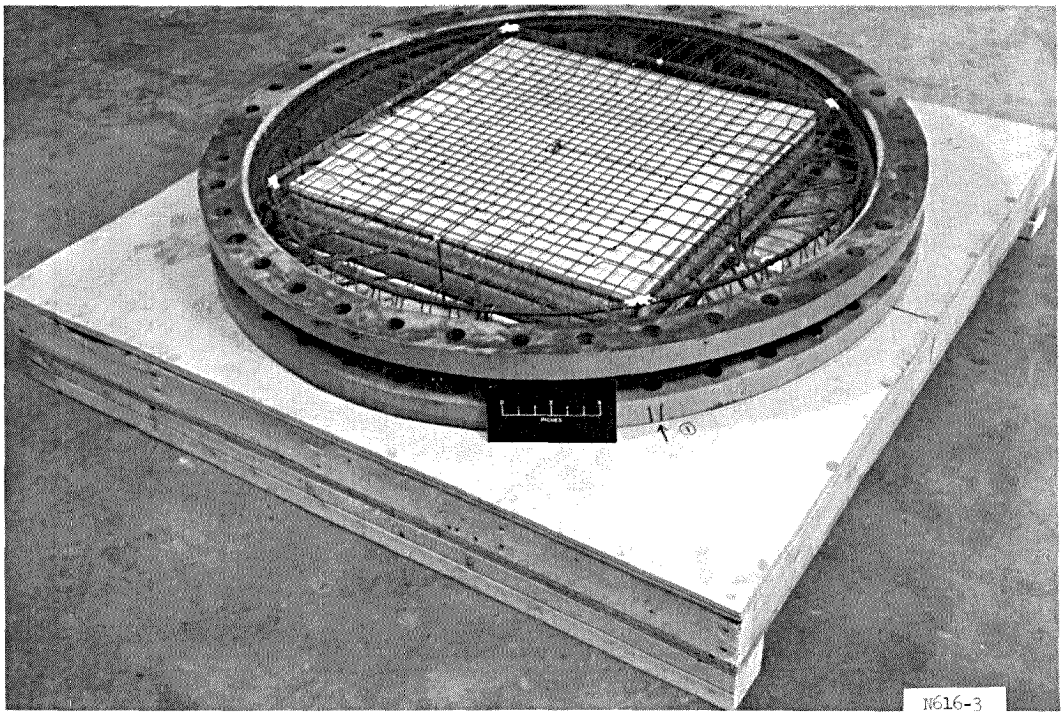

Figure 2.9 Slab form ready for casting.

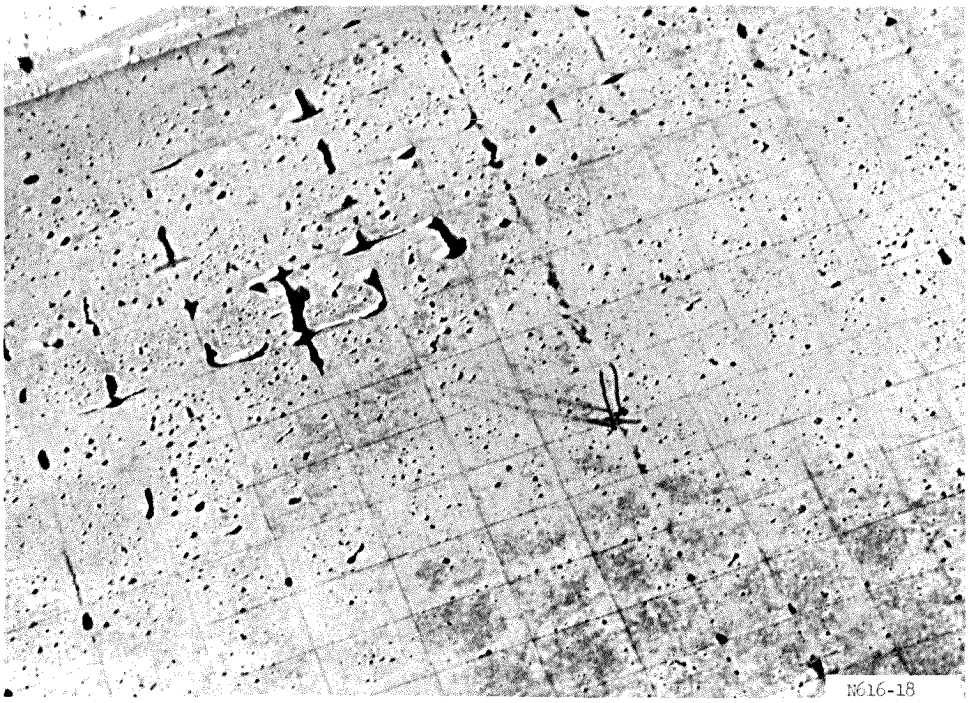

Figure 2.10 Voids in Slab IS2 due to inadequate vibration (typical of the first four slabs).

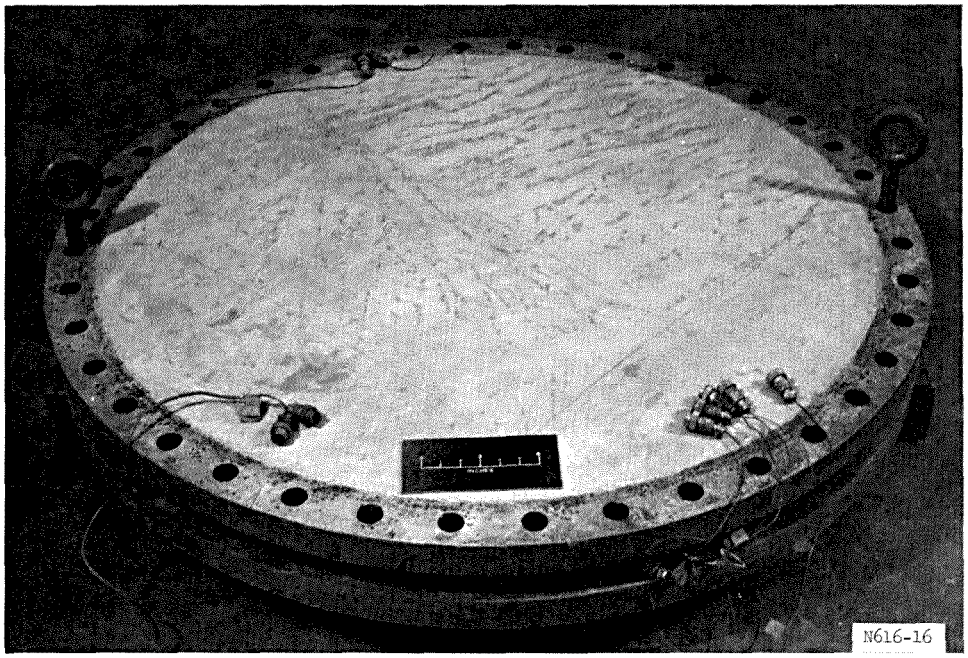

a. Top view.

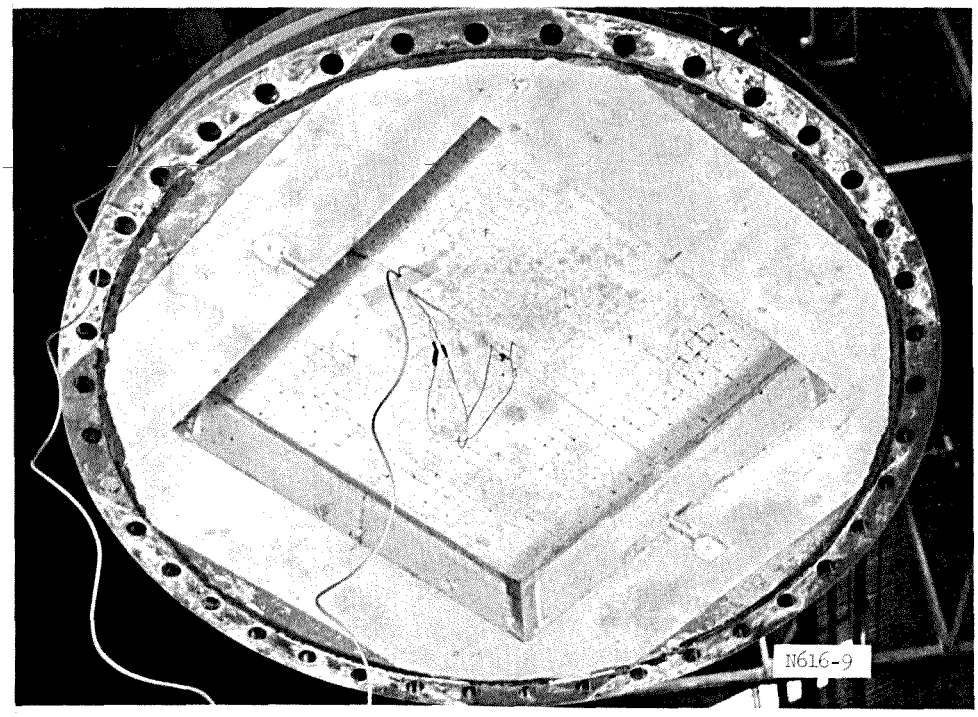

b. Bottom view.

Figure 2.11 Slab IS2 after casting and curing.

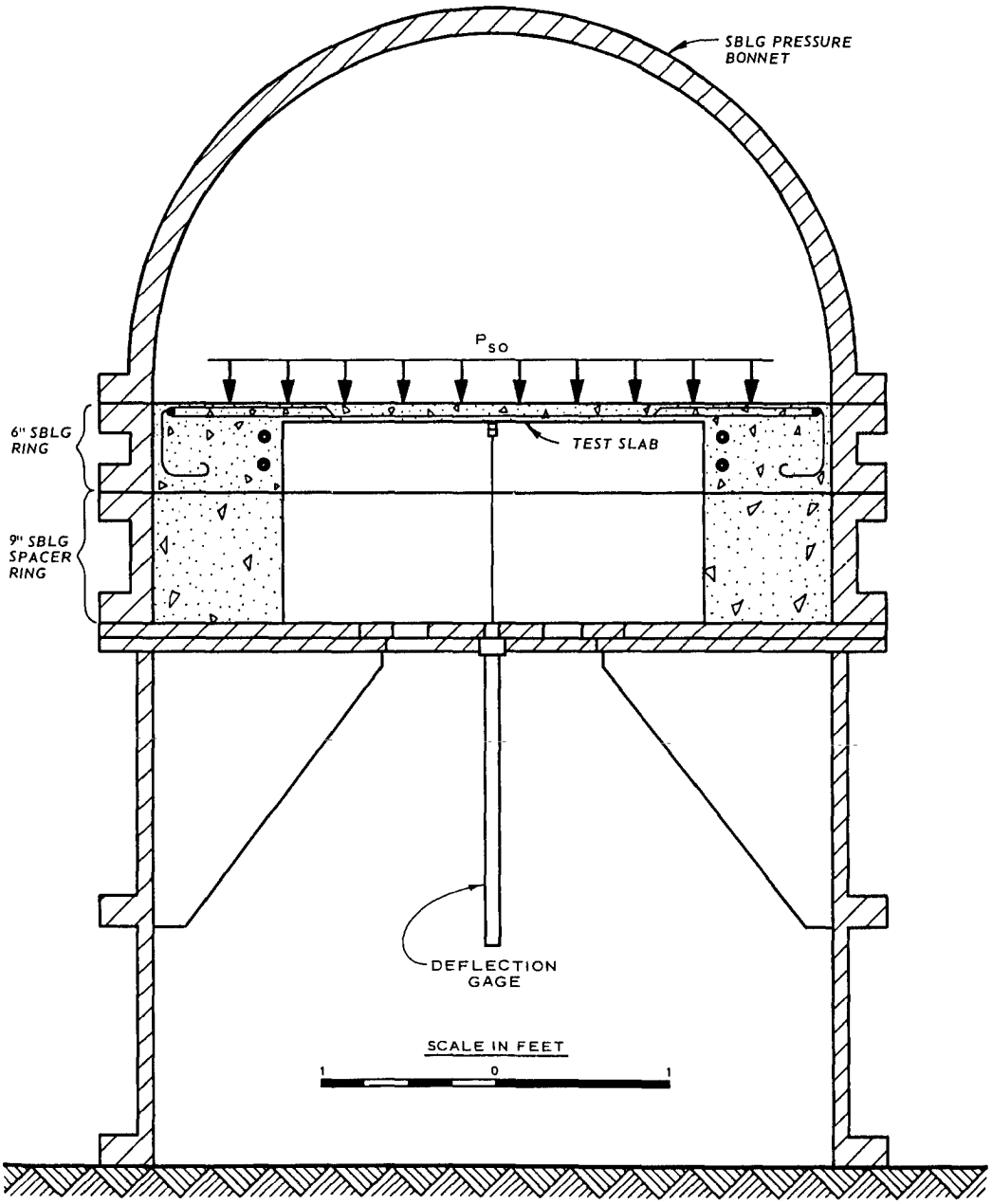

Figure 2.12 SBLG test configuration for slabs.

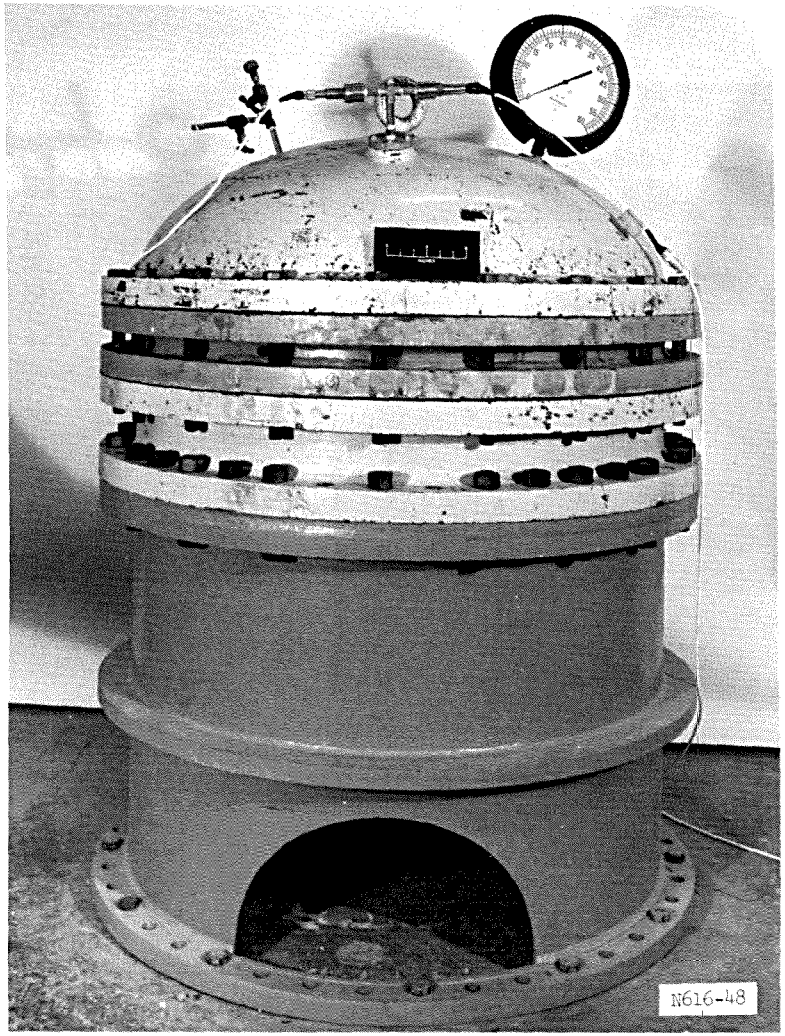

a. Static test setup.

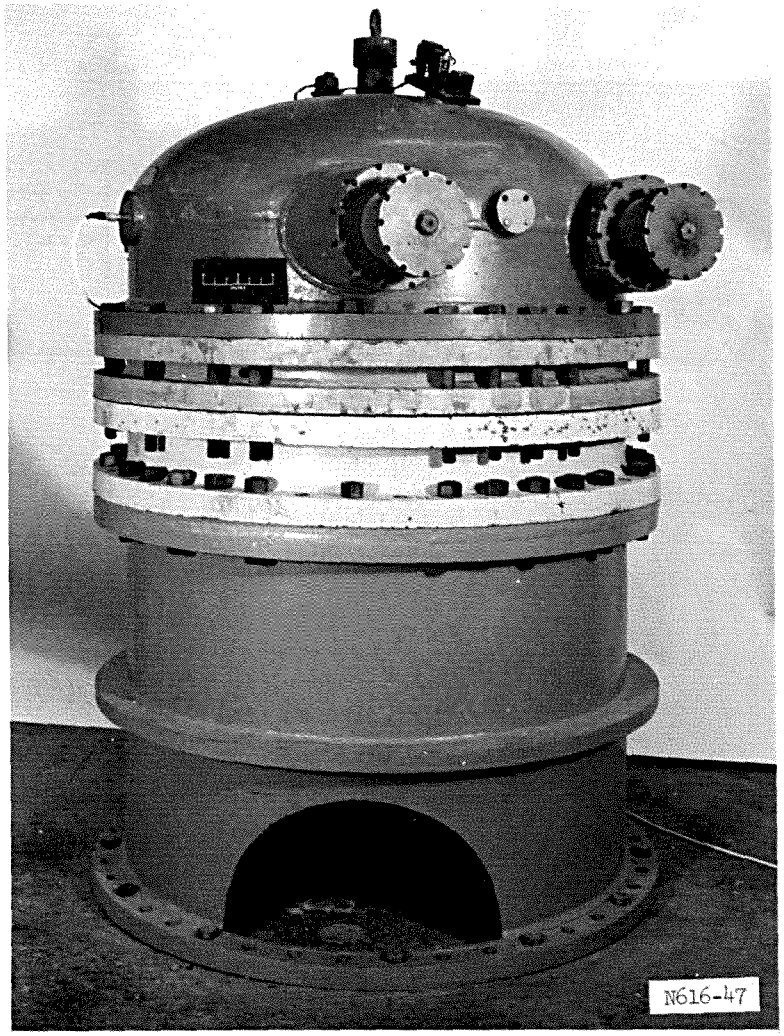

b. Dynamic test setup.

Figure 2.13 SBLG test setup.

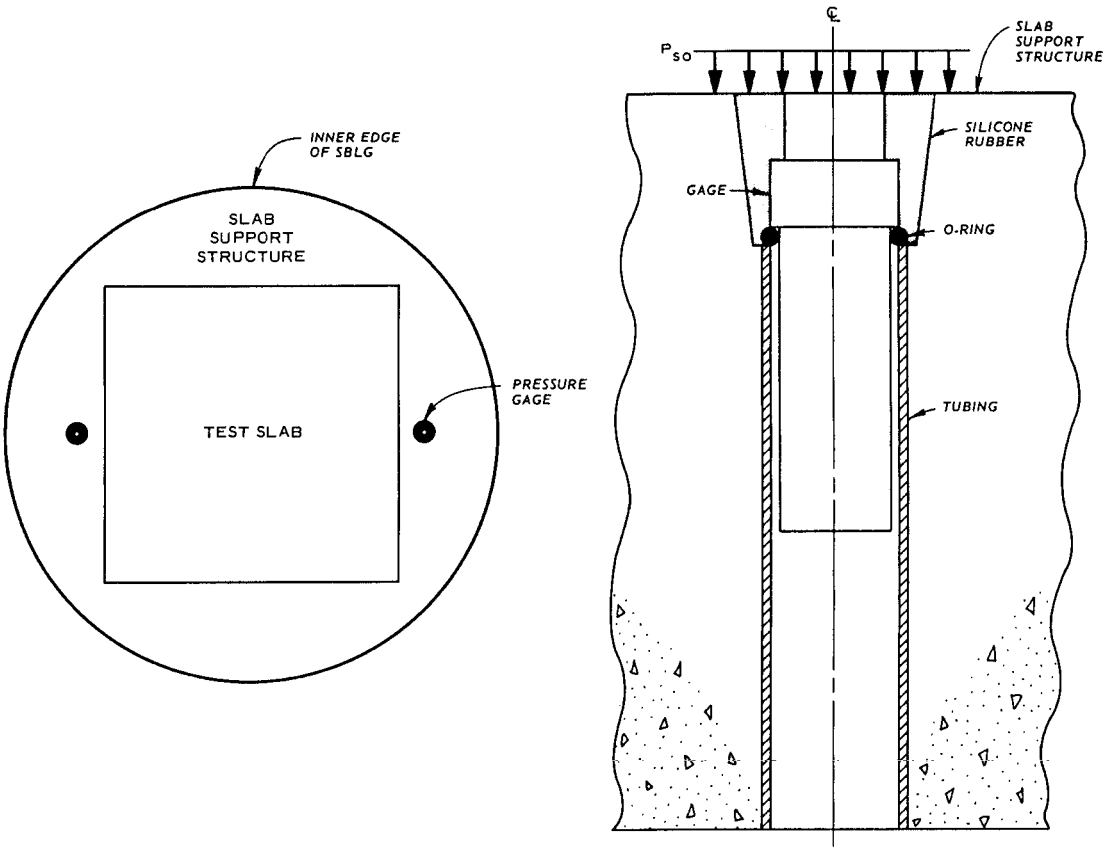

Figure 2.14 Pressure gage locations and gage mount assembly.

a. Slab surface gages and mounts.

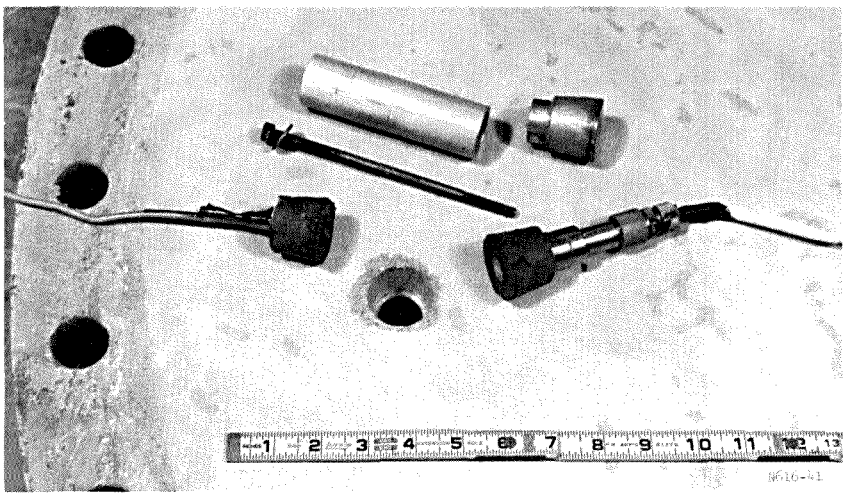

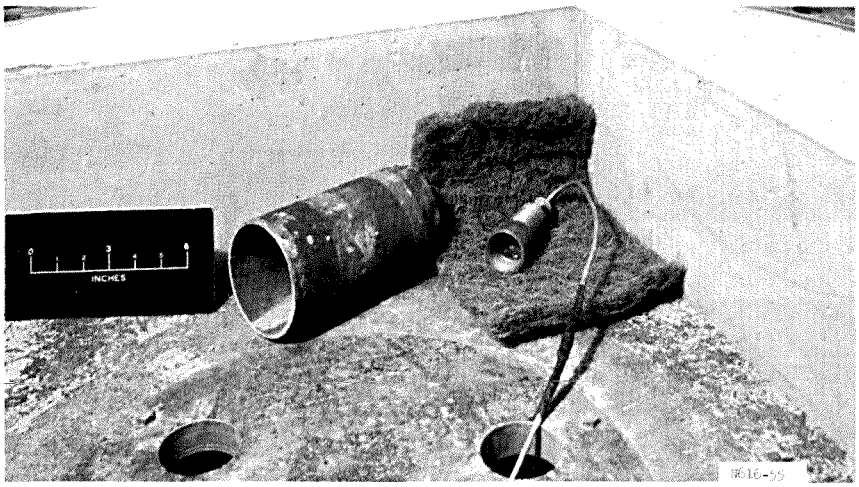

b. Internal pressure gage.

c. Internal pressure gage mounted.

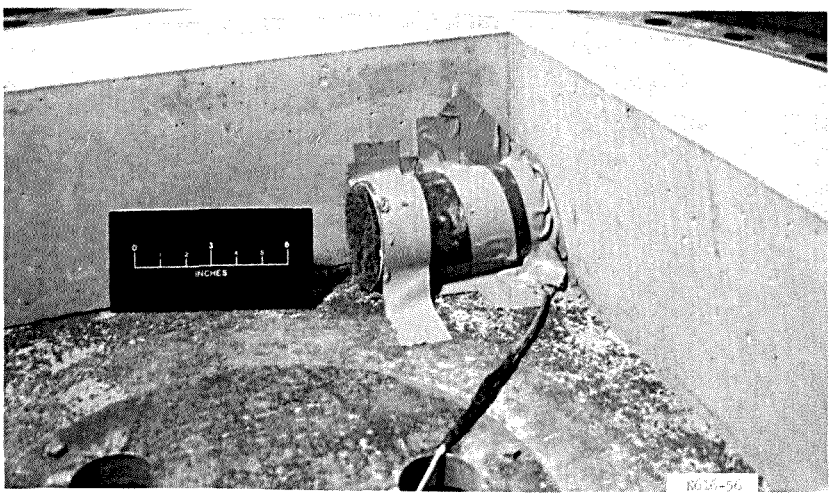

Figure 2.15 Pressure gages.

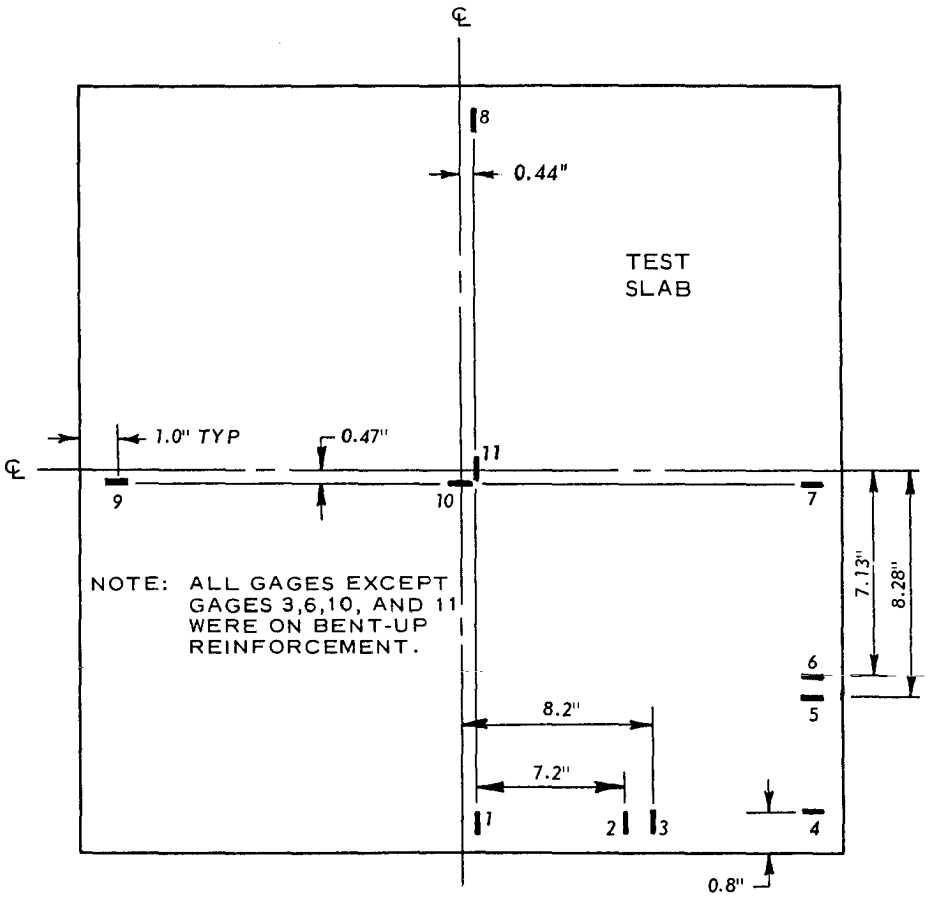

Figure 2.16 Strain gage layout.

CHAPTER 3

TEST RESULTS

3.1 METHOD OF PRESENTATION

The test results are presented in this chapter in graphical and tabular form. The pressure-time records from the dynamic tests were numerically integrated and are presented as impulse-time curves.

3.2 STATIC TESTS

Four slabs, three identical slabs in the first series and one slab in the second series, were tested statically in support of the dynamic experimental program. The top and bottom surfaces of each slab after testing are shown in Figure 3.1.

The curves of pressure versus midspan deflection for the four static tests are plotted in Figure 3.2. The pressure measurements obtained from the Norwood transducers during the static tests had to be corrected for two factors. One correction was necessary because the pressure gages did not read the pressure created by the water head because of their positions above the slab surface. This correction consisted of adding 0.6 psi to all the pressure measurements to correct for the weight of the water. The second correction was concerned with the neoprene diaphragm, which supported load as it deflected with the slab. If the deflection was between 4 and 6 inches, 0.3 psi was subtracted from the pressure measurements; if between 2 and 4 inches, 0.1 psi was subtracted; and if less than 2 inches, no correction was made. When more than one pressure gage was used, an average of all measurements was taken. The dual-peak, pressure-deflection curves are characteristic of the two failure mechanisms (flexural resistance and membrane resistance) present in a two-way reinforced slab. All four curves (Figure 3.2) show similar behavior throughout their response. The maximum recorded pressure in the first series of slabs corresponded to a deflection of about 6 inches, or approximately one-fifth of the

span length. Pertinent points on the pressure-deflection curves for the static tests are presented in Table 3.1. Slab IIS1, which had 50 percent more steel reinforcing, was considerably stronger than the Series I slabs. The increased steel percentage made the slab stiffer. This is evident from the deflection of Slab IIS1. The deflection corresponding to the maximum recorded pressure was approximately 5 inches, or about one-sixth of the span length.

3.3 DYNAMIC TESTS

Eight dynamic tests, five on Series I slabs and three on Series II slabs, were conducted. As stated previously, the Series II slabs contained 50 percent more steel reinforcing than the Series I slabs. A summary of the results of the dynamic tests is presented in Table 3.2. The only characteristic of the dynamic load that was controlled was the peak surface overpressure. This peak was varied during testing to obtain the desired slab response.

Typical surface overpressure-time records are shown in Figure 3.3. The pressure-time data for the dynamic tests were integrated and plotted as impulse-time curves, as shown in Figures 3.4 through 3.11. To obtain these curves, the analog tape records of the test were digitized with an analog-to-digital data reduction unit and then numerically integrated with the aid of a digital computer. Following the integration, the results were plotted using an X-Y plotter.

Each figure presents the impulse-time curve for each pressure gage that gave satisfactory results. Zero time for all tests was assumed to occur at the time the first slab pressure gage responded to the surface overpressure. The strain and deflection measurements were also referenced to this time base.

The top and bottom surfaces of each dynamically tested slab are shown in Figure 3.12. All slabs exhibited similar behavior and crack patterns, i.e. steel percentage had no significant effect on the general response characteristics.

Midspan deflection-time measurements were made during all the dynamic tests. A typical permanent dynamic deflection profile is shown

in Figure 3.13. Deflection-time histories are shown in Figure 3.14. The plot for Test IID1 is not shown because the deflection gage was faulty. In some instances, the deflections exceeded the linear range of the deflection gage, i.e., when the slab collapsed to the bottom of the reaction structure. If the linear range of the deflection gage was exceeded, the dynamic deflections were estimated and are shown as dashed lines in Figure 3.14.

Peak pressures, rise times, impulses, durations, deflections, and response times of the dynamically tested slabs are summarized in Table 3.2.

3.4 STRAIN MEASUREMENTS

Steel strain versus pressure data are shown in Figures 3.15 and 3.16 for the statically tested slabs. Strain-time curves for the dynamic tests of Slabs IID1 and IID3 are shown in Figures 3.17 and 3.18, respectively. During the static tests of Slab IS1, several gages became separated from their leads before the test was over because the leads broke as cracks opened. Steps were taken to prevent this in the rest of the tests.

The strain curves for Slab IS3 (Figure 3.15) exhibit a relatively slow rise until, at about a pressure of from 10 to 15 psi, they jump rapidly upward until the gages become discontinuous. At 10 to 15 psi, the corresponding strain is about 0.0018 in/in. The steel appears to yield at this point. Referring to Figure 2.7, it can be seen that at about this strain (0.0018 in/in) the steel is indeed yielding. The peak strain appears to be approximately 0.01 in/in excluding strains at Gages 10 and 11, which experience the greatest strains due to their location. In the case of Slab IIS1 (Figure 3.16), the strains show a greater tendency to loop around themselves and, as a result, do not experience the rapid rise of the Series I slab strains. However, the average peak reached by these strains is 0.015 in/in.

The strain-time curves for dynamic tests of Slabs IID1 and IID3 (Figures 3.17 and 3.18, respectively) exhibit somewhat similar characteristics. In some instances, the strains have a relatively short

duration (2 to 4 msec) before they experience a very rapid rise until the gage becomes discontinuous (Figures 3.17b and 3.18a for example). Some strains undergo more erratic behavior (Figures 3.17c and 3.18e), but still exhibit an overall rise. Still other strains exhibit a longer duration (7 to 9 msec) before jumping up rapidly, as shown in Figures 3.18b and 3.18c. The peaks of these various curves vary from 0.0055 to 0.04 in/in (in tension).

TABLE 3.1 STATIC RESISTANCE AND DEFLECTIONS

Slab	Ultimate Flexural Resistance		Secondary Flexural Resistance		Tensile Membrane Resistance		Collapse Midspan Deflection Z_c
	Pressure P_u	Midspan Deflection Z_u	Pressure P_s	Midspan Deflection Z_s	Pressure P_t	Midspan Deflection Z_t	
	psi	inches	psi	inches	psi	inches	inches
IS1	13.1	0.63	5.1	1.60	20.3	4.47	5.17
IS2	15.5	0.45	7.8	1.50	22.4	4.10	6.10
IS3	13.8	0.60	8.8	1.55	27.0	4.64	6.00
Average	14.1	0.56	7.2	1.55	23.2	4.40	5.76
IIS1	18.2	0.30	11.7	0.95	36.5	4.10	4.90

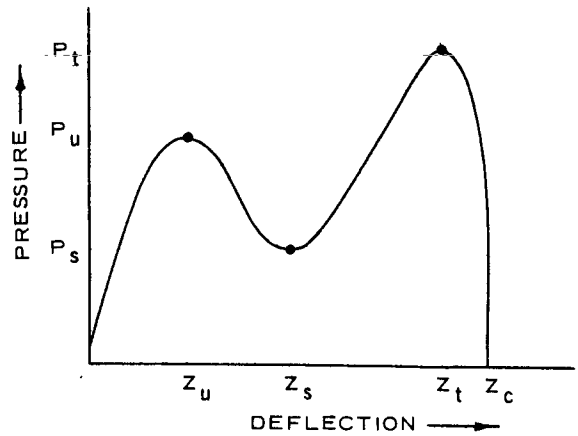

TABLE 3.2 DYNAMIC RESISTANCE

Test	Peak Pressure Direct from Pressure Curve	Peak Pressure from Impulse Curve	Average Peak Pressure	Rise Time	Maximum Midspan Deflection (Permanent)	Time to Maximum Midspan Deflection	Comment
	psi	psi	psi	msec	inches	msec	
ID1	≈15	--	≈15	--	0.25	--	Slight cracking around periphery of slab
ID1B	35.4	34.1	34.7	4.0	13[a]	24	Repeat test of Slab ID1, total collapse
ID2	26.8	26.1	26.5	4.3	7.5	31	Four corners held, sides ruptured
ID3	28.4	27.2	27.8	4.2	13[a]	31	Two corners held, sides ruptured
ID4	27.0	27.0	27.0	4.3	7.0	34	Four corners held, sides ruptured
ID5	27.7	27.2	27.4	4.3	13[a]	15	Total collapse
Series I average peak pressure =			28.7 psi[b]				
IID1	57.7	55.8	56.8	3.4	13[a]	15	Total collapse
IID2	37.5	35.6	36.6	4.0	8.1	28	Three corners held, sides ruptured
IID3	43.6	42.6	43.1	3.8	13[a]	28	Total collapse
Series II average peak pressure =			45.5 psi				

[a] Deflection gage bottomed out. Support structure allows 13 inches maximum slab deflection.

[b] Slab ID1 value not used in figuring average.

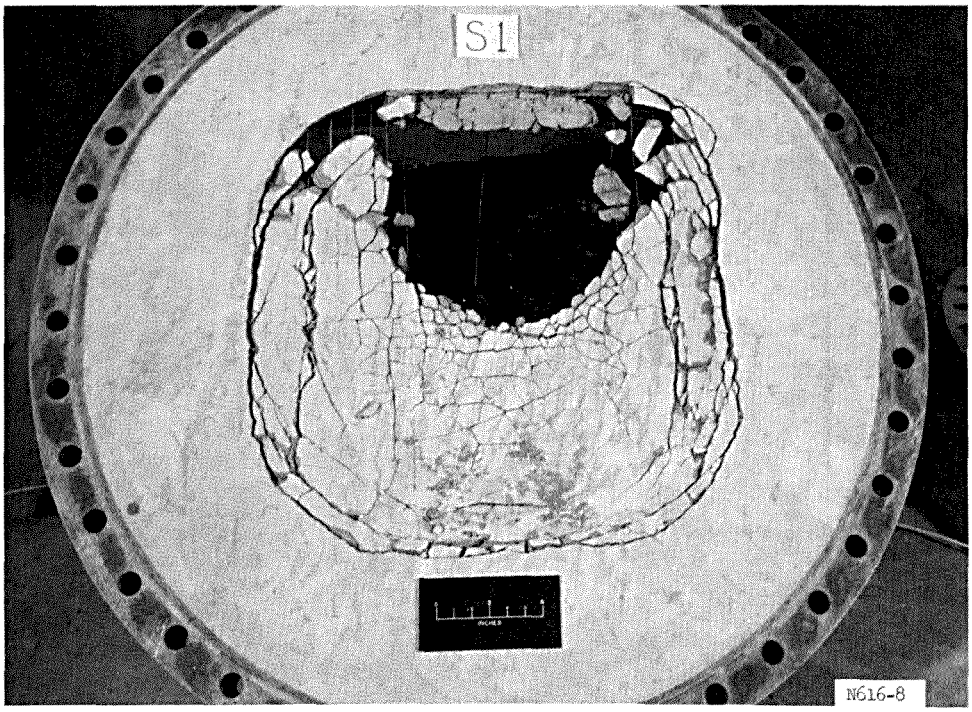

a. Slab IS1, top.

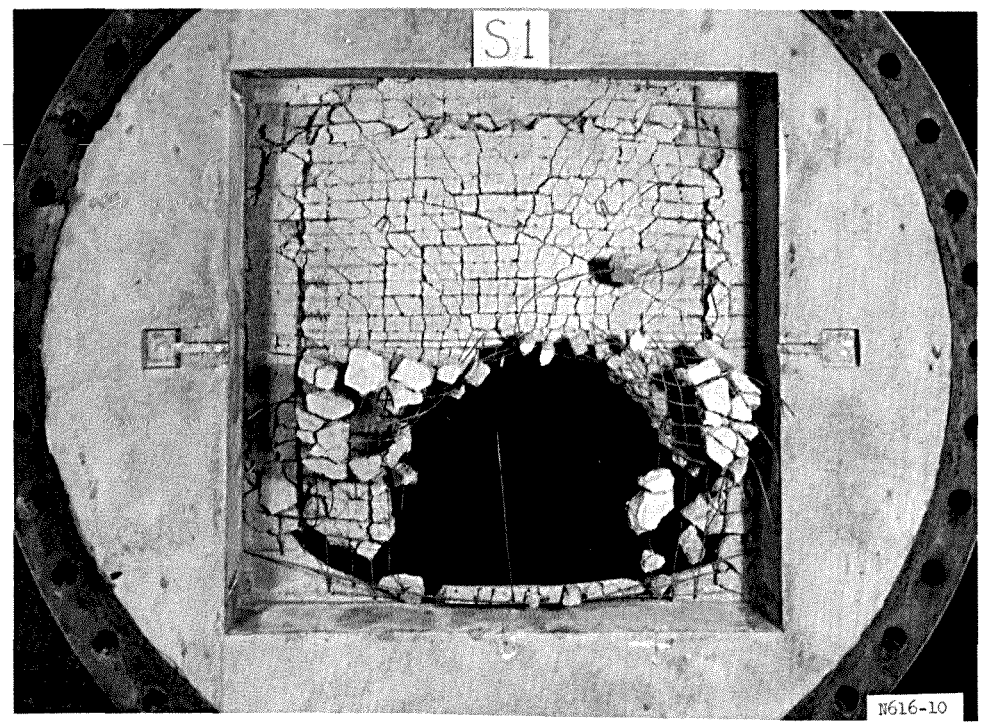

b. Slab IS1, bottom.

Figure 3.1 Conditions of slabs after static tests (sheet 1 of 4).

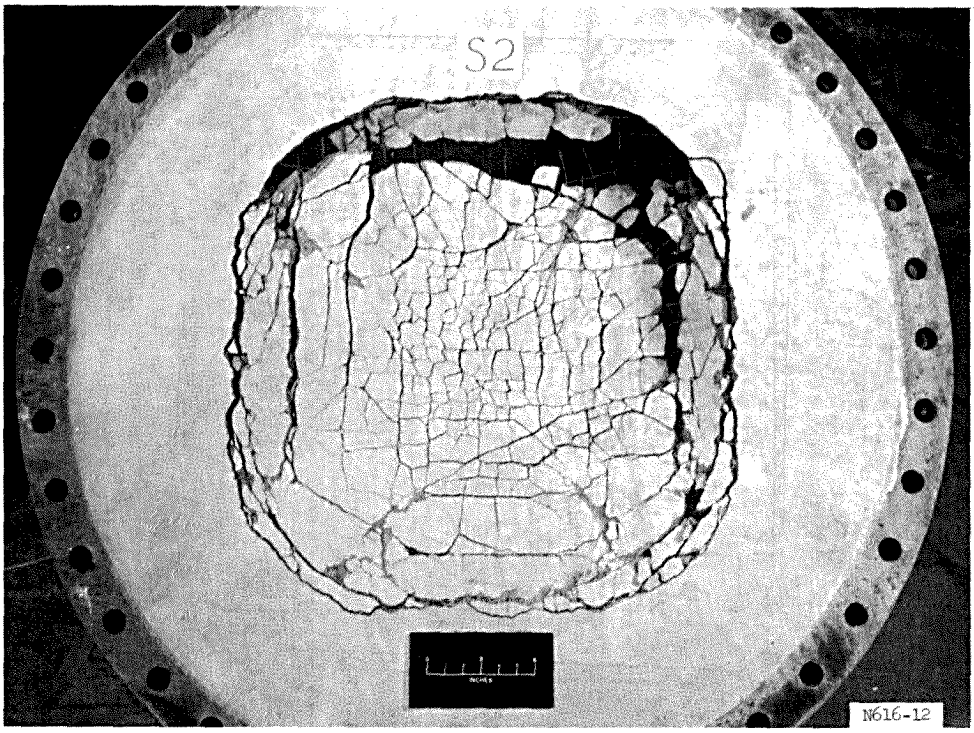

c. Slab IS2, top.

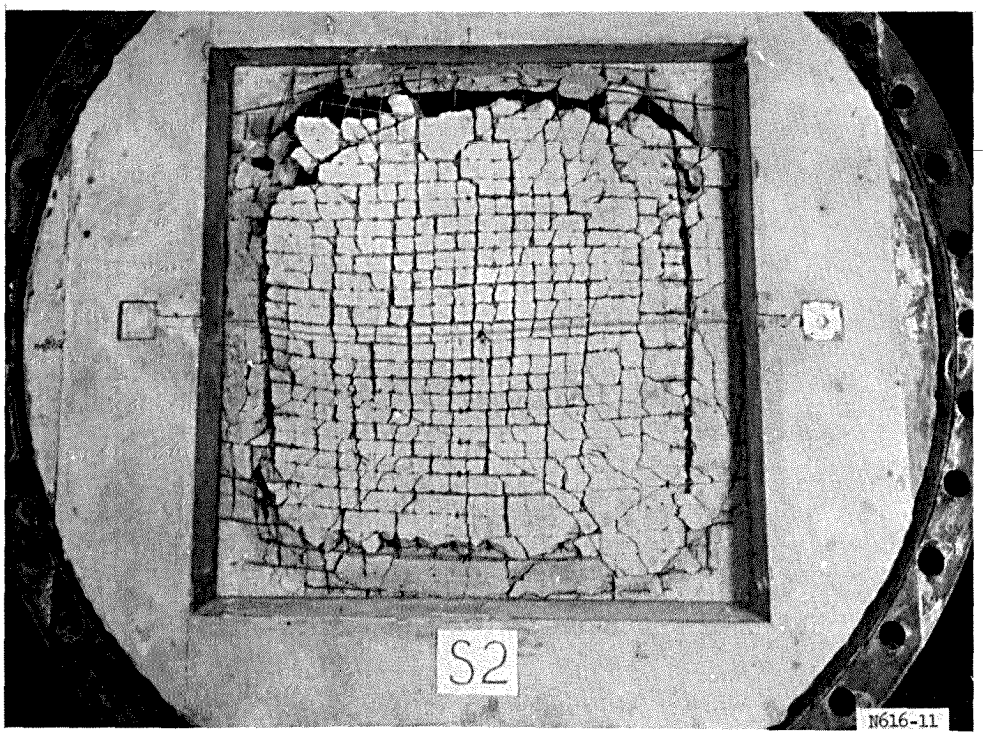

d. Slab IS2, bottom.

Figure 3.1 (sheet 2 of 4).

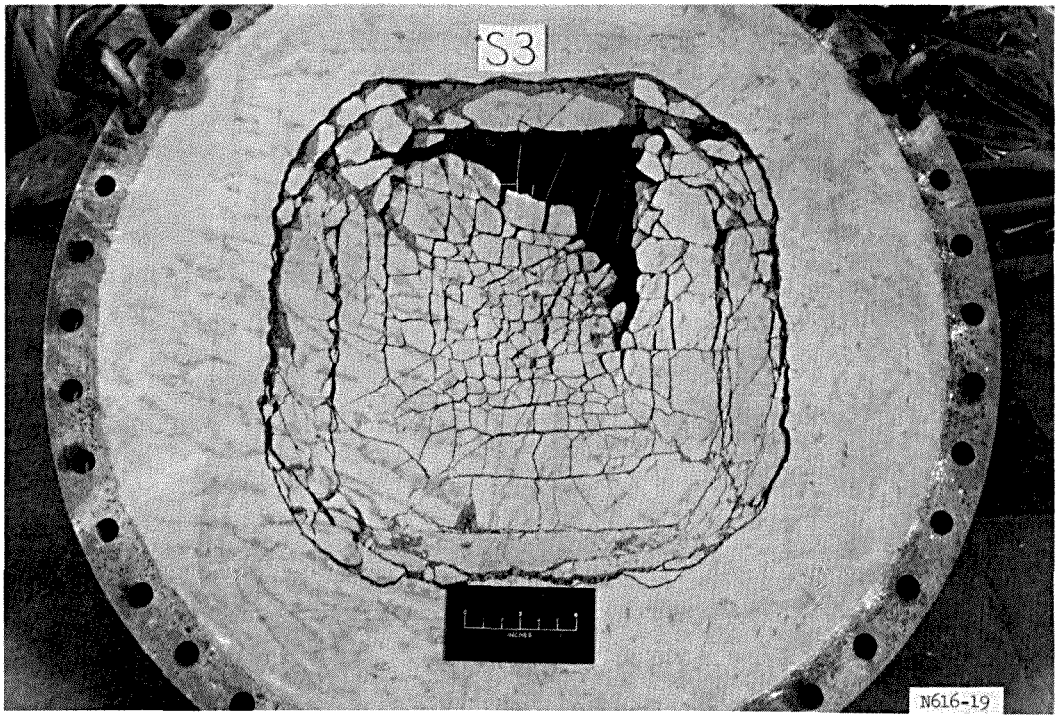

e. Slab IS3, top.

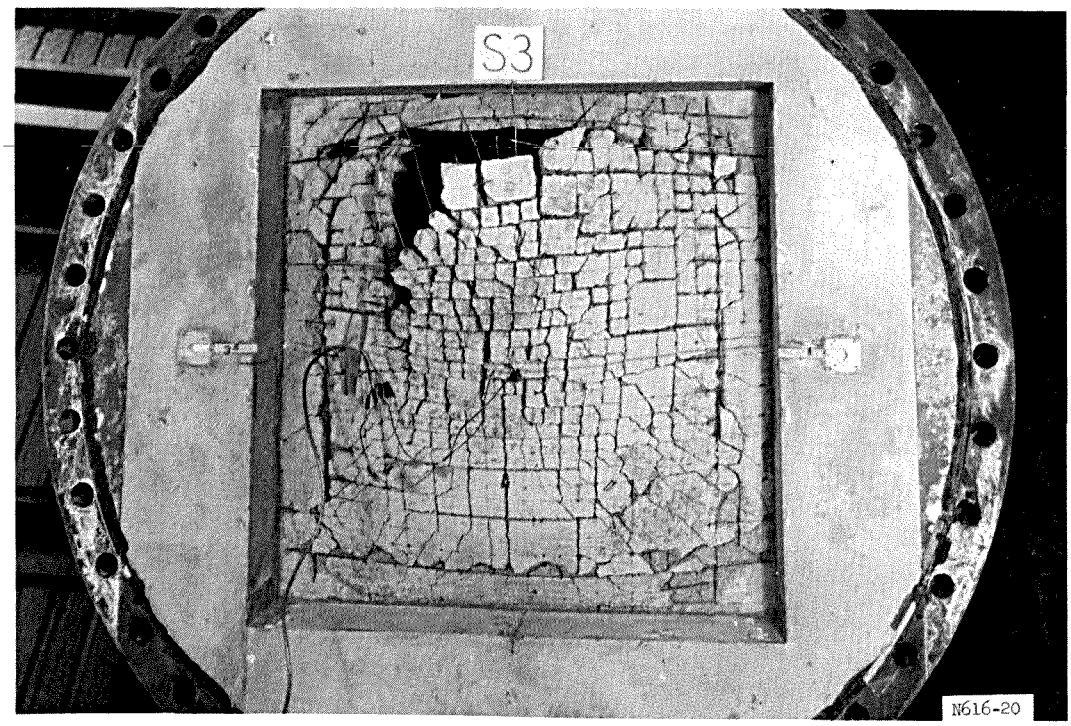

f. Slab IS3, bottom.

Figure 3.1 (sheet 3 of 4).

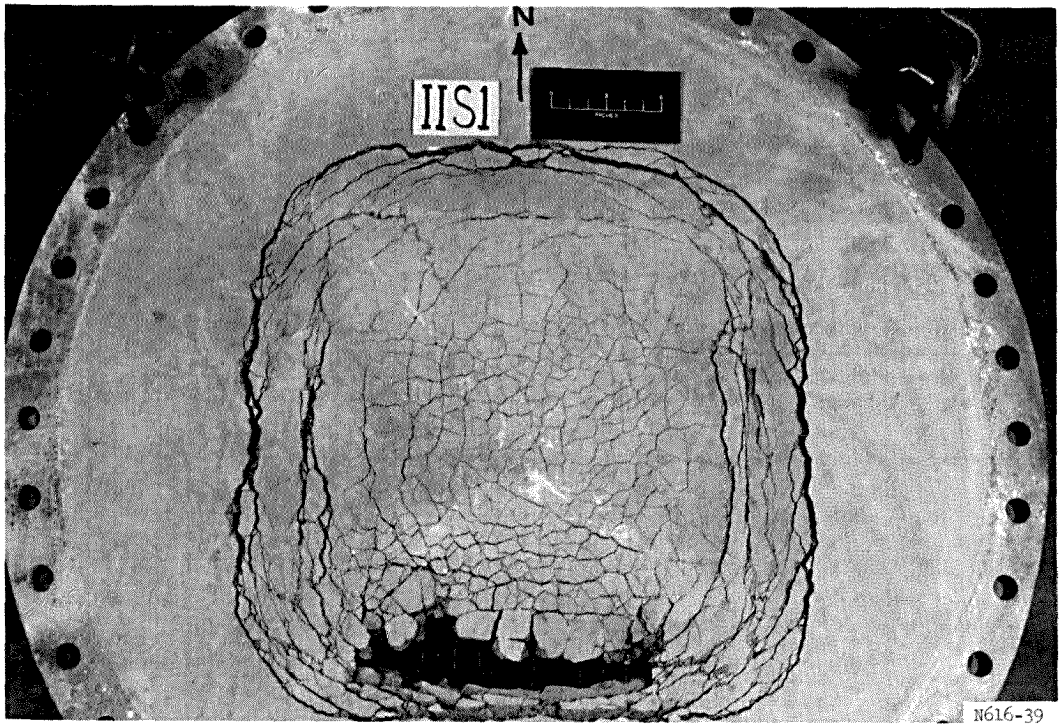

g. Slab IIS1, top.

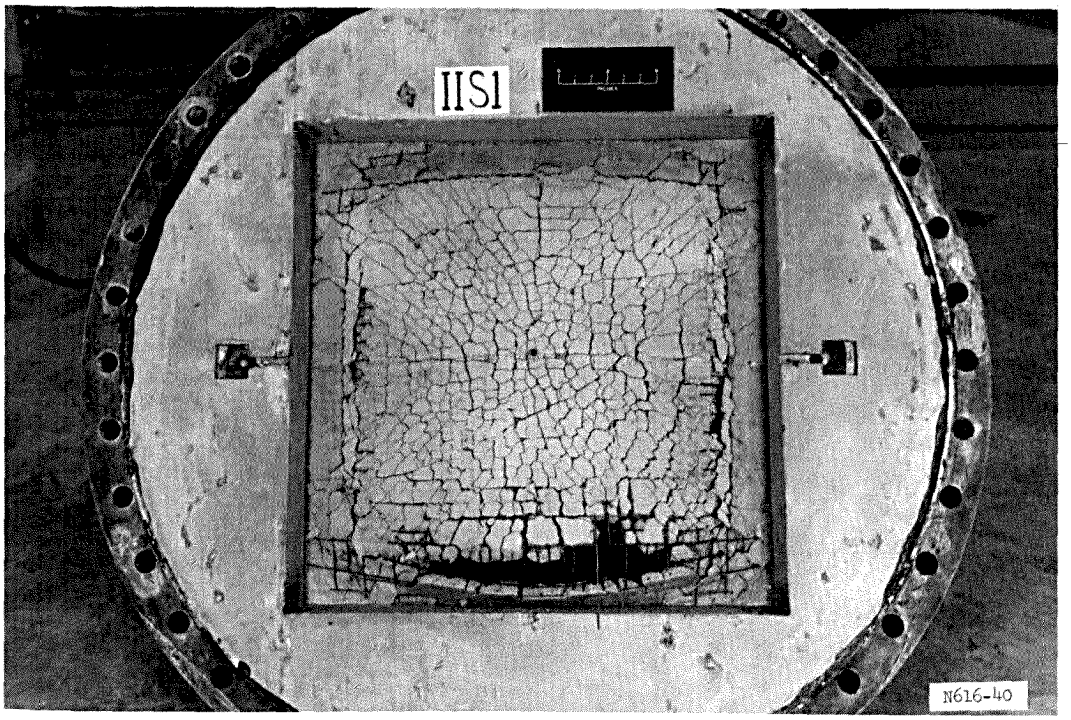

h. Slab IIS1, bottom.

Figure 3.1 (sheet 4 of 4).

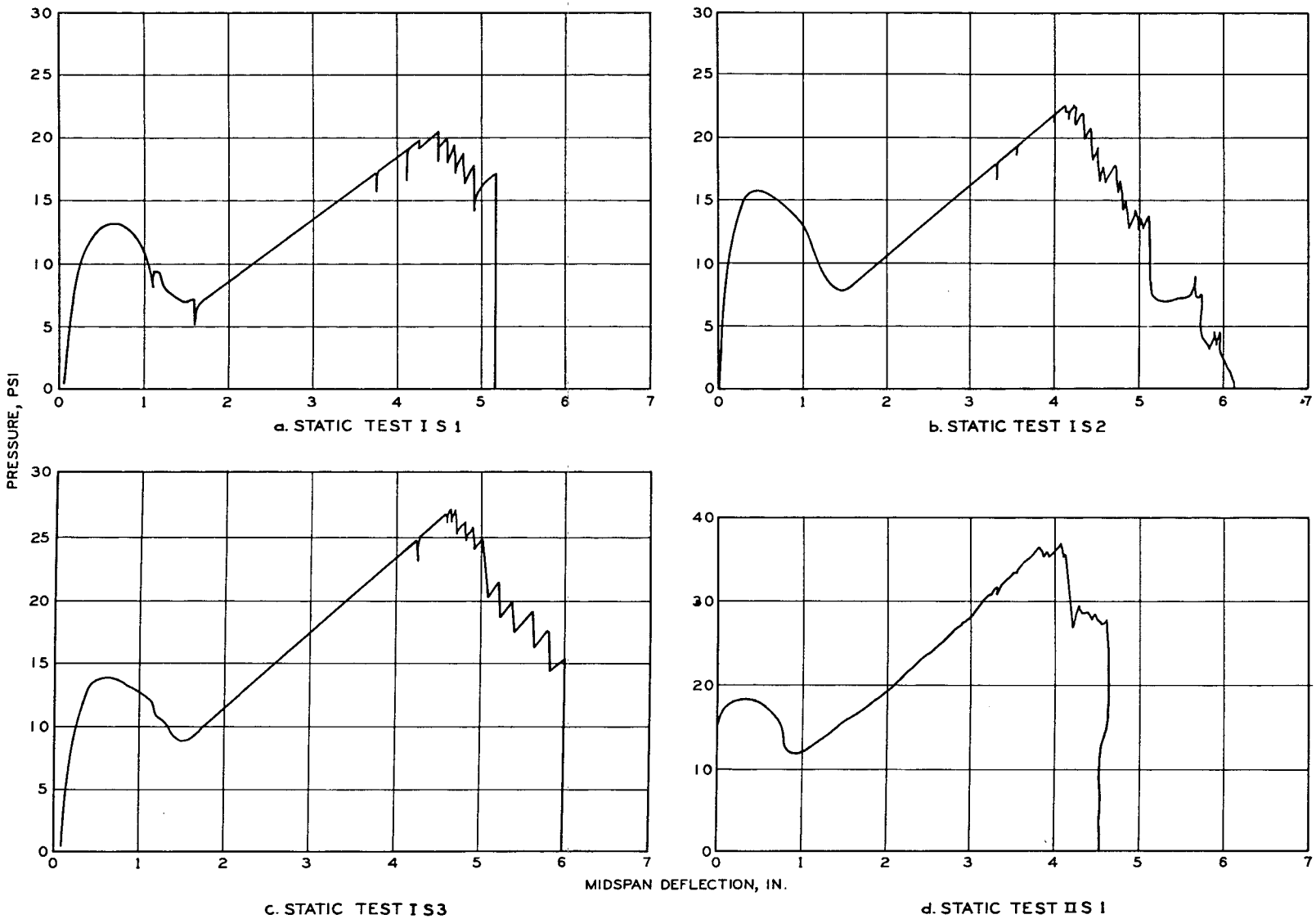

Figure 3.2 Pressure versus midspan deflection, static tests of Slabs IS1, IS2, IS3, and IIS1.

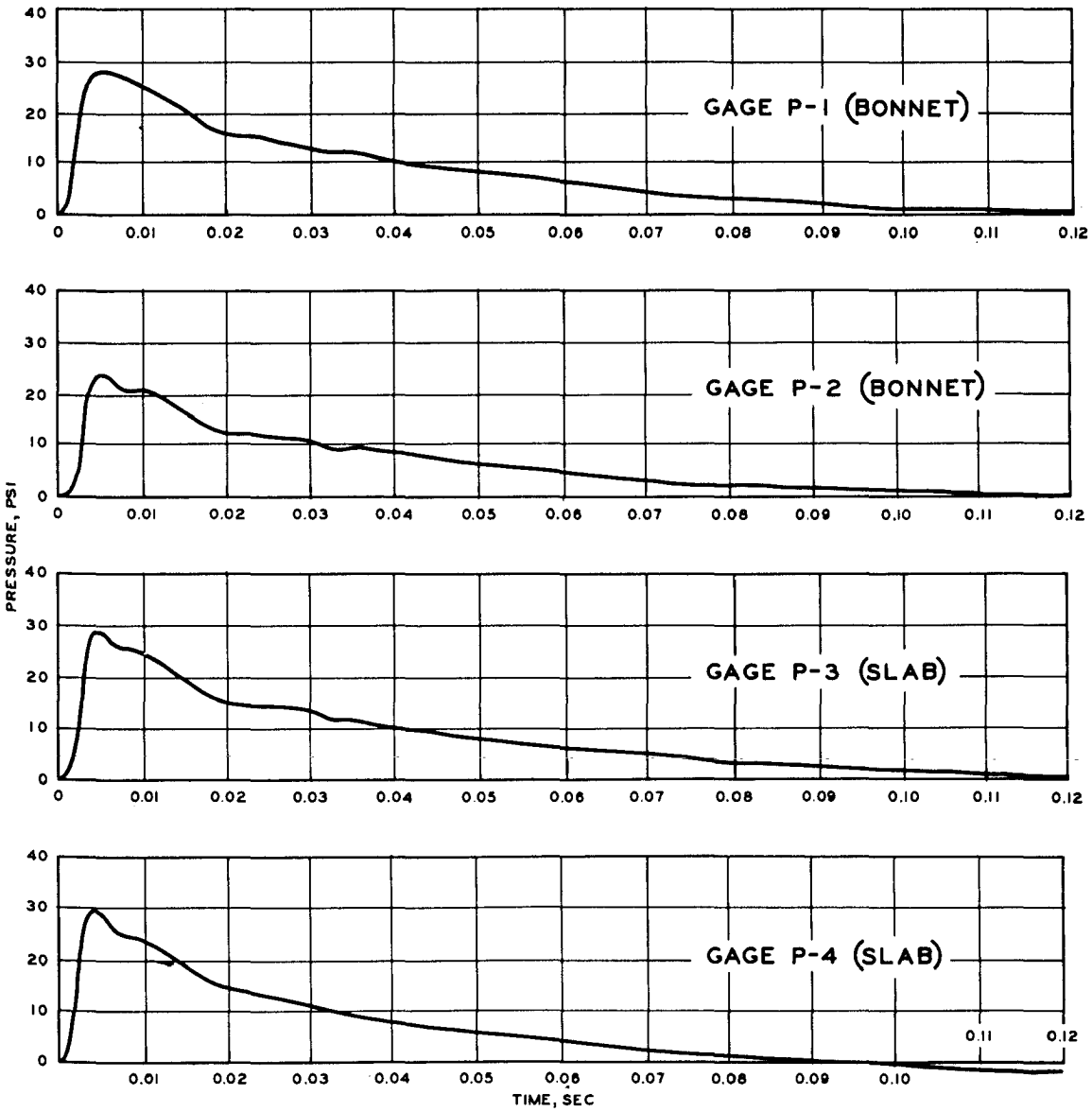

Figure 3.3 Overpressure-time records for Slab D2.

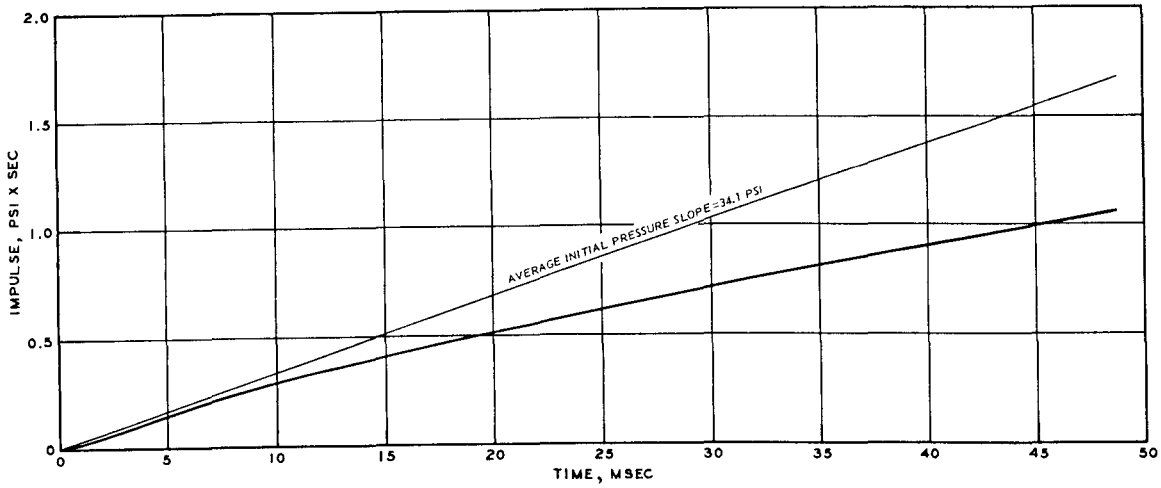

Figure 3.4 Impulse-time curve for Slab ID1B, Gage P1.

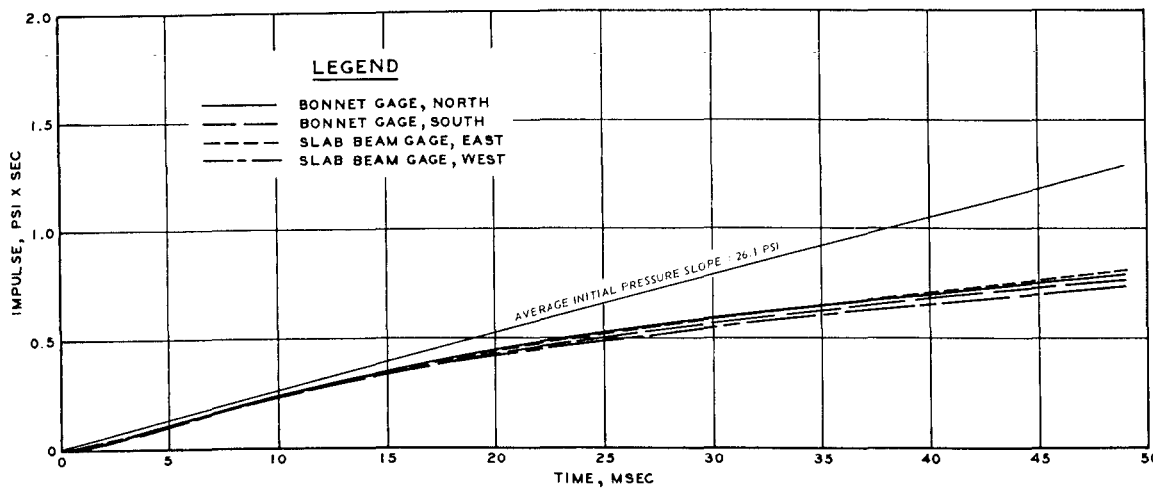

Figure 3.5 Impulse-time curves for Slab ID2.

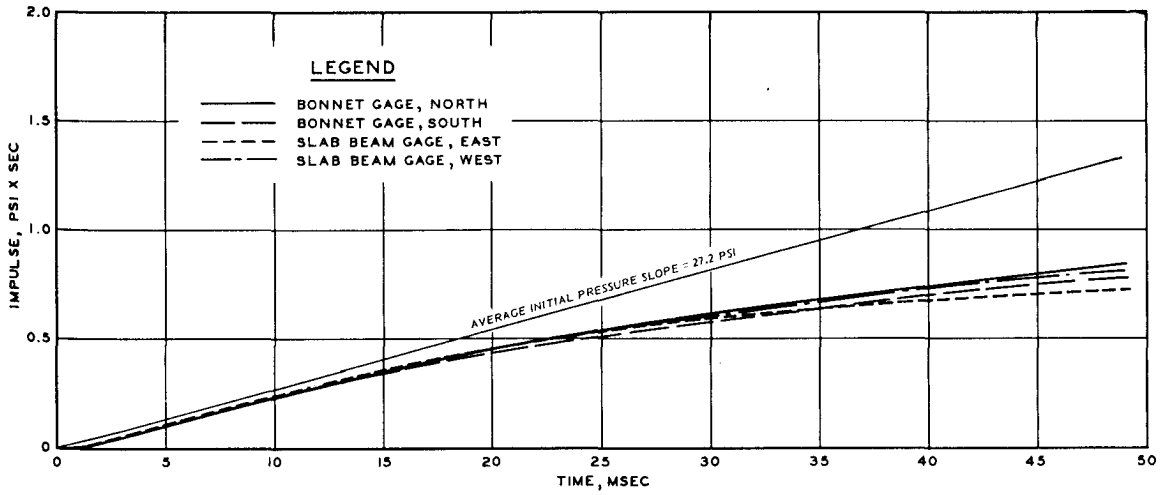

Figure 3.6 Impulse-time curves for Slab ID3.

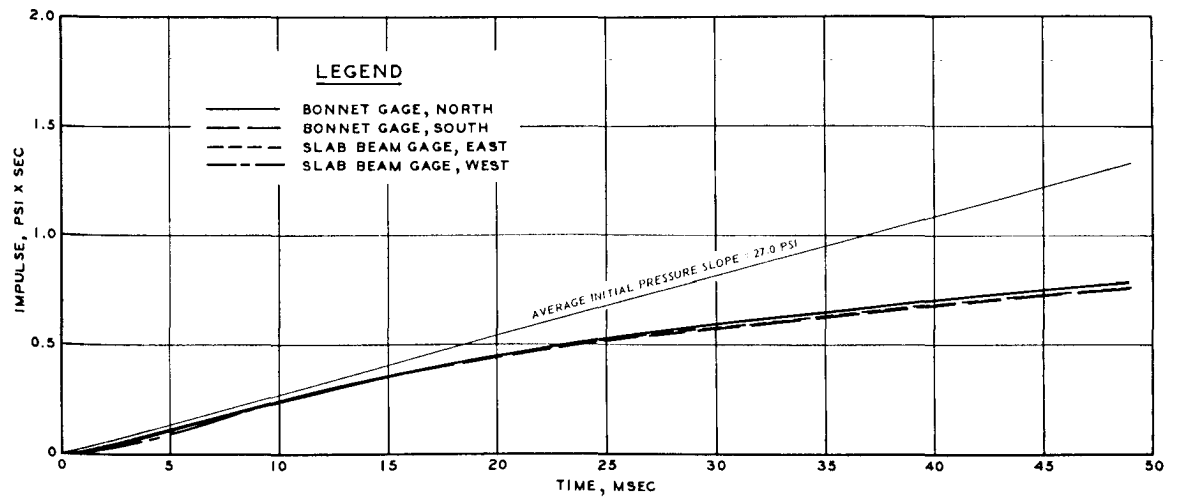

Figure 3.7 Impulse-time surves for Slab ID4.

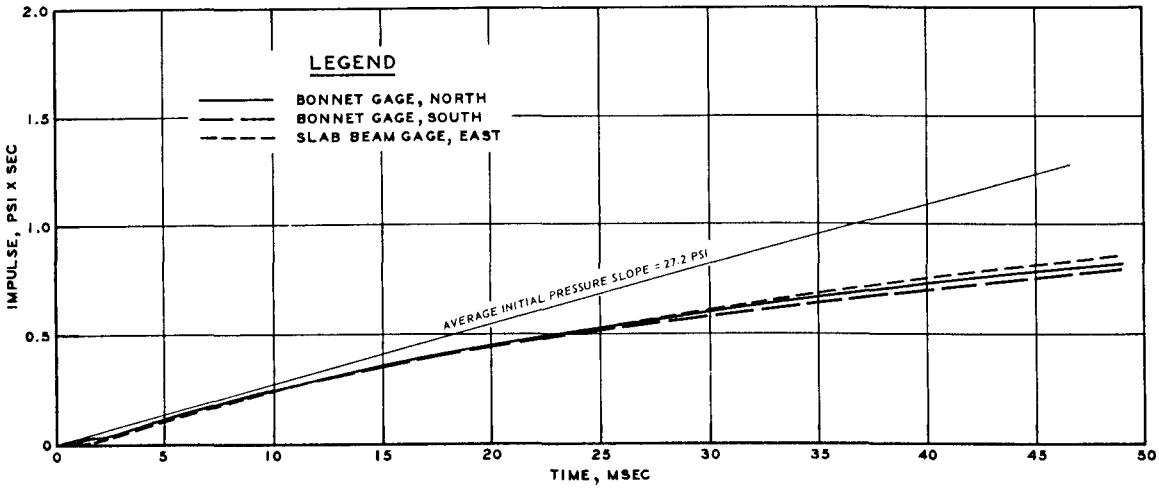

Figure 3.8 Impulse-time curves for Slab ID5.

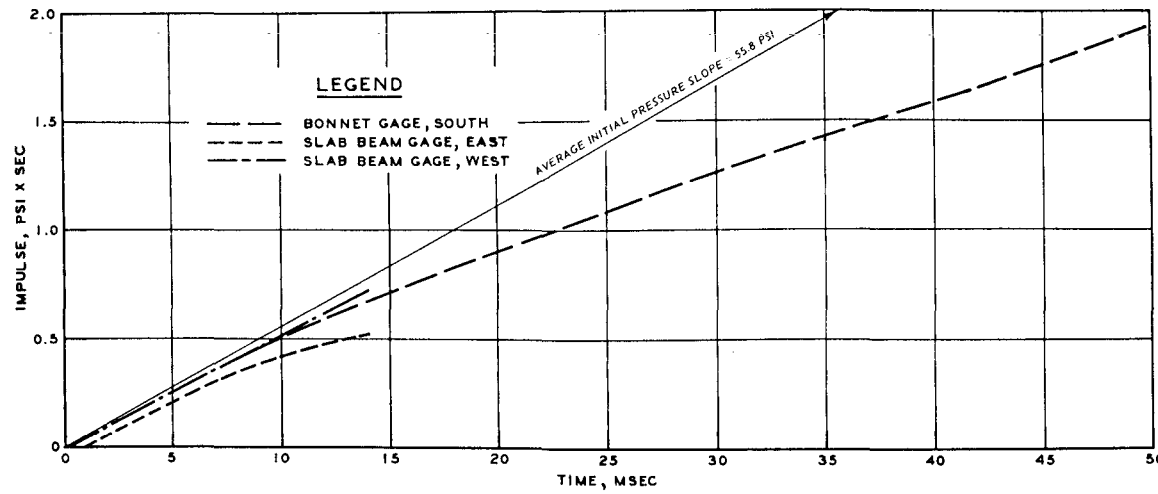

Figure 3.9 Impulse-time curves for Slab IID1.

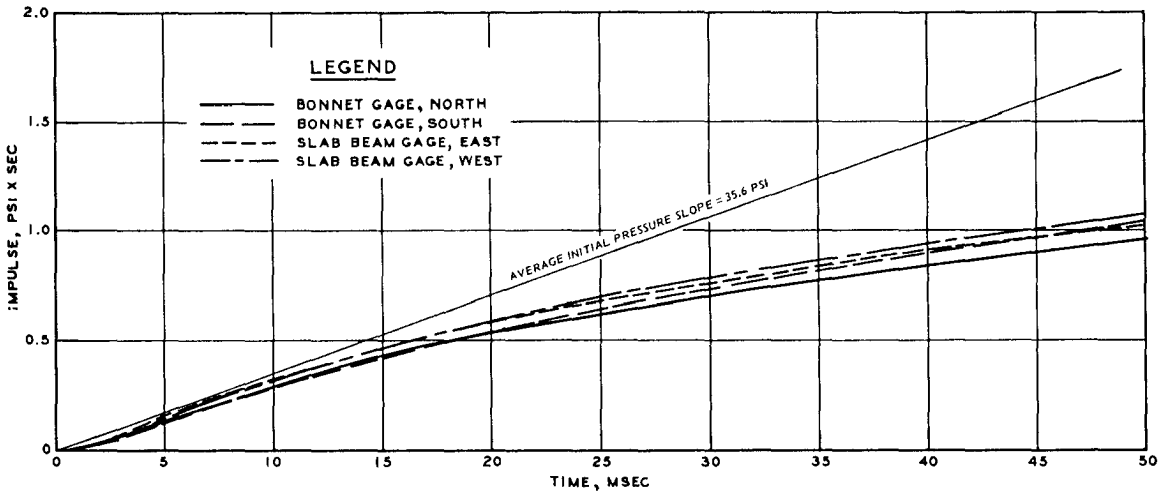

Figure 3.10 Impulse-time curves for Slab IID2.

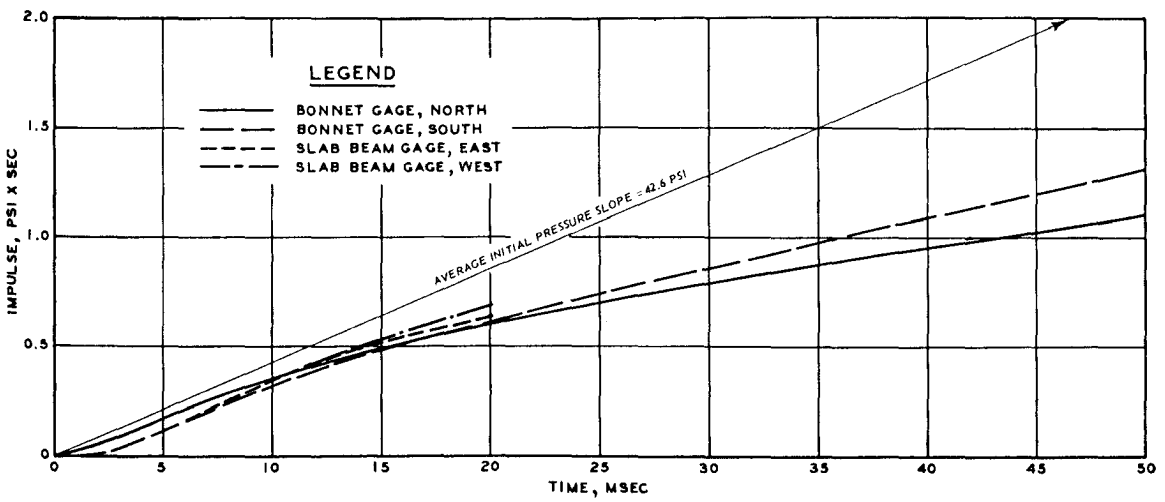

Figure 3.11 Impulse-time curves for Slab IID3.

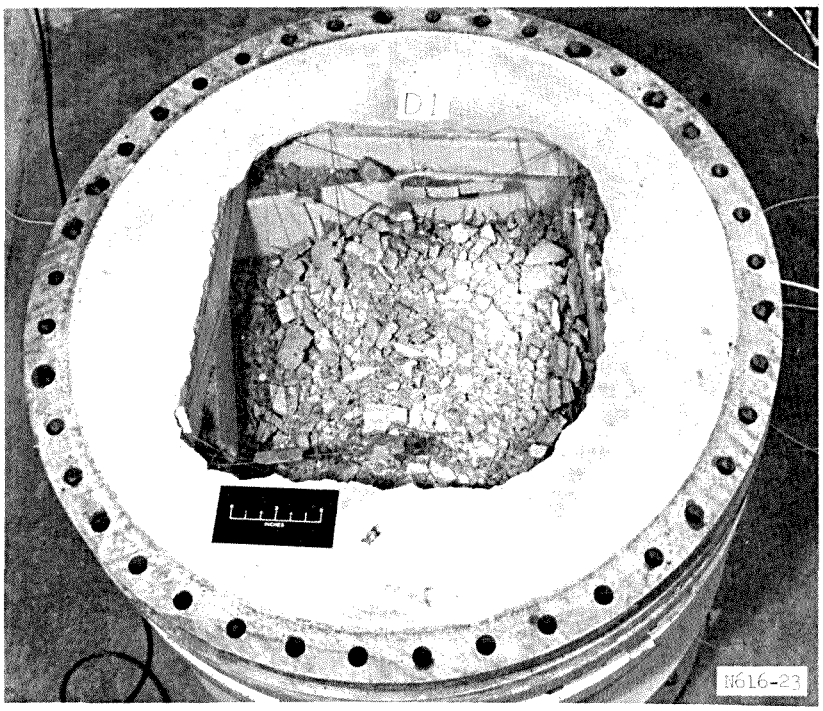

a. Slab ID1, top.

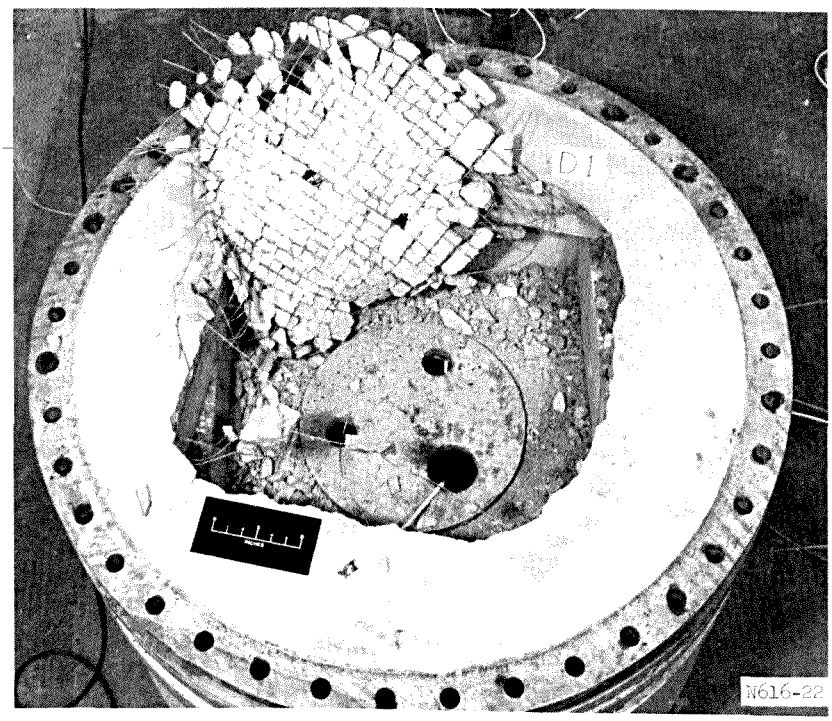

b. Slab ID1, bottom.

Figure 3.12 Conditions of slabs after dynamic tests (sheet 1 of 11).

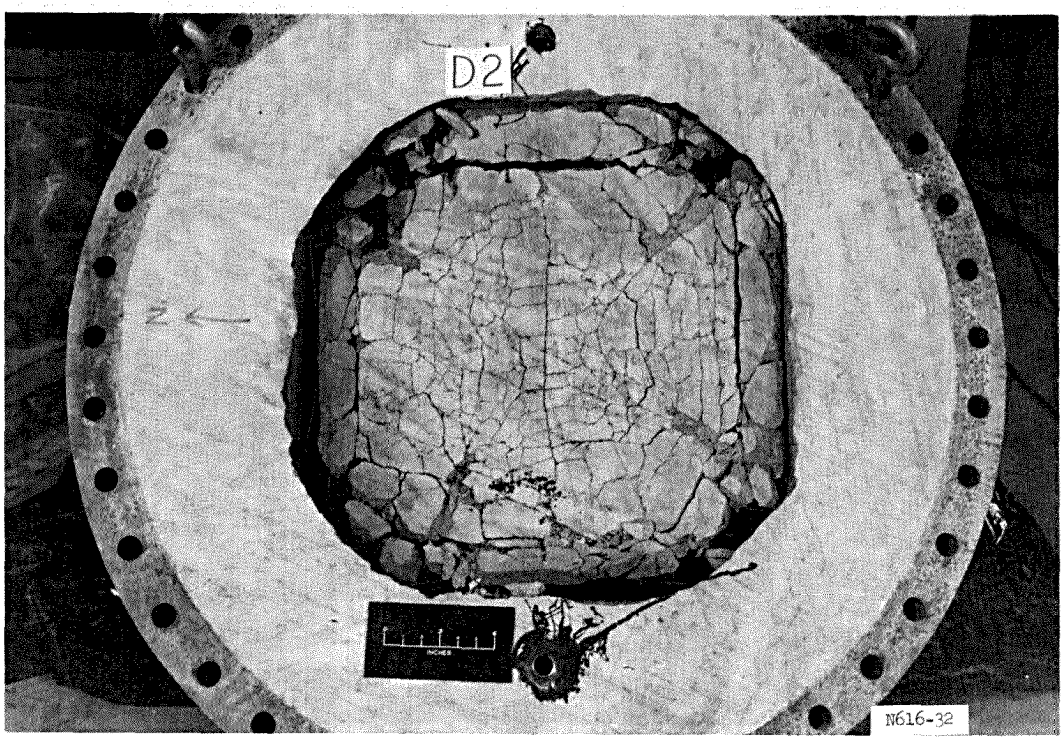

c. Slab ID2, top.

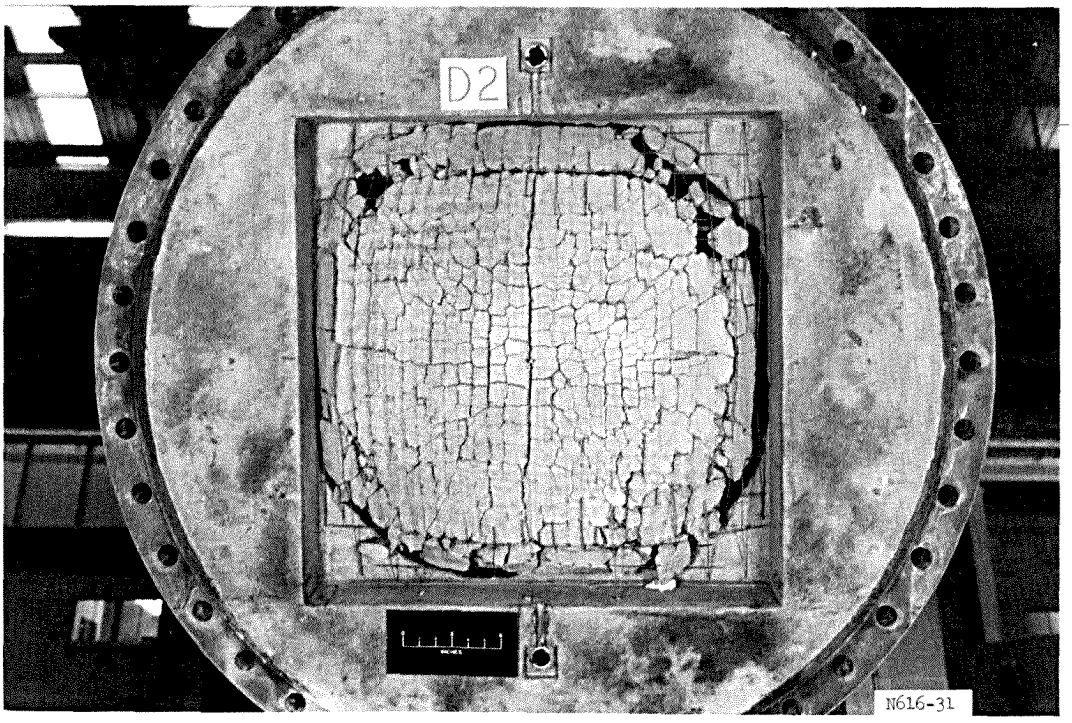

d. Slab ID2, bottom.

Figure 3.12 (sheet 2 of 11).

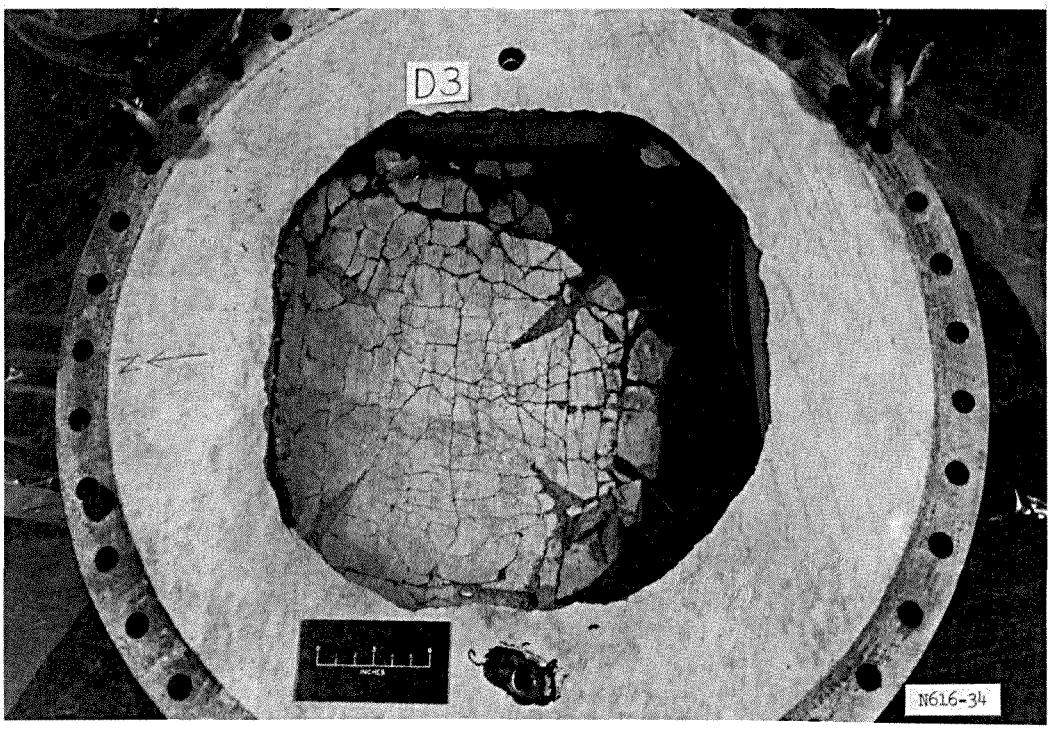

e. Slab ID3, top.

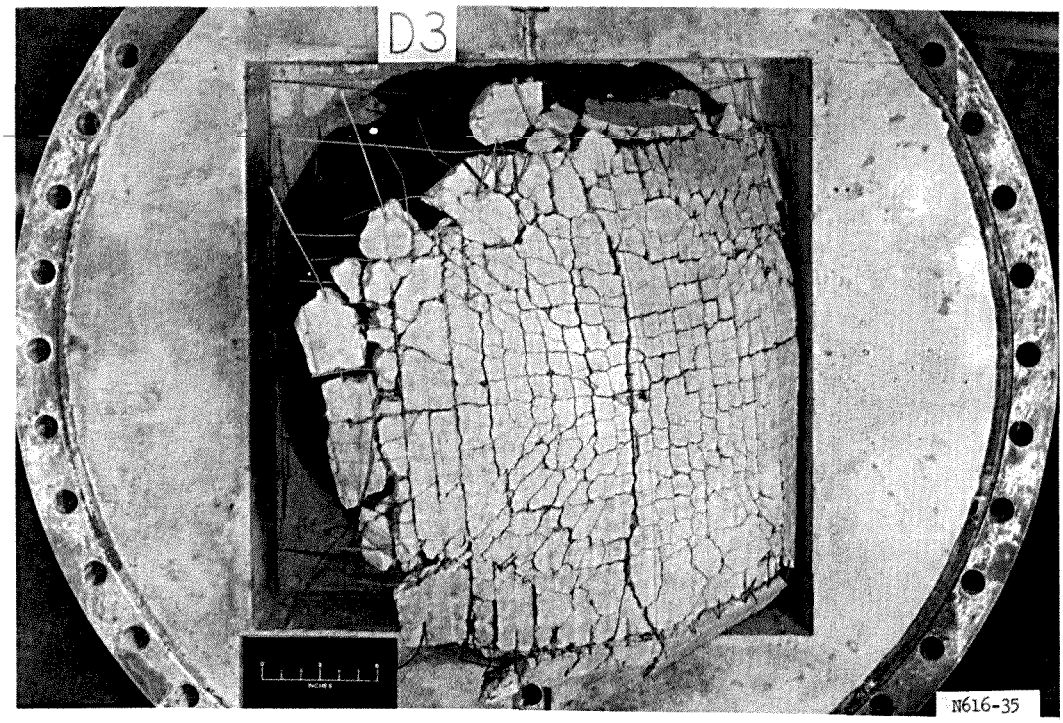

f. Slab ID3, bottom

Figure 3.12 (sheet 3 of 11).

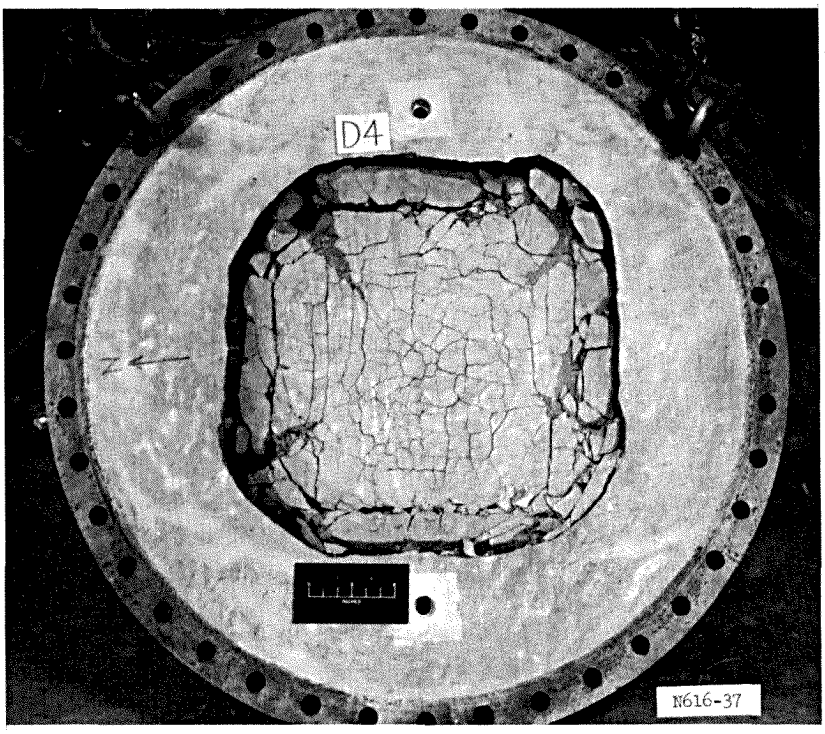

g. Slab ID4, top.

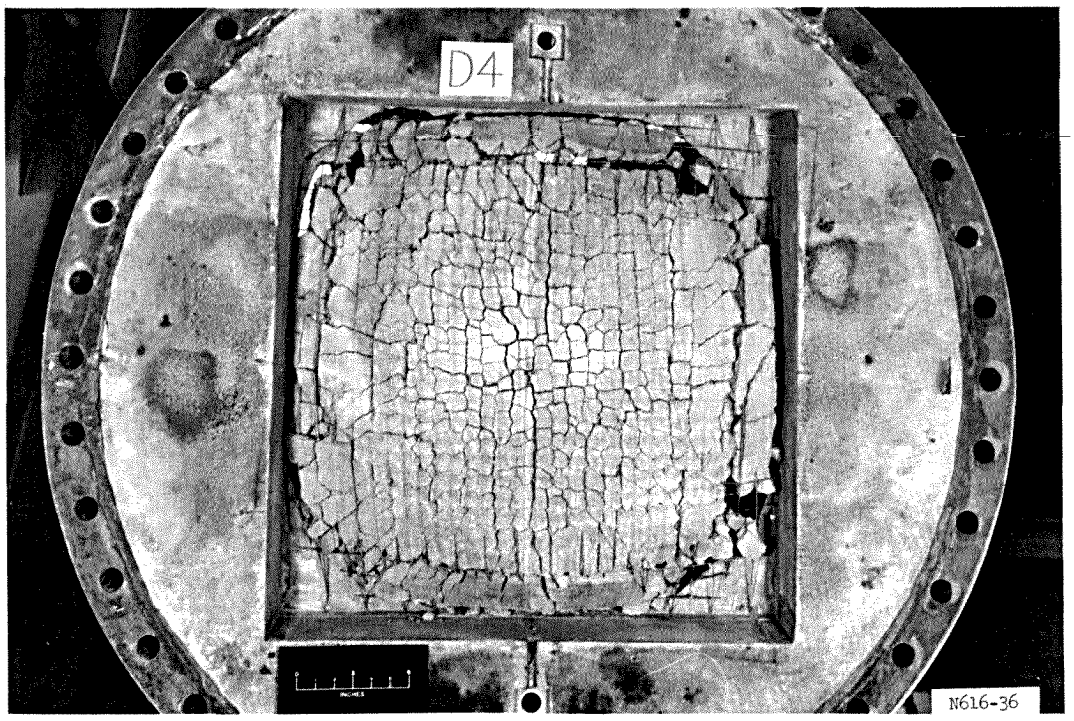

h. Slab ID4, bottom.

Figure 3.12 (sheet 4 of 11).

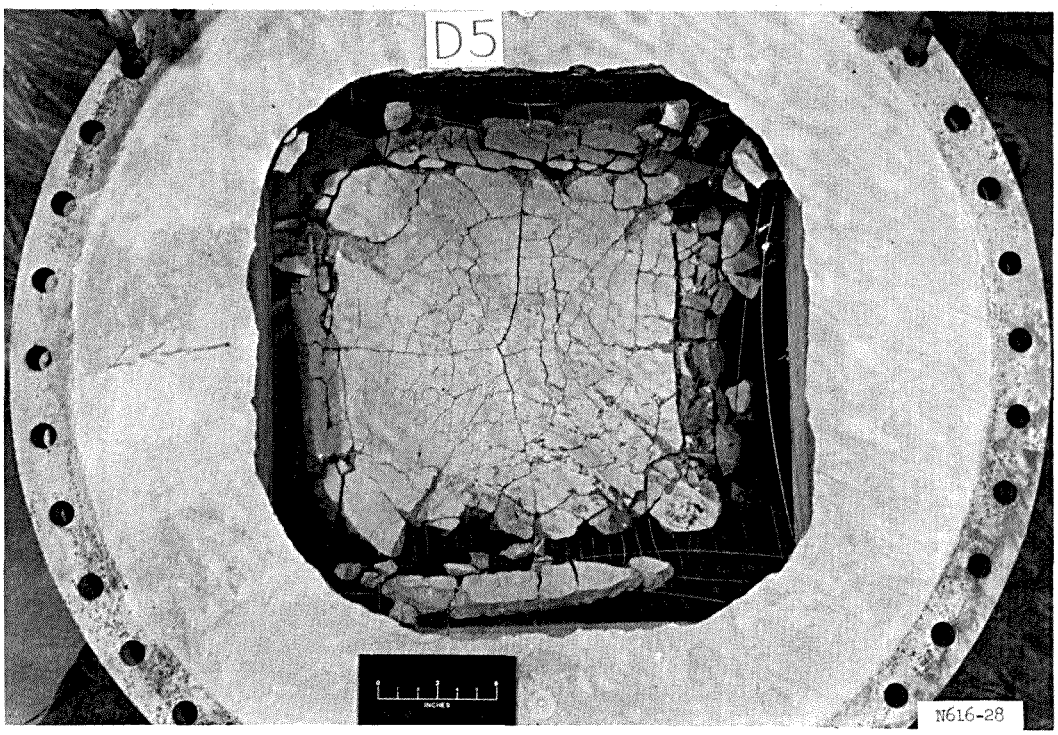

i. Slab ID5, top.

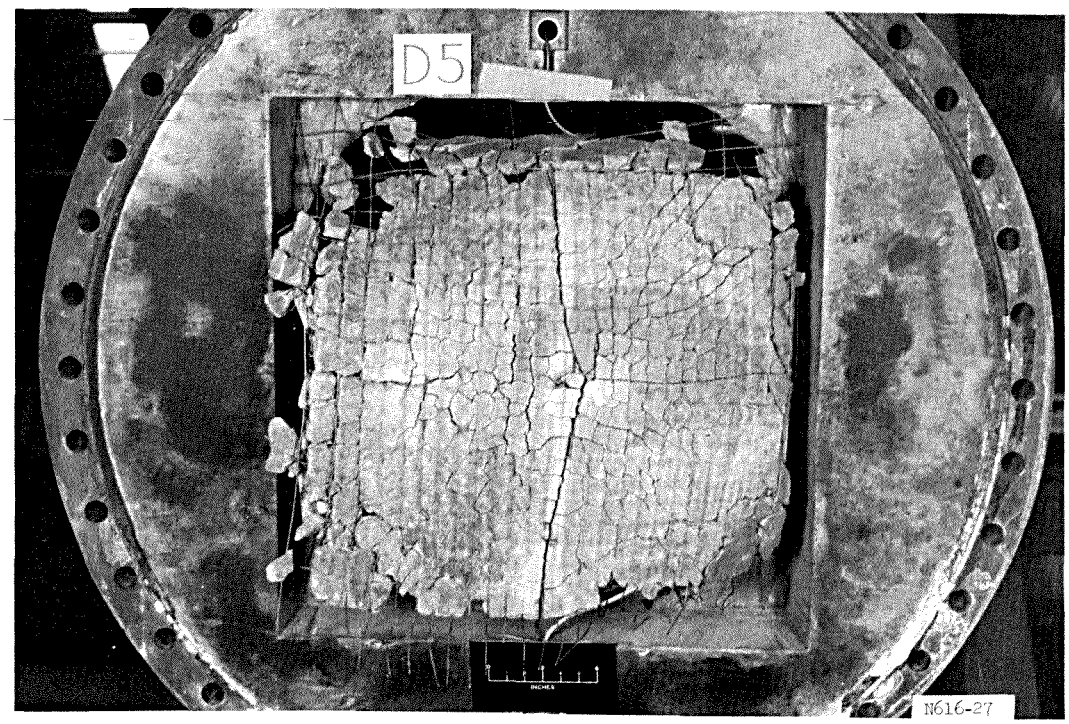

j. Slab ID5, bottom.

Figure 3.12 (sheet 5 of 11).

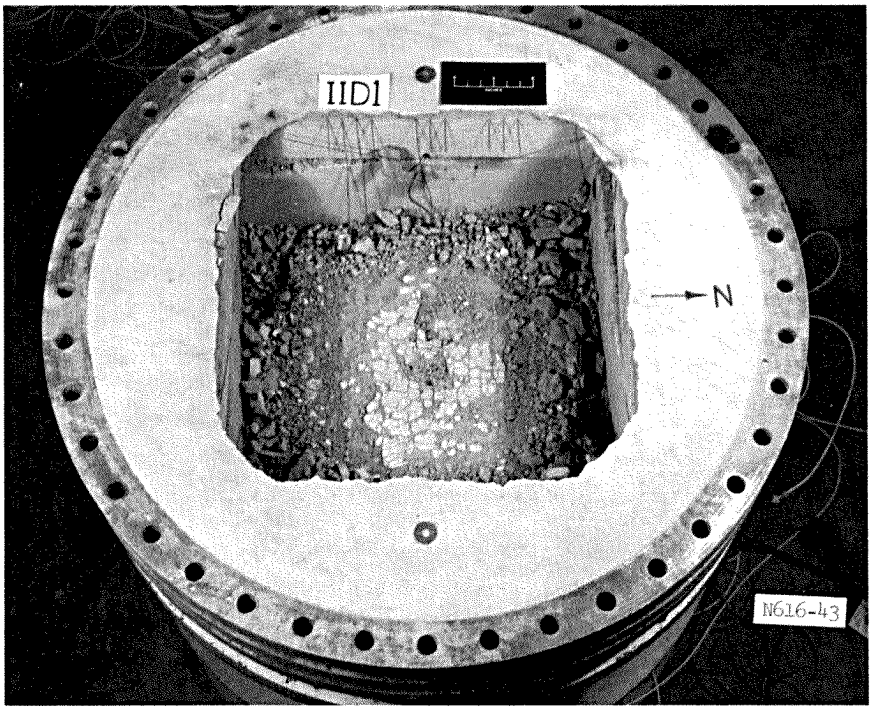

k. Slab IID1, top.

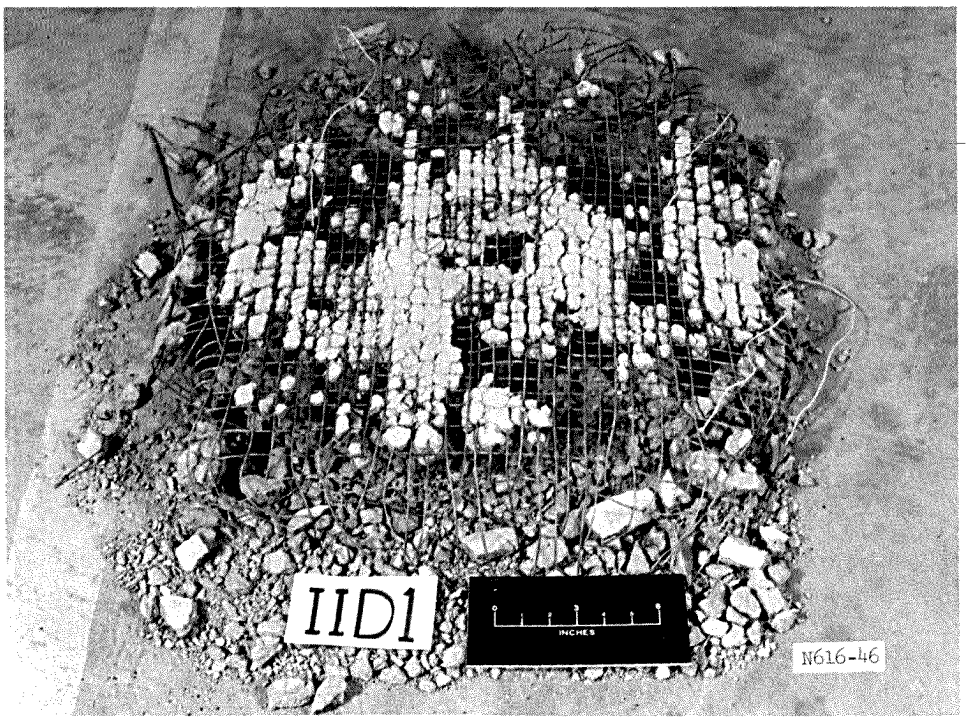

l. Slab IID1, bottom.

Figure 3.12 (sheet 6 of 11).

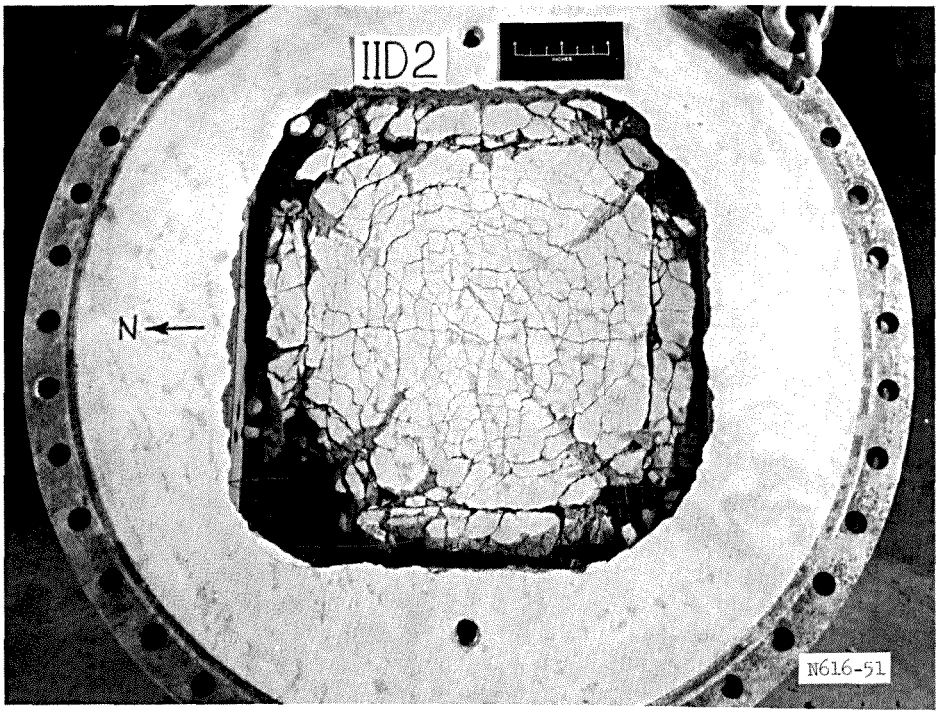

m. Slab IID2, top.

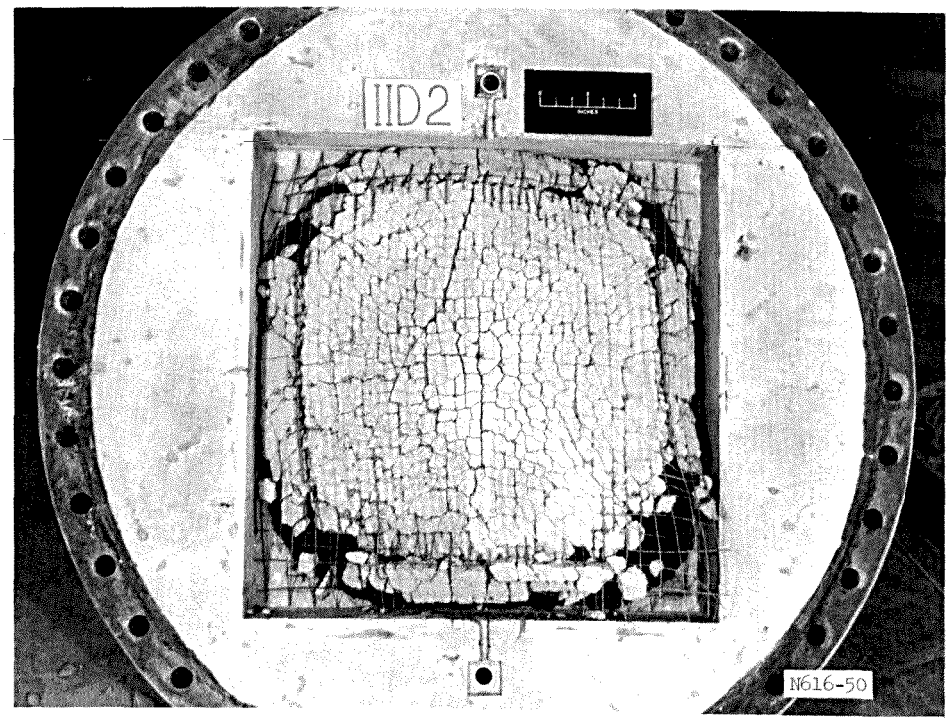

n. Slab IID2, bottom.

Figure 3.12 (sheet 7 of 11).

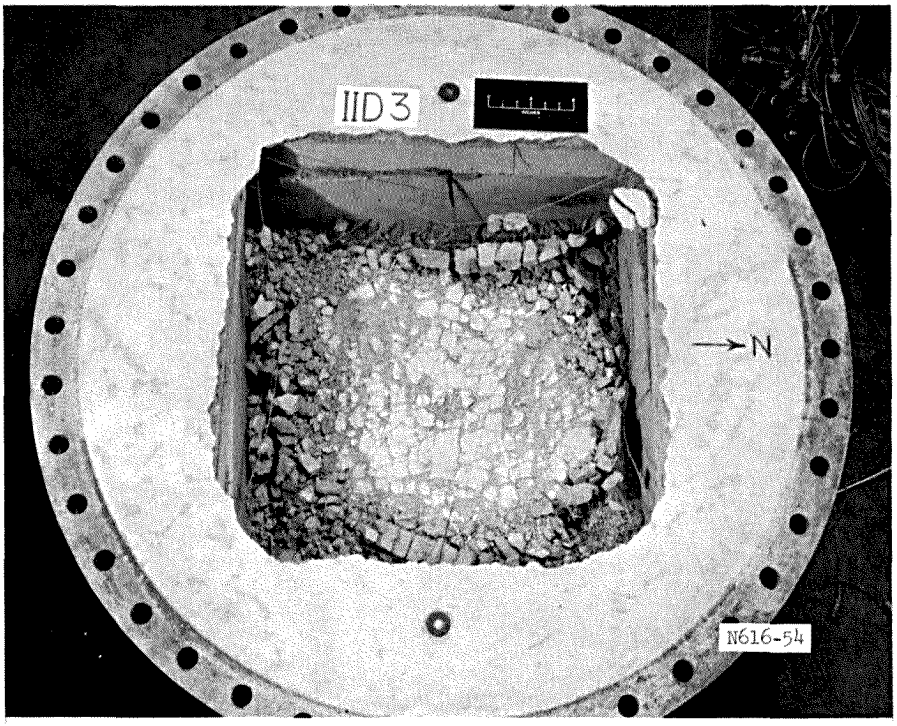

o. Slab IID3, top.

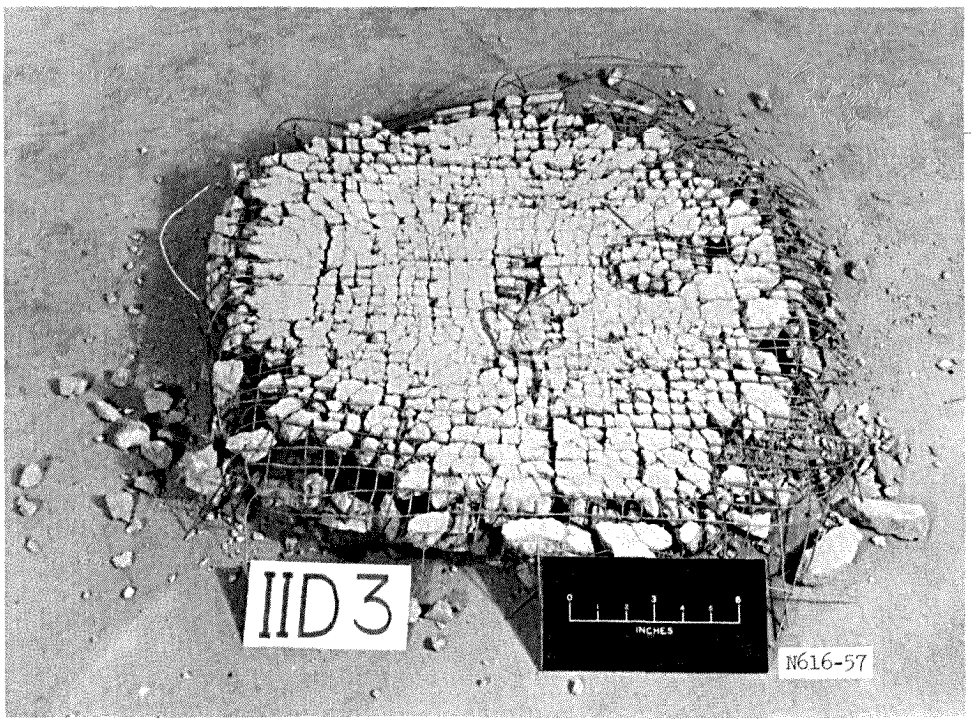

p. Slab IID3, bottom.

Figure 3.12 (sheet 8 of 11).

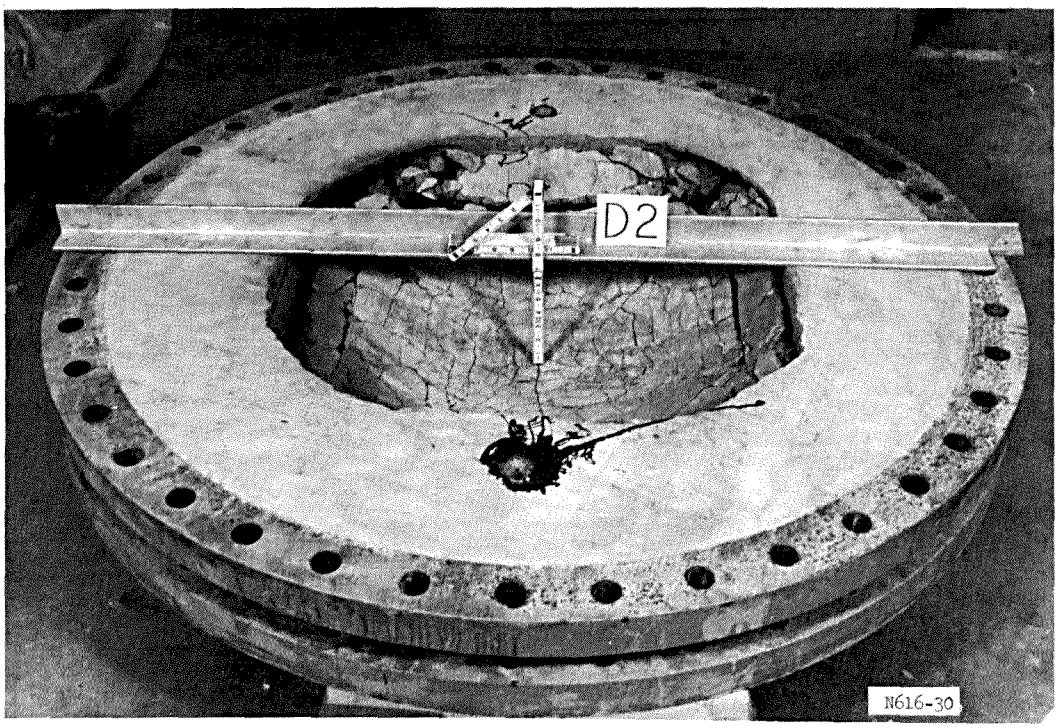

q. Slab ID2, maximum deflection.

r. Slab ID2, closeup of concrete cracking.

Figure 3.12 (sheet 9 of 11).

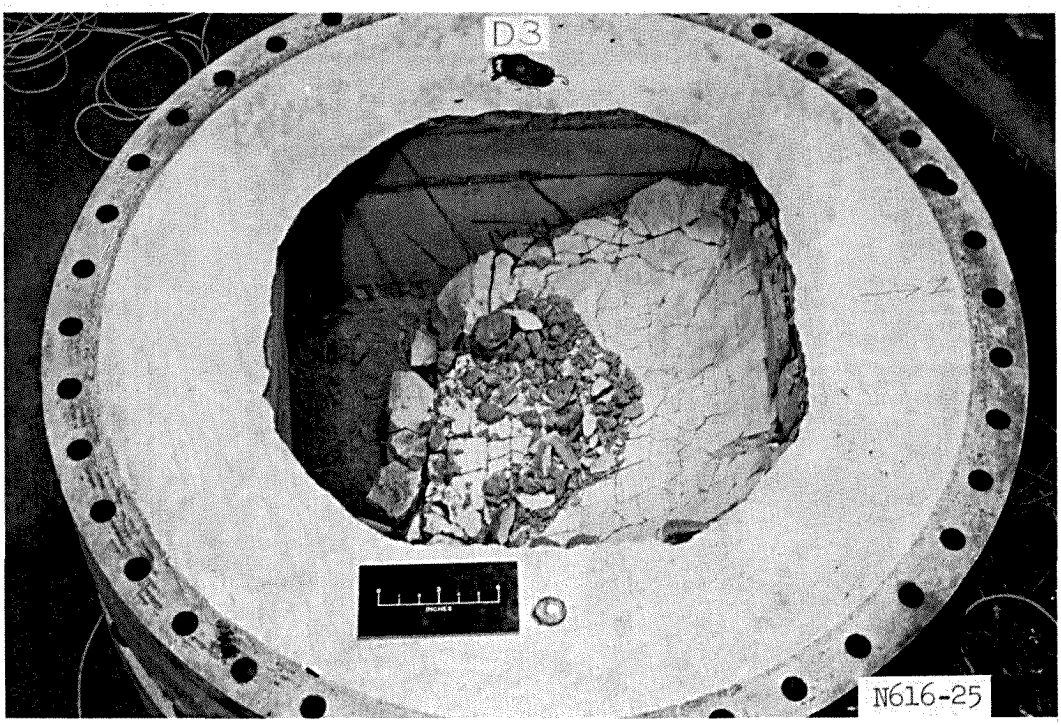

s. Slab ID3, maximum deflection.

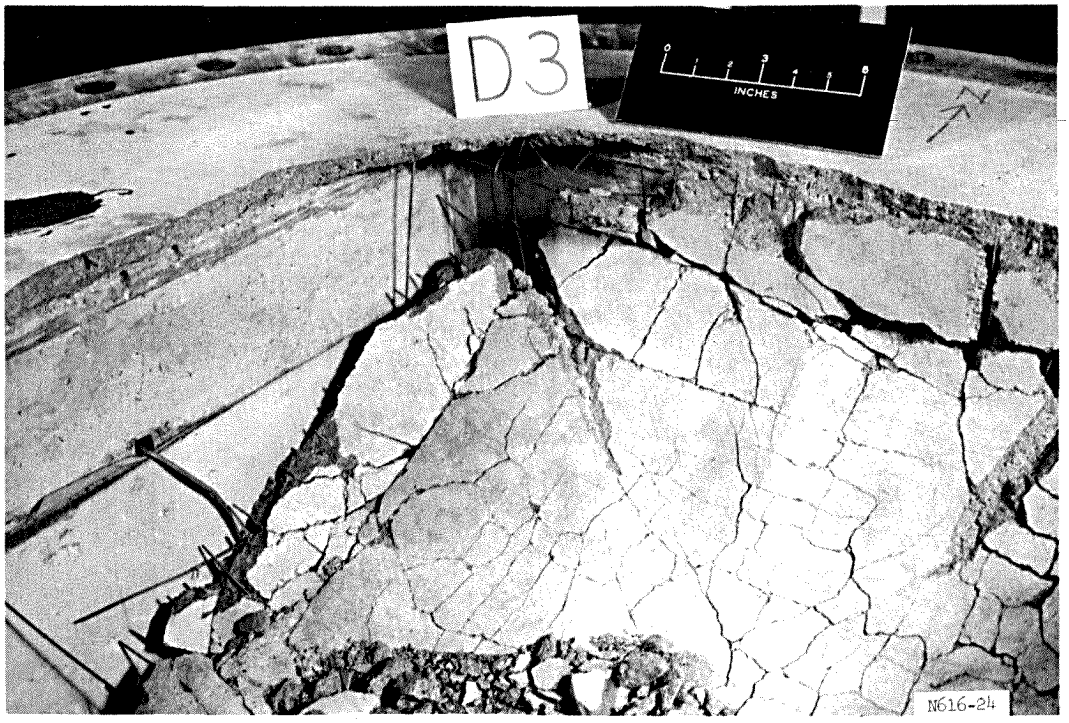

t. Slab ID3, steel rupture.

Figure 3.12 (sheet 10 of 11).

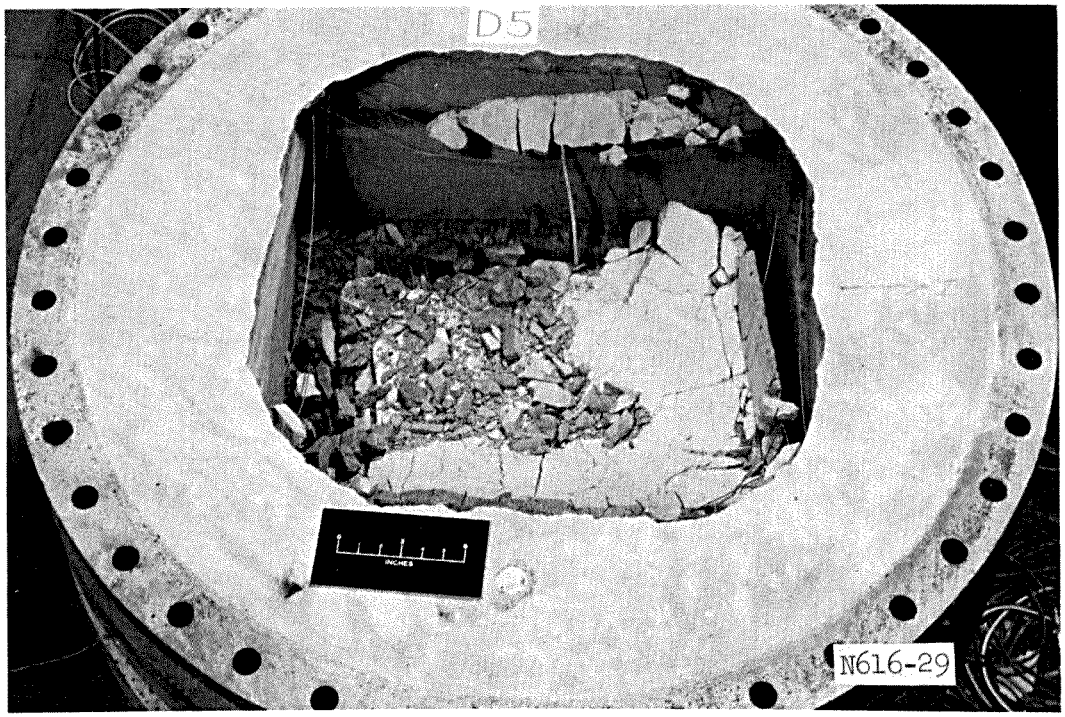

u. Slab ID5, maximum deflection

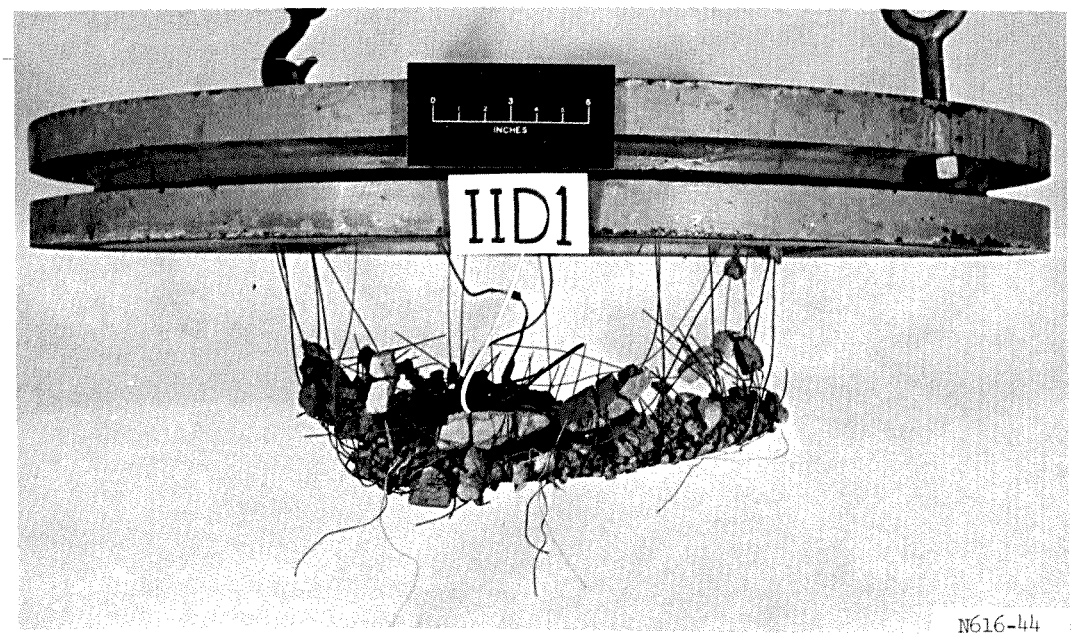

v. Slab IID1, maximum deflection.

Figure 3.12 (sheet 11 of 11).

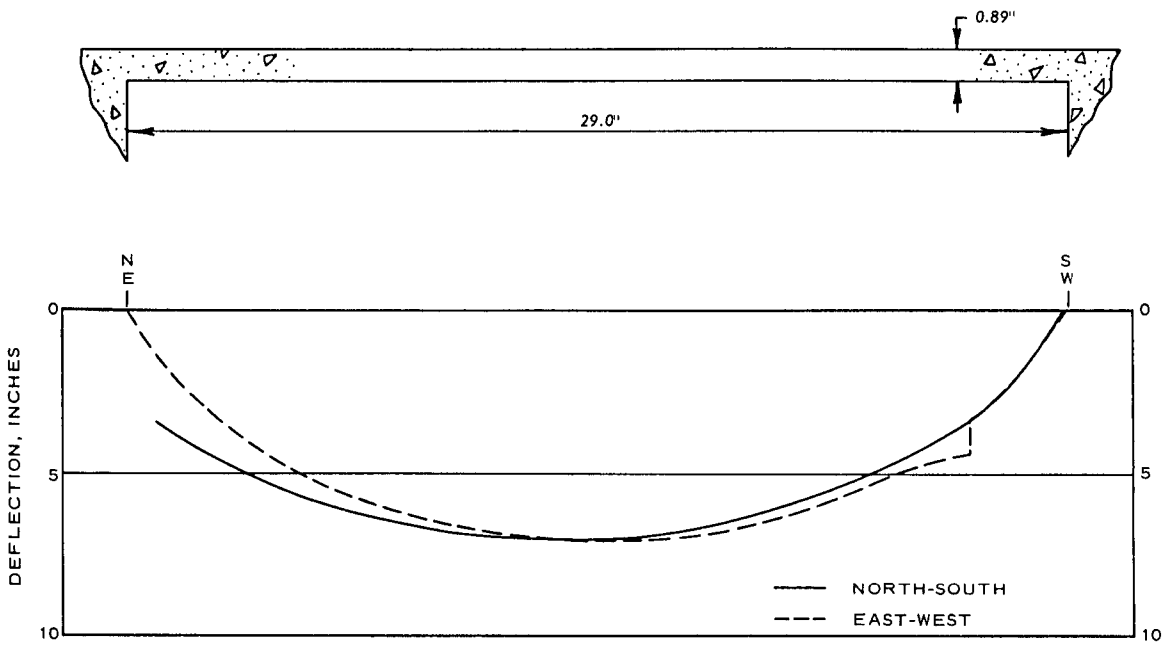

Figure 3.13 Permanent dynamic deflection profile, Slab ID4.

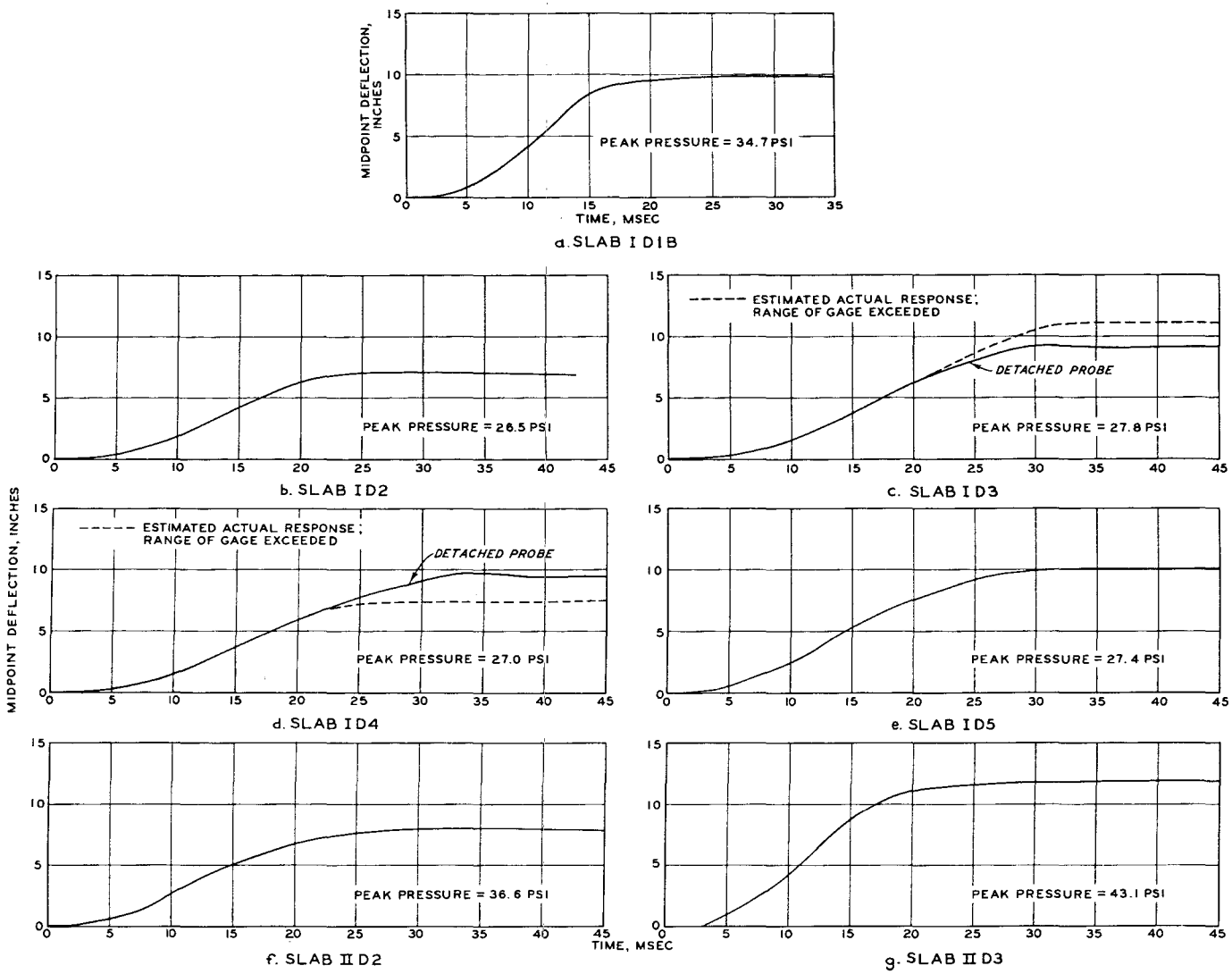

Figure 3.14 Dynamic deflection-time histories.

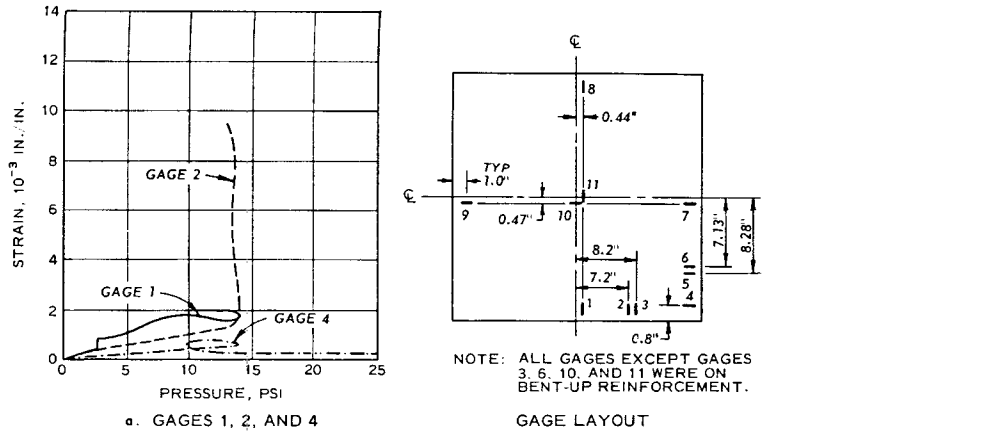

Figure 3.15 Steel strain-pressure curves, Slab IS3.

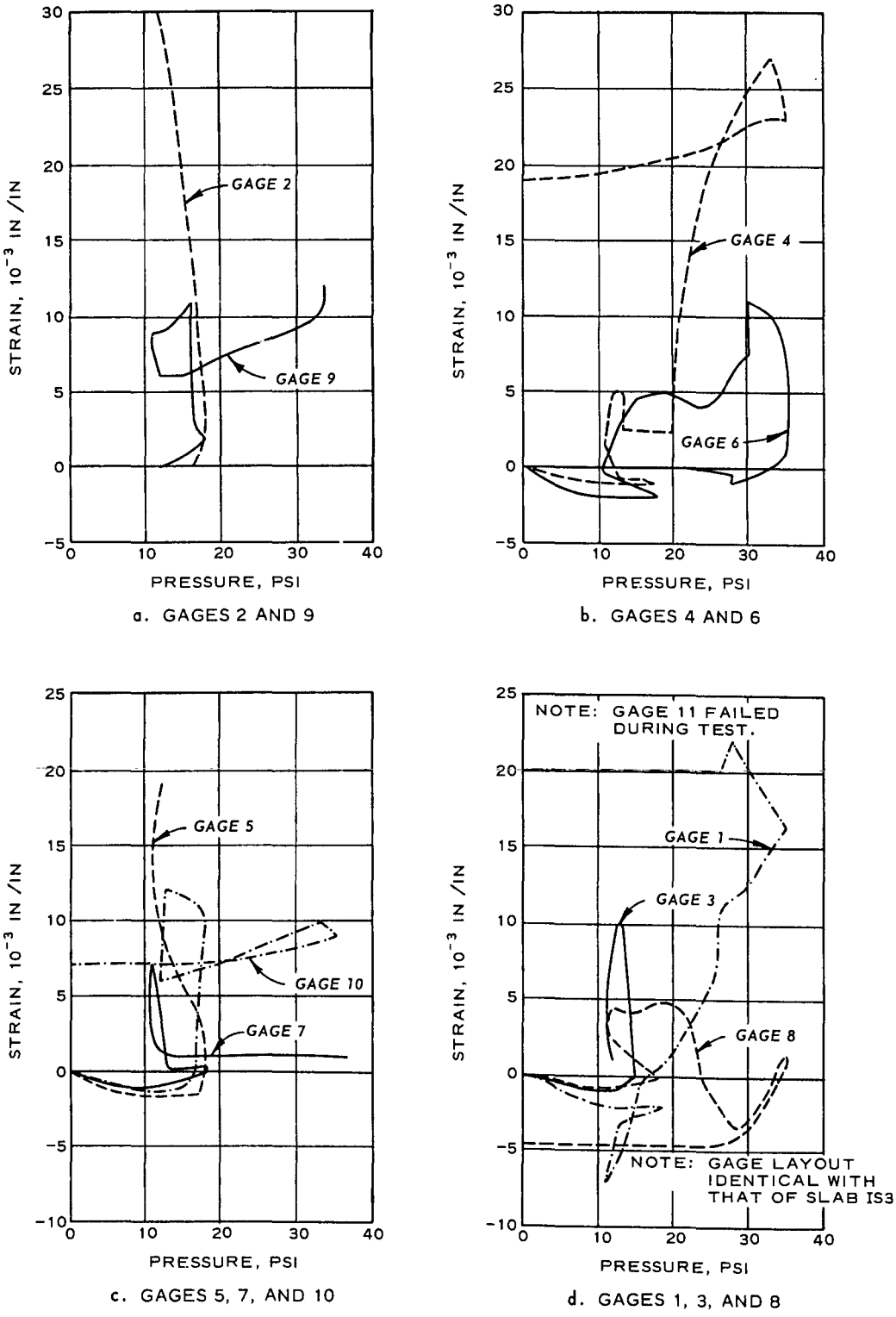

Figure 3.16 Steel strain-pressure curves, Slab IIS1.

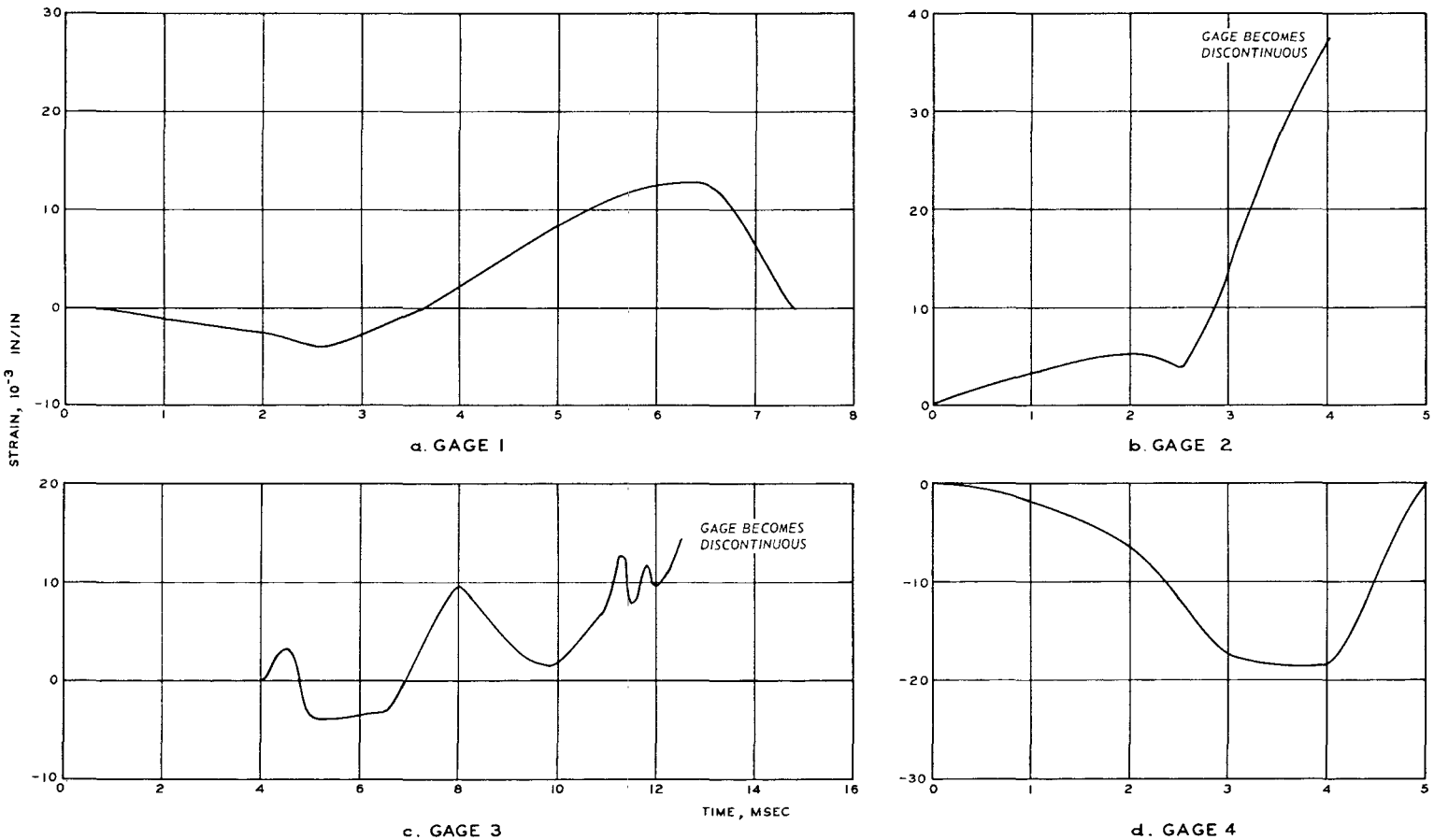

Figure 3.17 Steel strain-time curves for Slab IID1 (sheet 1 of 2).

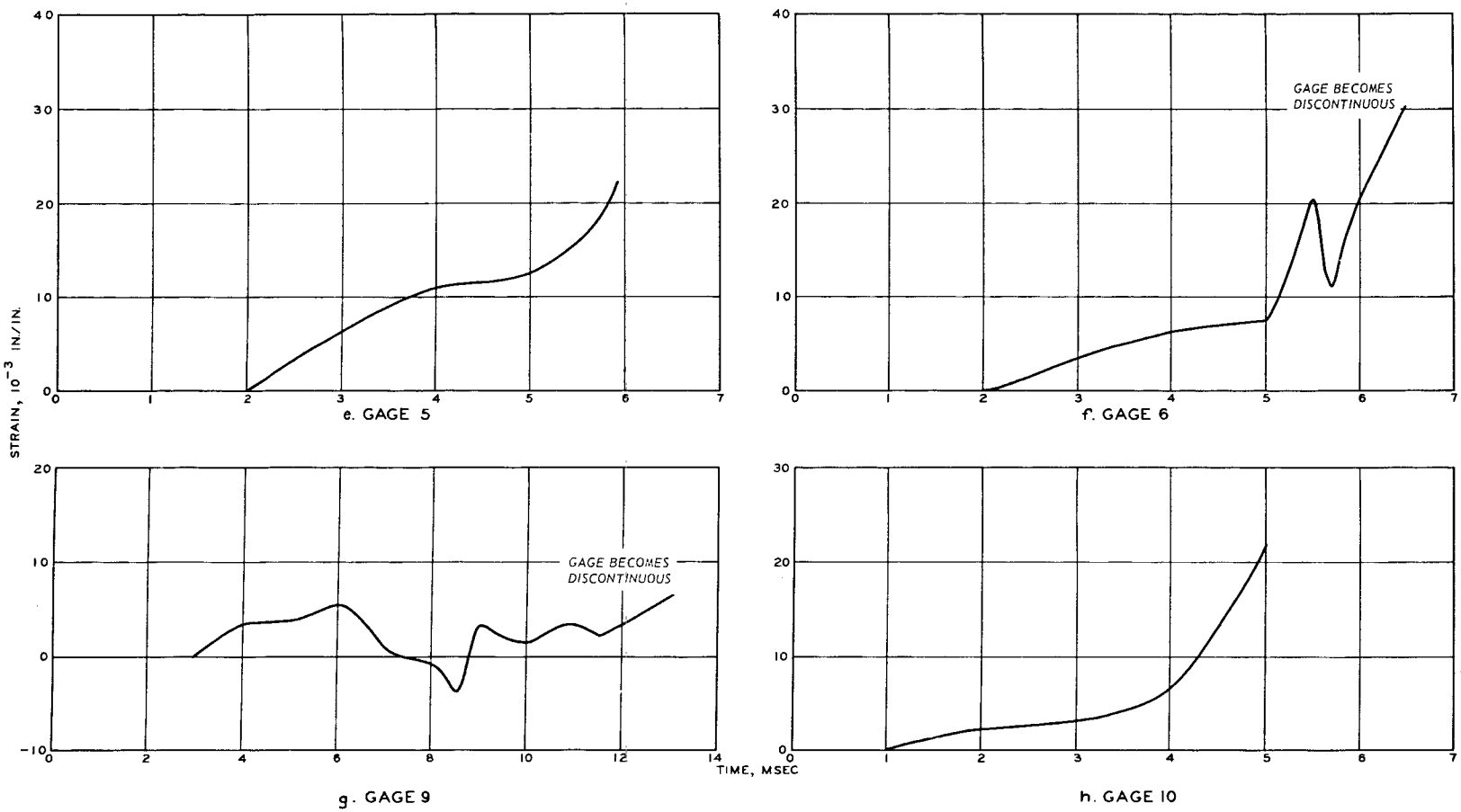

Figure 3.17 (sheet 2 of 2).

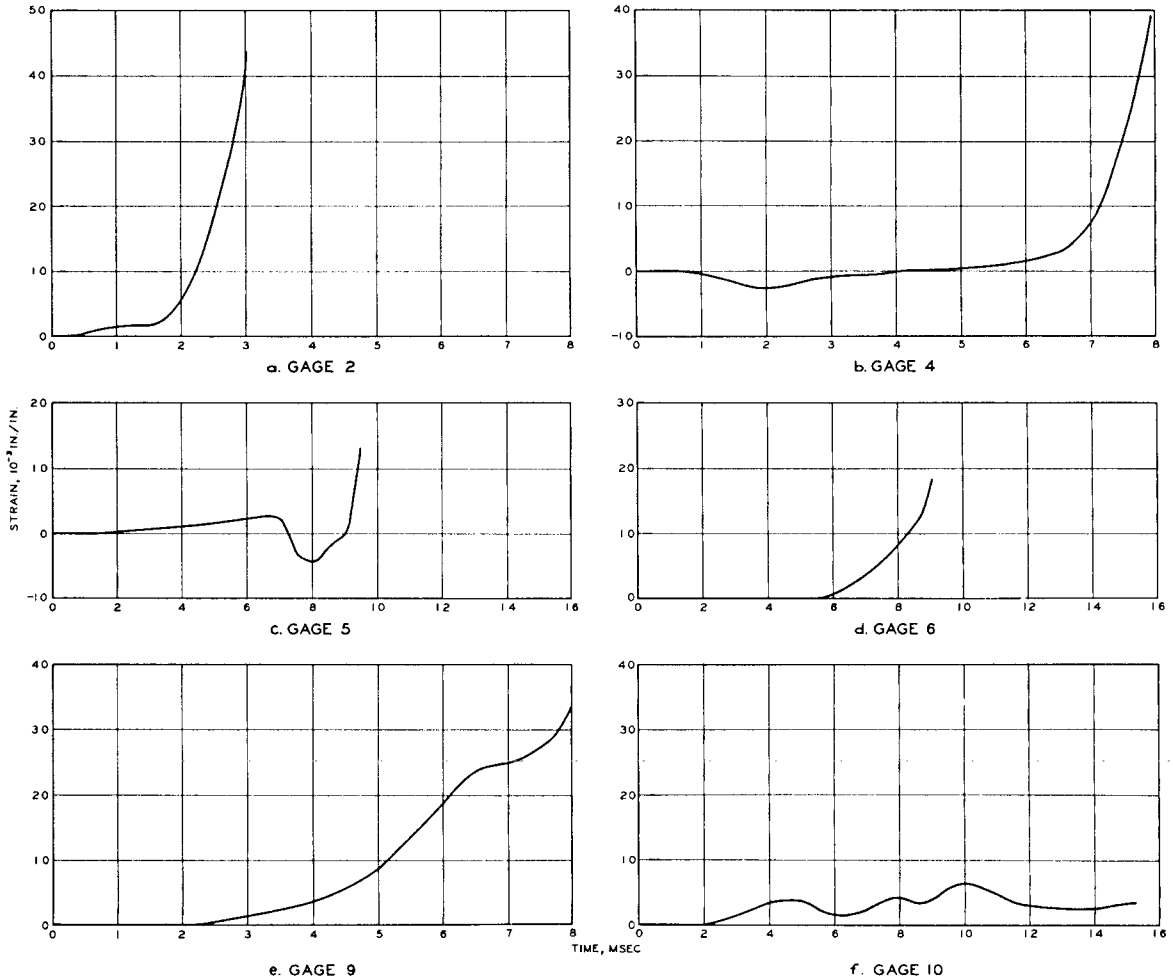

Figure 3.18 Steel strain-time curves for Slab IID3.

CHAPTER 4

DISCUSSION OF RESULTS

4.1 STATIC RESPONSE

The analysis and interpretation of the test results can best be discussed by taking a closer look at the graphic records of those tests.

The statically loaded slabs consistently behaved in a manner that produced dual-peak resistance curves, as shown in Figures 3.2 and 4.1. The first peak, which occurred at about a 1/2-inch midspan deflection, was due either to arching action of the slab, induced by the in-plane forces developed from the edge restraint, or initial yield line flexure.

Yield line theory (References 6 and 7) assumes that a constant load on a slab causes a concentration of strain in the reinforcing steel and concrete along lines of maximum moment. These lines, referred to as yield lines, form and spread into a pattern that divides the slab into segments. In the case of a square, longitudinally restrained slab, yield lines form an X pattern dividing the slab into four equal segments. Near failure, the elastic deformations of each segment are assumed negligible with respect to the plastic deformation at the yield lines. Consequently, all curvature in the slab at failure is assumed to be concentrated at the yield lines. These lines are the axes of rotation for the movements of each segment.

When the edges of a slab are free to translate, moment is developed in the loaded slab, but there are no in-plane forces developed because the edges are unrestrained. Therefore, the resistance curve takes the shape of that for the unrestrained slab in Figure 4.1. This was the case of the test slabs in the study described in Reference 2.

When the edges of a slab are restrained against outward movement, both moment and in-plane compressive forces are induced in the slab when the slab is loaded. Then the resistance curve takes the shape of that for the restrained slab in Figure 4.1. It is these in-plane forces induced by the edge restraint that give rise to the arching effect of the loaded slab.

To explain why arching and not yield line theory better describes the first peak of the static resistance curve, the deflection that occurs after the ultimate pressure P_u is reached must be observed (from Point A to B in Figure 4.1). Even after ultimate flexural pressure has been reached, the deflection of the slab still increases although the corresponding load is actually decreasing. According to yield line theory, an increasing deflection, however small, requires a constant load. Therefore, yield line theory cannot explain why deflection continues to increase under decreasing load. Arching action, however, can explain the phenomenon. Arching induced in the slab due to the fixed edges strengthens the slab, thus requiring a higher load to cause it to yield. Once this resistance is overcome, the slab experiences snapthrough (ultimate flexural resistance, Point A, Figure 4.1). Snapthrough indicates that the concrete is failing. Cracks are forming and penetrating the slab, thus causing pressure reduction. However, the overpressure is still high enough to cause deflection along the yield lines. Hence, the deflection increases as the load decreases. This action proceeds until the dropping pressure corresponds to the yielding steel plateau and forms the trough of the resistance curve (Point B in Figure 4.1).

Another explanation for the behavior of the resistance curve from Point A to Point B (Figure 4.1) is the fact that water (an incompressible fluid) was used as the load producing medium. As the slab experienced ultimate flexural resistance, deflection increased but the corresponding load decreased due to the increase in volume above the slab caused by the slab deflection. The loading rate was constant throughout the test, but if the loading rate had been increased when the slab experienced ultimate flexural resistance, the increased load due to the faster loading rate might have offset the volume change brought about by the slab deflection and the dip in the resistance curve from Point A to Point B might not have occurred.

It cannot be determined whether the behavior of the curve in Figure 4.1 from Point A to Point B is attributable to arching action induced from the fixed edges or due to using water as the loading medium.

It is suspected, however, that the behavior of the curve from Point A to Point B is a combination of both effects.

The latter part of the resistance curve (from Point B to C in Figure 4.1) represents the tensile membrane resistance of the slab. The major difference between the Series I and II tests, relative to this part of the curve, was maximum pressure. Sharp drops and recoveries near the end of the resistance curves (Figure 3.2) probably were produced when reinforcing wire broke. The peak was reached after several breaks, and once the peak was attained, pressure dropped as successive wires were broken.

Apparently, a side of the slab will begin to rupture with the breaking of the top reinforcing until the load is increased to a high enough level to break the bottom reinforcing. The bottom reinforcing was apparently the primary load-carrying component of the system after membrane action had fully developed. Once the bottom reinforcing began to break, load capability was lost and little extra pressure was required to rupture the entire side. Final pressure loss occurred when the diaphragm pushed through the severed side, thus ending the test.

The scattering of values of peak pressure (Table 3.1) cannot readily be explained. Maximum midspan deflections were fairly consistent and corresponded to about a 7 to 12 percent elongation of the reinforcing.

The beginning of the resistance curve for Slab IIS1 (Figure 3.2d) is different from that for the Series I slabs. Apparently, the higher percentage of steel made the slab stiffer. The higher strength of the Series II static slab was also consistent with the higher steel percentage. At the beginning of the test of Slab IIS1, the pressure had to be held at 10 psi until the calibration step for instrumentation had been recorded, as it had not been done prior to the test. This may explain the unusual beginning of the resistance curve for Slab IIS1.

All four statically tested slabs had one of the two sides that contained the "shallow-bent" wires ruptured. The wires are termed "shallow-bent" because the height of bend was only 0.46 inch, as compared with a height of bend of 0.62 inch for the wires laid perpendicular to the

shallow-bent wires. The shallow-bent wires were placed on top of the 0.62-inch-bend wires, as shown in Figure 2.8b. Of the two reinforcing mats in the slab, the one with the least negative moment capability (based on the area of steel, A_s) was the mat containing the shallow-bent wires. Therefore, failure should have occurred at either of the two sides that had the shallow-bent wires, as was the case for the four statically loaded slabs.

Yield lines were apparent on Slabs IS2 and IS3, but they were not well developed and occurred only near the corners. The yield lines generally appeared to lie not on the diagonals of the slab but slightly off to either side. This may correspond to the Y-pattern corner segments in yield line theory (Reference 8).

Typical of membrane action are the numerous tensile concrete cracks that occurred near the center of all the slabs. These cracks were fairly random except in those slabs that had excessive voids under the reinforcing wire. Also, radial cracks occurred on the bottoms of the slabs near the corner diagonals. These were apparently tension cracks in the concrete caused during formation of yield lines.

Large cracks were typical along the line where reinforcing was bent up. An explanation of this would be that after the initial yield lines occurred and the slab went into membrane tension, the bent-up wires were forced to straighten out. This pulled the concrete apart at those points, thus resulting in the cracks.

Slab IIS1 was quite different in appearance from the Series I slabs. Cracking was much more intense, especially around the edge. Concrete crushing was extensive around the edges of the slab due to the higher steel percentage. Development of yield lines on this slab was not apparent, but radial cracks were prevalent on the bottom surface.

4.2 DYNAMIC RESPONSE

The dynamically tested slabs differed greatly from the statically tested slabs for several reasons. First, dynamically tested slabs tend to fail more uniformly than statically tested slabs, which start to fail in one area, thus unloading the rest of the slab. Thus, failure is

concentrated in one area of a statically tested slab. Second, dynamic testing is a "hit or miss" situation with respect to determining the collapse pressure. For this reason, many tests are required to obtain a reasonably valid collapse pressure. Third, in dynamic tests, the reinforcing steel stretches at a very high rate of strain, which tends to increase the steel's strength. This change in strength is very important to the overall strength of the slab. Finally, dynamic airloads, as produced in the laboratory, produce both venting in the slab and back pressure under the slab. This phenomenon is very difficult to evaluate but is also important to the strength of the slab.

Before the dynamic testing is discussed, some comment on measurement and the pressure environment is necessary. Four pressure gages were placed above the slab, two in the bonnet and two near the edge of the slab. A gage was placed under the Series II slabs. Records from these pressure gages showed a rapid rise time followed by a fairly rapid decay time due to venting through the slab into the lower chamber. Once venting was completed, at about 20 msec, the decrease in pressure was less rapid since the gases could then escape only through the vent holes in the lower chamber and in the bonnet. The pressures given herein are actually average pressures for the first few milliseconds. Because of the pressure reduction due to venting and the consequential increase in pressure under the slab, it would seem that the response of the slab would have been slowed and a higher than actual collapse pressure would have been attained. However, from a practical standpoint, venting and the presence of pressure underneath the slab would occur in an actual situation on a full-sized shelter also. Therefore, the response of an actual slab should be similar to that of the model.

In measuring deflection, a little trouble was encountered because the probe was separated from the slab at times. Also, deflection measurements experienced some electrical interference caused by grounding of the transducer. However, all the deflection curves showed a smooth response. Time of response to maximum deflection varied and depended on the overpressure and amount of reinforcing. Maximum deflections without collapse were between 7 and 8 inches.

Steel elongation was approximated after the tests. It was realized that a correction factor was needed due to the fact that the reinforcing had separated from the sides of the slab. Measurements were taken directly from the slab with a ruler, and an inch was subtracted from these measurements to compensate for the separation of the reinforcement from the sides. For a 6- to 7-inch center deflection, elongation was estimated to be 12 to 16 percent. This is close to the maximum deflection possible based on full utilization of the elongation capability of the steel used.

The first dynamic test, ID1, resulted in a low pressure of 15 psi due to bad primacord. Therefore, a different size cord was used for the rest of the tests. Only hairline cracks occurred around the periphery of Slab ID1. A second shot at 35 psi collapsed the slab. The slab dished before it separated from the sides.

The dynamic tests yielded a relatively valid collapse pressure for the slabs. For Series I dynamic slabs, the collapse pressure was 23.7 percent above static strength; for Series II slabs, the collapse pressure was 24.6 percent above static strength.

The sequence of failure of the slabs followed yield line behavior. The dynamically tested slabs showed better developed yield lines and greater deflections than the statically tested slabs. All the dynamically tested slabs showed well developed tensile membrane action. Collapse was apparently initiated with the breaking of the top reinforcing along the center of all four sides. This was followed by rupture of the bottom reinforcing at the center of the sides, with rupture progressing to the corners of the slab. The rupture of the corner wires determined the point at which collapse occurred. At this point, venting had virtually equalized pressure between the top and bottom of the slab, and final rupture depended upon the inertia of the slab as it blew through.

4.3 THEORETICAL DETERMINATION OF SLAB STRENGTH

4.3.1 Static Analysis. Tensile membrane resistance begins to develop at a point near that designated as Point B in Figure 4.1. The

membrane forces in the central region of the slab begin to change from compression to tension. Beyond Point B, the tensile membrane region grows outward toward the edges of the slab, which begin to resist inward movement. Cracks begin to penetrate the entire depth of the concrete, and yielding of reinforcement spreads throughout this region. The reinforcement acts as a tensile membrane, causing the slab resistance to increase with deflection until the reinforcement ruptures.

The following expression has been developed (Reference 9) for the resistance of a uniformly loaded slab acting as a tensile membrane:

$$\frac{wL_x^2}{T_x\Delta} = \frac{\pi^3}{4\sum_{n=1,3,5\ldots}^{\infty} \frac{1}{n^3}(-1)^{\frac{n-1}{2}}\left(1 - \frac{1}{\cosh\left(\frac{n\pi L_y}{2L_x}\sqrt{\frac{T_x}{T_y}}\right)}\right)}$$

Where: w = uniformly distributed load per unit area of slab

L_x = span of slab in x direction

T_x = yield force, per unit width, of reinforcement in x direction

Δ = maximum deflection of any point of slab in a direction of the normal to the x-y plane (positive in direction of loading)

n = odd integers

L_y = span of slab in y direction

T_y = yield force, per unit width, of reinforcement in y direction

This equation gives a linear relation between w and Δ and defines that portion of the pressure-deflection curve between Points B and C in Figure 4.1.

To simplify the use of Equation 4.1, values of $wL_x^2/T_x\Delta$ for various values of L_y/L_x and T_x/T_y have been plotted (Figure 4.2). Only $T_x \geq T_y$ for slabs with $L_y \geq L_x$ was considered since economy of steel will always require more steel in the direction of the short span than in the direction of the long span (Reference 9).

Therefore, the right side of Equation 4.1 becomes a constant, and for a square slab ($L_x = L_y$) Equation 4.1 becomes:

$$q = k(p + p') \frac{df_s}{L^2} Z \qquad (4.2)$$

Where: q = tensile membrane resistance

k = a constant

p = ratio of tension reinforcement per unit width of slab

p' = ratio of compression reinforcement per unit width of slab

f_s = stress in tension reinforcement

L = clear span length of slab

Z = midspan deflection

Assuming pure tensile membrane action ($T_x = T_y$), k would equal 13.5 based on Figure 4.2 (Reference 9). However, based on test results reported in Reference 9, pure membrane action does not occur, particularly in deep slabs and at slab deflections near the secondary resistance level. The error in Equation 4.2 resulting from assuming that the slab is a pure membrane can be adjusted by setting k equal to 20, as was done in Reference 3. By setting k equal to 20, the ratio T_x/T_y is less than 1, which is saying that the reinforcement in the two directions is not yielding at the same time.

It has been found, Reference 9, that a safe maximum value for central deflection after tensile membrane action is:

$$Z_t = 0.1L \qquad (4.3)$$

Using Equation 4.3 to calculate deflection yields 2.9 inches. This value is a conservative estimate of the actual experimental values (Table 3.1). As stated earlier, the primary objective of this study was to study total collapse response of the slabs. Therefore, a safe value for deflection is not useful. The static deflections at collapse found during this study were 15 and 14 percent of the span length for the Series I and II slabs, respectively. A more applicable approximation

of static collapse based on results of this study would be:

$$Z_t' = 0.15L \tag{4.4}$$

Tensile membrane resistance was computed using the preceding equations. Table 4.1 is a summary of the results of computations made using different values of k, f_s, and Z in Equation 4.2. The values of k and f_s in Column A of Table 4.1 are the values used in Reference 3. Also in Columns A through D, the deflection equation from Reference 9 (Equation 4.3) was used, whereas in Columns E through H, the deflection equation of this study (Equation 4.4) was used. The best correlation between experimental and theoretical values of membrane resistance is in Column E of Table 4.1. The k and f_s values are taken from Reference 9, and the deflection value is from Equation 4.4. The difference between the theoretical values in Column E and the experimental values is less than 1 percent. To attain the values in Column E, f_s was set equal to f_y. This could be a source of some error because during membrane resistance the stress in the reinforcing steel should be nearer the ultimate level, as was also noted in Reference 3. The results in Column E of Table 4.1 appear to justify the use of f_y rather than f_u for f_s. This conclusion was also reached in Reference 3, and f_y was used for f_s in the calculations therein. When f_u is substituted for f_s in Equation 4.2, the results (Column F) are off by as much as 70 percent when compared with experimental values. Therefore, based on the correlation between theoretical and experimental values of membrane resistance, it seems logical to assume that $f_s = f_y$ in Equation 4.2.

The Reference 9 k value for pure tensile membrane resistance was used in Columns C, D, G, and H of Table 4.1. The best correlation between experimental and theoretical response is given in Column H, but even these values are 15 percent higher than experimental values. It seems apparent from this that the slabs did not exhibit pure tensile membrane action and that the use of $k = 20$ is justified.

Prediction of ultimate collapse pressure using Equation 4.1 for

the static slabs in this study appears to be very good. However, the deflection equation developed herein (Equation 4.4) had to be used in conjunction with Equation 4.1 to obtain a close correlation with the experimental results.

4.3.2 Dynamic Analysis. Equation 4.1 was also used to predict the tensile membrane resistance for the dynamic slabs. Then the value obtained for tensile membrane resistance was compared with the average peak overpressure obtained experimentally. However, Equation 4.4 had to be revised to accurately describe the dynamic deflections obtained experimentally. The dynamic deflections ranged from 25 percent of the span length for the Series I slabs to 28 percent for the Series II slabs. Therefore, the deflection equation would take the form of:

$$Z_t = 0.25L \tag{4.5}$$

Using Equations 4.2 and 4.5, values were calculated and are presented in Table 4.2. For the statically tested slabs, the values in Column E of Table 4.1 represented the best correlation between theoretical and experimental values. For the values in Column E of Table 4.2, however, the correlation is not as favorable. The values for membrane resistance in Column E are 36 percent higher than the peak pressure attained experimentally for the Series I dynamically tested slabs and 33 percent higher than the peak pressure attained experimentally for the Series II dynamically tested slabs. The best correlation between experimental and theoretical values for the dynamically tested slabs is given in Column B or G of Table 4.2. However, the deflection value in Column B is not representative of experimental results. Even though the deflection value in Column G is indicative of the experimental value, the k value is not, based on the results of the static analysis. The statically tested slabs did not exhibit pure tensile membrane action, so it does not seem logical to assume that the same slabs when loaded dynamically will behave with pure tensile membrane action.

However, it was apparent from observation of the dynamically

tested slabs and the larger deflections encountered that concrete crushing was more intense than in the statically tested slabs. As concrete crushing increases, only the tensile strength of the reinforcement is left to resist loading; hence, tensile membrane action increases and pure membrane action is approached, which justifies the 13.5 value for k in Column G in Table 4.1. So the results in Column G of Table 4.2 appear to give the closest correlation between experimental and theoretical values. These values in Column G are conservative and differ from experimental results by about 9 percent for the Series I slabs and 11.5 percent for the Series II slabs.

Based on the test results, it appears that the dynamically tested slabs more closely approached pure membrane tension than the statically tested slabs. Although Equation 4.1 did not give as accurate predictions of dynamic strength as it did in the case of static response, it did yield a conservative value of overpressure that is a reasonable approximation of dynamic response; also, it exhibits how important membrane action is to the overall strength of the slab.

TABLE 4.1 THEORETICAL VALUES OF TENSILE MEMBRANE RESISTANCE q_t FOR STATICALLY TESTED SLABS

Average experimental values--Series I, q_t = 23.2 psi, Z = 4.40 in; Series II, q_t = 36.5 psi, Z = 4.10 in.

	q_t as Determined Using Indicated Parameters						
Column A	Column B	Column C	Column D	Column E	Column F	Column G	Column H
k = 20 $f_s = f_y$ Z = 2.9 in	k = 20 $f_s = f_u$ Z = 2.9 in	k = 13.5 $f_s = f_y$ Z = 2.9 in	k = 13.5 $f_s = f_u$ Z = 2.9 in	k = 20 $f_s = f_y$ Z = 4.35 in	k = 20 $f_s = f_u$ Z = 4.35 in	k = 13.5 $f_s = f_y$ Z = 4.35 in	k = 13.5 $f_s = f_u$ Z = 4.35 in
Series I:							
15.6	26.4	10.5	17.8	23.4	39.6	15.8	26.7
Series II:							
24.2	41.0	16.3	27.6	36.3	61.4	24.5	41.5

TABLE 4.2 THEORETICAL VALUES OF TENSILE MEMBRANE RESISTANCE q_t FOR DYNAMICALLY TESTED SLABS

Average experimental values--Series I, peak overpressure = 28.7 psi, Z = 7.25 in; Series II, peak overpressure = 45.5 psi, Z = 8.10 in.

	q_t as Determined Using Indicated Parameters						
Column A	Column B	Column C	Column D	Column E	Column F	Column G	Column H
k = 20 $f_s = f_y$ Z = 2.9 in	k = 20 $f_s = f_u$ Z = 2.9 in	k = 13.5 $f_s = f_y$ Z = 2.9 in	k = 13.5 $f_s = f_u$ Z = 2.9 in	k = 20 $f_s = f_y$ Z = 7.25 in	k = 20 $f_s = f_u$ Z = 7.25 in	k = 13.5 $f_s = f_y$ Z = 7.25 in	k = 13.5 $f_s = f_u$ Z = 7.25 in
Series I:							
15.6	26.4	10.5	17.8	39.0	66.0	26.3	44.6
Series II:							
24.2	41.0	16.3	27.6	60.5	102.4	40.8	69.1

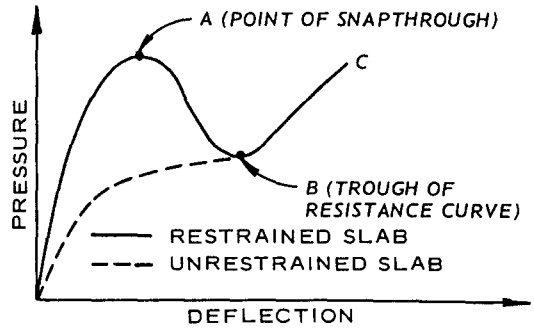

Figure 4.1 Typical dual-peak resistance curve.

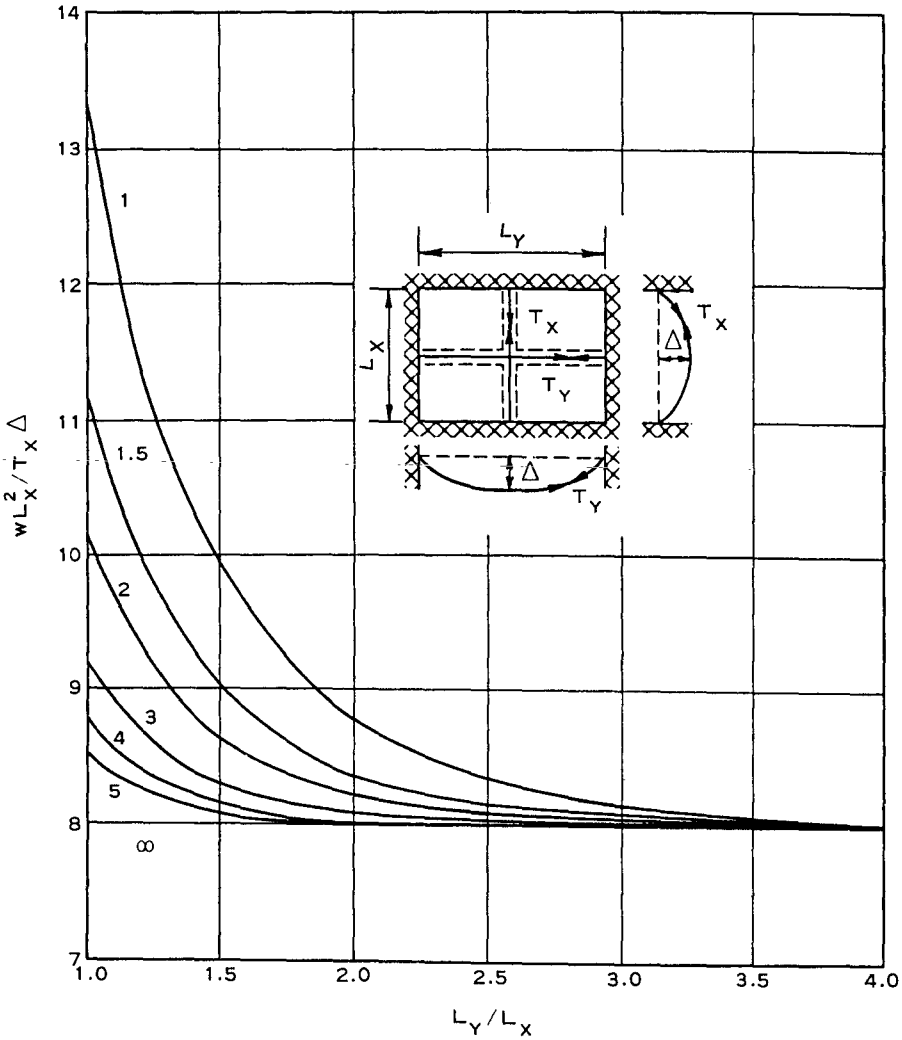

Figure 4.2 Load-deflection relations from Equation 4.1 for uniformly loaded plastic tensile membranes with rigid rectangular boundaries. Values of T_x/T_y are shown beside each curve.

CHAPTER 5

SUMMARY OF RESULTS, CONCLUSIONS, AND RECOMMENDATIONS

5.1 SUMMARY OF RESULTS AND CONCLUSIONS

The results of four static and eight dynamic tests on fixed-edge, longitudinally restrained, two-way reinforced concrete slabs and the conclusions drawn therefrom are summarized below.

5.1.1 Slabs Subjected to Uniformly Distributed Static Loads. The average ultimate collapse strengths of the slabs tested under static loading, as determined from the actual dual-peak resistance curves, were 23.2 psi for the Series I slabs and 36.5 psi for the Series II slab. The average values of ultimate flexural resistance were 14.1 psi for the Series I slabs and 18.2 psi for the Series II slab.

A comparison of the value of tensile membrane resistance with that of ultimate flexural resistance indicates that an increase in load-carrying capability of 64.5 percent was realized for the Series I slabs and 100.5 percent for the Series II slab. It can be concluded that the ultimate strength of the slabs was substantially increased by membrane action.

Deflections of the static slabs averaged 4.40 inches for the Series I slabs and 4.10 inches for the Series II slab. This corresponds to a deflection of 15.2 percent of the slab span for the Series I slabs and 14 percent for the Series II slab.

5.1.2 Slabs Subjected to Dynamic Loads. The average ultimate collapse strengths of the dynamically tested slabs were 28.7 psi for the Series I slabs and 45.5 psi for the Series II slabs.

Comparing the values of ultimate collapse strength for the dynamic slabs with those for the static slabs shows increases in ultimate strength of 23.7 percent for the Series I slabs and 24.6 percent for the Series II slabs.

Deflections for the dynamic slabs are a bit more difficult to present due to the fact that so many of the test slabs totally collapsed. However, for the Series I slabs, the deflection averaged 7.25 inches,

disregarding deflections of the slabs that totally collapsed. This deflection represents 25 percent of the slab span. For the Series II slabs, average deflection was 8.1 inches (28 percent of slab span), again neglecting deflections of slabs that totally collapsed. Compared with the statically tested slabs, deflection of the dynamically tested slabs was 64.8 percent greater for the Series I slabs and 97.5 percent greater for the Series II slabs.

5.1.3 Comparison of Results. This study was similar to that reported in Reference 2 and actually serves as a continuation of the Reference 2 study. Primarily, this study establishes an upper boundary for ultimate slab strength relative to the values presented in Reference 2. To illustrate this point, Table 5.1 was developed to compare the results of this study with those obtained in the Reference 2 study.

5.2 RECOMMENDATIONS

This study and the Reference 2 study have established an upper and lower boundary for the dynamic response of two-way reinforced concrete floor slabs; the lower boundary was established in the Reference 2 study. The lower limits for the Series I and III dynamic slabs are 11.0 and 15.0 psi, as shown in Table 5.1. The upper limits are 28.7 psi and 45.5 psi for Series I and II, respectively.

In Figures 5.1 through 5.3, a comparison of pressure-midspan deflection curves is presented. Since the test slabs in the Reference 2 study were three times as large as the test slabs of this study, the pressure-midspan deflection curves had to be scaled accordingly to make an adequate comparison. Looking at these curves, one can readily see how the different edge constraints affected slab resistance. It can also be seen that the test slabs of the Reference 2 study experienced very little tensile membrane action, while those of this study experienced a high degree of tensile membrane action.

As mentioned earlier, the Reference 2 slabs had simple supports on all edges; those tested in this study had edges that were completely fixed. Neither condition represents exactly a real-world slab, which would be supported on all four sides by beams. The actual support

condition can best be simulated by testing a model of a multipanel floor system. Presently, dynamic and static testing of a multipanel floor system is under way at WES. The multipanel floor system being tested consists of nine concrete panels incorporated into a steel frame system. Results indicate that the multipanel slab system has a collapse loading nearer the lower bound. However, it is further recommended that a concrete beam and slab system be dynamically tested to correlate with the steel frame slab system and further narrow the range of collapse pressures for the two-way slab system.

TABLE 5.1 COMPARISON OF ULTIMATE LOAD CAPACITIES

Study	Series	Slab Dimensions			Ultimate Load Capacity	
		Span	Thickness	% Steel	Static	Dynamic
		inches	inches		psi	psi
This study	I	29	0.89	0.78	23.2	28.7
	II[a]	29	0.89	1.17	36.5	45.5
Reference 2	I	90	2.625	0.78	7.7	11.0
	III[a]	90	2.625	1.17	11.8	15.0

[a] Series II and III slabs each had 1.17 percent steel reinforcement.

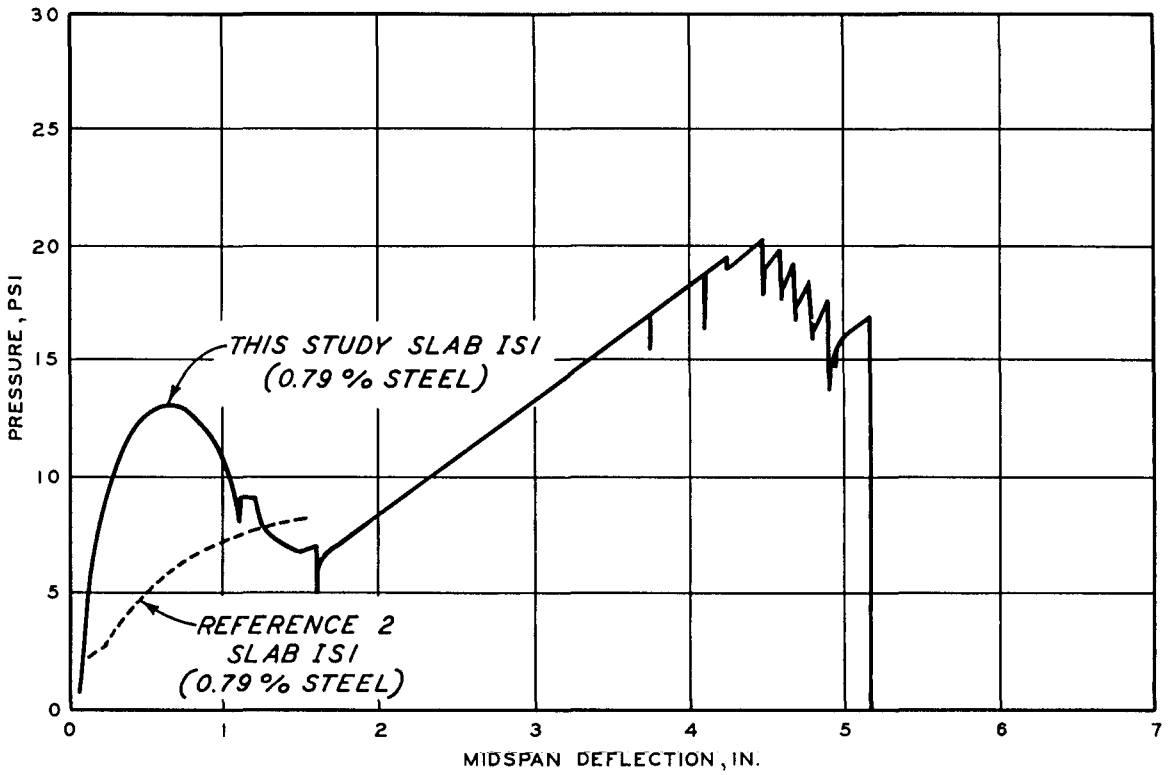

Figure 5.1 Comparison of pressure-midspan deflection curves, Slab IS1.

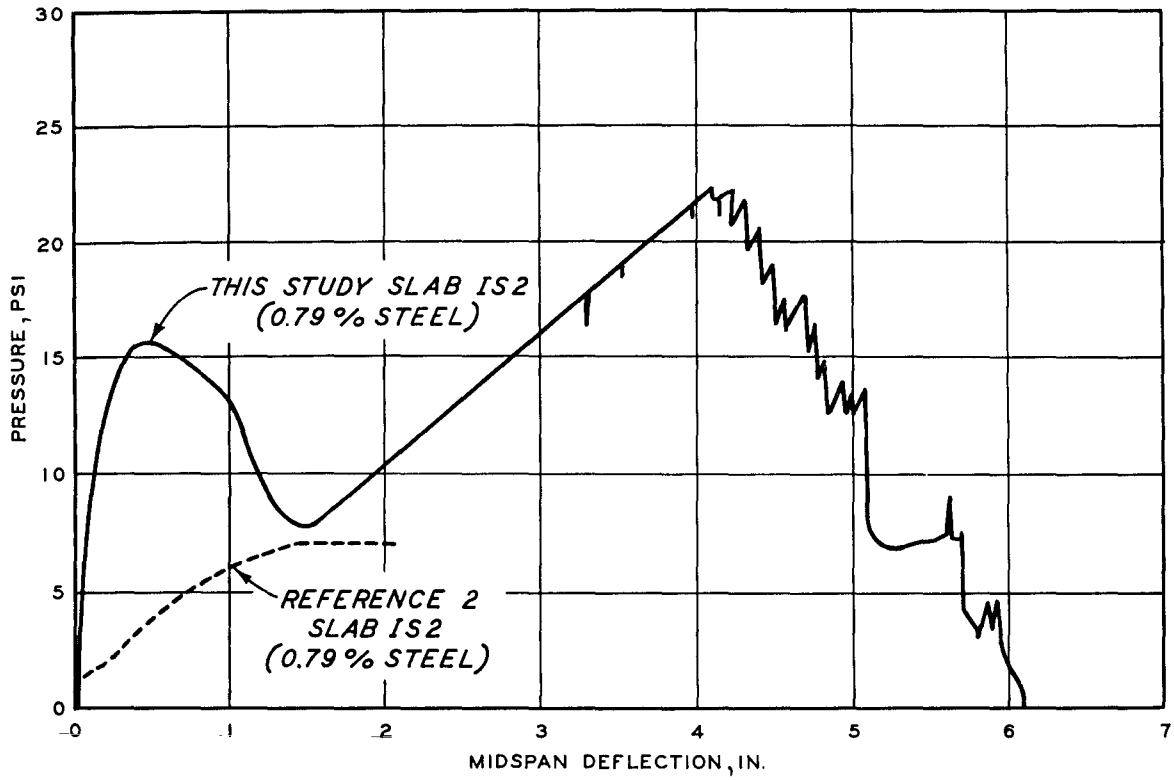

Figure 5.2 Comparison of pressure-midspan deflection curves, Slab IS2.

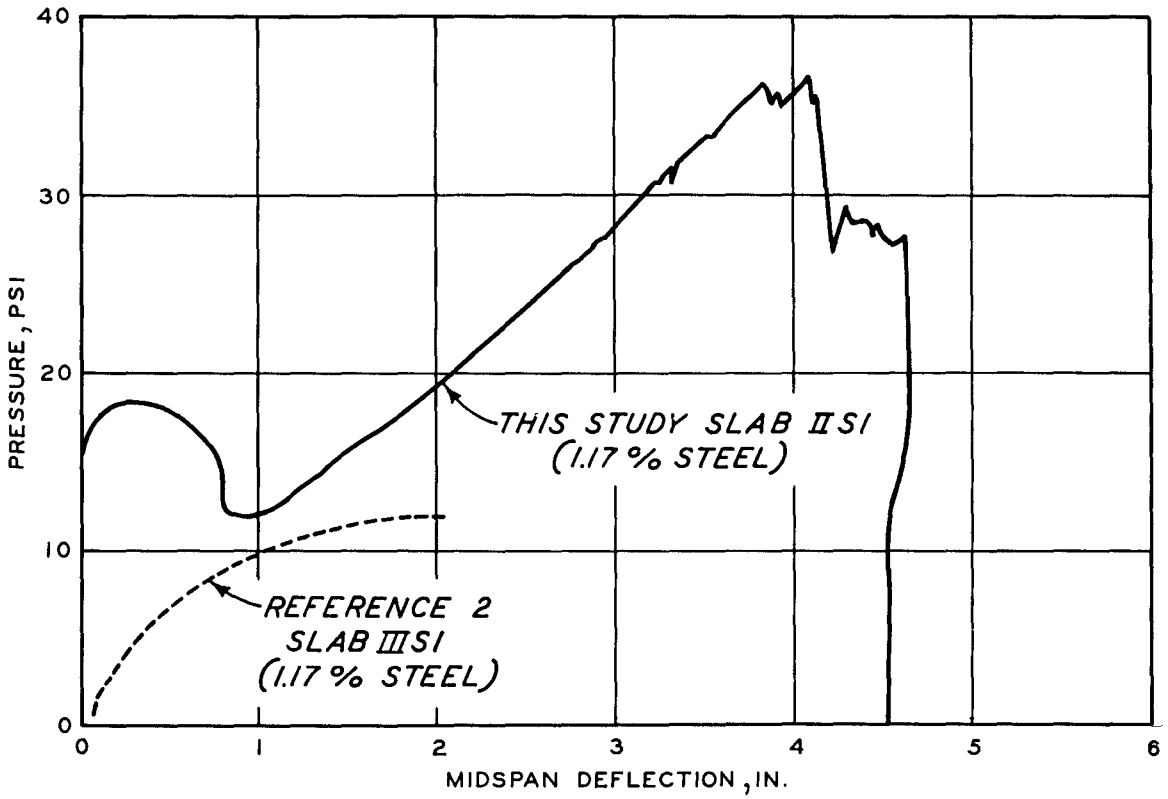

Figure 5.3 Comparison of pressure-midspan deflection curves, Slabs IISl and IIISl.

REFERENCES

1. U. S. Department of Defense and Atomic Energy Commission; "The Effects of Nuclear Weapons"; 1962; Washington, D. C.; Unclassified.

2. D. R. Denton; "A Dynamic Ultimate Strength Study of Simply Supported Two-Way Reinforced Concrete Slabs;" Technical Report No. 1-789, July 1967; U. S. Army Engineer Waterways Experiment Station, CE, Vicksburg, Mississippi; Unclassified.

3. W. A. Keenan; "Strength and Behavior of Restrained Reinforced Concrete Slabs Under Static and Dynamic Loadings"; Technical Report R621, April 1969; U. S. Naval Civil Engineering Laboratory, Port Hueneme, California; Unclassified.

4. ACI Committee 318; "Building Code Requirements for Reinforced Concrete (ACI 318-56)"; ACI Standard 318-56, 1959; American Concrete Institute, Detroit, Michigan; Unclassified.

5. "Standard Specification for Deformed Billet-Steel Bars for Concrete Reinforcement"; ASTM Designation: A615-68, 1972 Book of Standards, Pages 757-762; American Society for Testing and Materials, Philadelphia, Pennsylvania; Unclassified.

6. A. Ingerslev; "The Strength of Rectangular Slabs"; Journal, Institution of Structural Engineers, 1923, Vol. 1; Unclassified.

7. K. W. Johansen; "Yield Line Theory"; 1962; Cement and Concrete Association, London, England; Unclassified.

8. P. M. Ferguson; "Reinforced Concrete Fundamentals with Emphasis on Ultimate Strength"; Second Edition, 1966; Wiley, New York; Unclassified.

9. R. Park; "Tensile Membrane Behavior of Uniformly Loaded Rectangular Reinforced Concrete Slabs with Fully Restrained Edges"; Magazine of Concrete Research, March 1964, Vol. 16, No. 46, Pages 39-44; Cement and Concrete Association, London, England; Unclassified.

DISTRIBUTION LIST FOR TECHNICAL REPORT N-73-8

Address	No. of Copies
Defense Civil Preparedness Agency, Research and Engineering ATTN: Administrative Officer Washington, D. C. 20301	50
Assistant Secretary of the Army (R&D) ATTN: Assistant for Research Washington, D. C. 20310	1
Chief of Naval Research Washington, D. C. 20360	1
Commander, Naval Sypply Systems Command (Code 0652) Department of the Navy Washington, D. C. 20390	1
Commander, Naval Facilities Engineering Command Research and Development (Code 0322C) Department of the Navy Washington, D. C. 20390	1
Advisory Committee on Civil Defense National Academy of Sciences ATTN: Mr. Richard Park 2101 Constitution Avenue, N. W. Washington, D. C. 20418	1
Defense Documentation Center ATTN: Mr. Myer Kahn Cameron Station Alexandria, Virginia 22314	12
Civil Defense Research Project Oak Ridge National Laboratory ATTN: Librarian P. O. Box X Oak Ridge, Tennessee 37830	1
Chief of Naval Personnel (Code Pers M12) Department of the Navy Washington, D. C. 20360	1
Commanding Officer and Director U. S. Naval Civil Engineering Laboratory ATTN: Document Library Port Hueneme, California 93041	1

Address	No. of Copies
Director, Civil Effects Branch Division of Biology and Medicine Atomic Energy Commission ATTN: Mr. L. J. Deal Washington, D. C. 20545	1
Commander Air Force Special Weapons Laboratory (AFSC) ATTN: Technical Library (DOGL) Kirtland Air Force Base Albuquerque, New Mexico 87117	1
Headquarters, Department of the Army ATTN: DAEN-MER-D Washington, D. C. 20314	1
Director, U. S. Army Engineer Waterways Experiment Station ATTN: Document Library P. O. Box 631 Vicksburg, Mississippi 39180	3
Mr. Milton D. Wright, Research Triangle Institute P. O. Box 12194 Research Triangle Park, North Carolina 27709	1
Director, Defense Civil Preparedness Agency ATTN: Mr. George N. Sisson (RE-SR) Washington, D. C. 20301	1
Research and Engineering Directorate Defense Civil Preparedness Agency ATTN: Mr. James E. Roembke Washington, D. C. 20301	1
Director, Defense Nuclear Agency ATTN: Mr. Jack R. Kelso Washington, D. C. 20305	1
Prof. Robert Bailey, Nuclear Engineering Department Duncan Annex, Purdue University Lafayette, Indiana 47907	1
Mr. Anatole Longinow IIT Research Institute 10 West 35th Street Chicago, Illinois 60616	1

Address	No. of Copies
Dr. Stanley B. Martin Stanford Research Institute 333 Ravenswood Avenue Menlo Park, California 94025	1
Dr. Clayton S. White, President-Director Lovelace Foundation 5200 Gibson Boulevard, S. E. Albuquerque, New Mexico 87108	1
Dr. Clarence R. Mehl, Dept. 5230 Sandia Corporation Sandia Base, Albuquerque, New Mexico 87115	1
Mr. Luke J. Vortman, Division 5412 Sandia Corporation Box 5800, Sandia Base Albuquerque, New Mexico 87115	1
Dr. Lewis V. Spencer National Bureau of Standards Room C313, Building 245 Washington, D. C. 20234	1
Mr. Lyndon Welch Eberle Smith Associates, Inc. 950 West Fort Street Detroit, Michigan 48226	1
Worcester Polytechnic Institute Department of Civil Engineering ATTN: Dr. Carl H. Koontz Worcester, Massachusetts 01609	1
University of Florida, Department of Mechanical Engineering ATTN: Prof. John A. Samuel Gainesville, Florida 32601	1
Pennsylvania State University ATTN: Prof. Richard E. Kummer 101 Engineer A University Park, Pennsylvania 16802	1
George Washington University Nuclear Defense Design Center ATTN: Prof. Raymond R. Fox School of Engineering and Applied Science Washington, D. C. 20006	1

Address	No. of Copies
Purdue University, Purdue Research Foundation School of Civil Engineering ATTN: Prof. M. B. Scott Lafayette, Indiana 47907	1
University of Colorado, School of Architecture ATTN: Prof. Gale K. Vetter Boulder, Colorado 80302	1
San Jose State College Department of Civil Engineering ATTN: Dr. Robert G. Spicher San Jose, California 95114	
University of Washington, Department of Civil Engineering ATTN: Prof. William M. Miller 307 More Hall Seattle, Washington 98105	1
Mr. Henry S. Wakabayashi Research and Engineering Directorate Defense Civil Preparedness Agency Washington, D. C. 20301	1
Director, U. S. Army Ballistic Research Laboratories ATTN: Technical Library Aberdeen Proving Ground, Maryland 21005	1
Director, U. S. Army Ballistic Research Laboratories ATTN: Mr. William Taylor Aberdeen Proving Ground, Maryland 21005	1
Director, Defense Nuclear Agency ATTN: Technical Library Washington, D. C. 20305	1
Director, U. S. Army Engineer Waterways Experiment Station ATTN: Weapons Effects Laboratory P. O. Box 631 Vicksburg, Mississippi 39180	1
Civil Engineering Center/AF/PRECET Wright-Patterson AFB, Ohio 45433	1
AFWL/Civil Engineering Division Kirtland AFB, New Mexico 87117	1

Address	No. of Copies
Mr. Carl K. Wiehle Stanford Research Institute 333 Ravenswood Avenue Menlo Park, California 94025	1
Mr. H. L. Murphy Stanford Research Institute 333 Ravenswood Avenue Menlo Park, California 94025	1
The Dikewood Corporation 1009 Bardbury Drive, S. E. University Research Park Albuquerque, New Mexico 87106	1
Research Triangle Institute P. O. Box 12194 Research Triangle Park, North Carolina 27709	1
URS Research Company 155 Bovet Road San Mateo, California 94402	1
University of Illinois ATTN: Dr. William J. Hall 111 Talbot Laboratory Urbana, Illinois 61801	1
University of Arizona ATTN: Miss Nancy K. Barberii OCD Professional Advisory Service Center Tucson, Arizona 85721	1
Bell Telephone Laboratories ATTN: Mr. R. W. Mayo Whippany Road Whippany, New Jersey 07981	1
Bell Telephone Laboratories ATTN: Mr. Eugene F. Witt Whippany Road Whippany, New Jersey 07981	1
Bell Telephone Laboratories ATTN: Mr. J. W. Foss Whippany Road Whippany, New Jersey 07981	1

Address	No. of Copies
Mr. Paul Zigman Environmental Science Associates 770 Airport Boulevard Burlingame, California 94010	1
Mr. Jack Halpern 8232 Greta Court Alexandria, Virginia 22309	1
University of Massachusetts School of Engineering ATTN: Dr. Merit P. White Amherst, Massachusetts	1
Dr. Abner Sachs Institute for Defense Analysis 400 Army-Navy Drive Arlington, Virginia 22202	1
R&D Associates ATTN: Dr. Harold L. Brode P. O. Box 3580 Santa Monica, California 90403	1
General American Transportation Corporation General American Research Division 7449 North Natchez Avenue Niles, Illinois 60648	1
Agbabian Associates, Engineering Consultants 250 N. Nash Street El Segundo, California 90245	1
Mr. Arthur D. Caster, Chairman Coordinating Committee on Civil Defense American Society of Civil Engineers 2864 McFarlan Park Drive Cincinnati, Ohio 45211	1
Mr. Thomas E. Waterman IIT Research Institute Technology Center 10 West 35th Street Chicago, Illinois 60616	1

Address	No. of Copies
Mr. Samuel Kramer, Chief Office of Federal Building Technology Center for Building Technology National Bureau of Standards Washington, D. C. 20234	1
University of Illinois, Urbana Campus ATTN: Prof. M. A. Sozen Department of Civil Engineering 3112 Civil Engineering Building Urbana, Illinois 61801	1

DOCUMENT CONTROL DATA - R & D

(Security classification of title, body of abstract and indexing annotation must be entered when the overall report is classified)

1. ORIGINATING ACTIVITY *(Corporate author)*

U. S. Army Engineer Waterways Experiment Station
Vicksburg, Mississippi

2a. REPORT SECURITY CLASSIFICATION

Unclassified

2b. GROUP

3. REPORT TITLE

DYNAMIC STRENGTH STUDY OF SMALL, FIXED-EDGE, LONGITUDINALLY RESTRAINED, TWO-WAY REINFORCED CONCRETE SLABS

4. DESCRIPTIVE NOTES *(Type of report and inclusive dates)*

Final report

5. AUTHOR(S) *(First name, middle initial, last name)*

Wayne M. Brown
Michael S. Black

6. REPORT DATE	7a. TOTAL NO. OF PAGES	7b. NO. OF REFS
December 1973	106	9

8a. CONTRACT OR GRANT NO.	9a. ORIGINATOR'S REPORT NUMBER(S)
b. PROJECT NO.	Technical Report N-73-8
c. Contract No. DAHC 20-68-W-0192	9b. OTHER REPORT NO(S) *(Any other numbers that may be assigned this report)*
d. Work Unit 1127E	

10. DISTRIBUTION STATEMENT

Approved for public release; distribution unlimited

11. SUPPLEMENTARY NOTES	12. SPONSORING MILITARY ACTIVITY
	Defense Civil Preparedness Agency Washington, D. C.

13. ABSTRACT

The study reported herein is one phase of an effort to develop criteria that will be helpful in evaluating or predicting the airblast load-carrying capacity of conventional floor slabs in existing Defense Civil Preparedness Agency approved shelters. The general objective of this study was to investigate the static and dynamic behavior of small, fixed-edge, longitudinally restrained, two-way reinforced concrete slabs. Twelve tests, four static and eight dynamic, were conducted on slabs with a clear span of 29 inches and a thickness of 0.89 inch. Two series of slabs (I and II) corresponding to two different percentages of steel reinforcement (0.78 and 1.17 percent) were used. The slabs were subjected to uniformly distributed static loads up to 36.5 psi using water pressure and to dynamic airblast overpressures ranging from 26.5 to 56.8 psi using explosives. Measurements of pressure, deflection, and reinforcement strains were made, and results are presented herein. The average ultimate collapse strengths of the slabs tested under static loading were 23.2 and 36.5 psi for the Series I and II slabs, respectively. The average values of ultimate flexural resistance were 14.1 and 18.2 psi for the Series I and II slabs, respectively. It was noted that the ultimate strength of the slabs was substantially increased by membrane action. Midspan deflections at the peak of tensile membrane action for the slabs tested statically averaged 4.40 inches for the Series I slabs and 4.10 inches for the Series II slab. The ultimate collapse strengths of the dynamically tested slabs averaged 28.7 and 45.5 psi for the Series I and II slabs, respectively. Midspan deflections at collapse of the slabs tested dynamically averaged 7.25 inches for the Series I slabs and 8.1 inches for the Series II slabs. A comparison of the ultimate collapse strengths of the slabs tested dynamically with those tested statically shows that increases in ultimate strength of 23.7 and 24.6 percent under dynamic loading were obtained for the Series I and II slabs, respectively. Slab strength was determined theoretically through the use of equations for predicting tensile membrane resistance and midspan deflection. After some modification of the equations used, good predictions of tensile membrane resistance of the static slabs were realized. These equations were also used in predicting the peak pressures sustained by the dynamic slabs. Using the equations to predict dynamic slab strength was less successful than using the equations to predict static slab strength.

14. KEY WORDS	LINK A		LINK B		LINK C	
	ROLE	WT	ROLE	WT	ROLE	WT
Dynamic loads						
Reinforced concrete						
Slabs						
Static loads						

U. S. Army Engineer Waterways Experiment Station, CE, Vicksburg, Miss. DYNAMIC STRENGTH STUDY OF SMALL, FIXED-EDGE, LONGITUDINALLY RESTRAINED, TWO-WAY REINFORCED CONCRETE SLABS, by W. M. Brown and M. S. Black. November 1973, 106 pp. (Technical Report N-73-8)
Unclassified report

Contract No. DAHC 20-68-W-0192
Work Unit 1127E

This study is part of an effort to develop helpful criteria for evaluating or predicting airblast load-carrying capacity of conventional floor slabs in existing DCPA approved shelters. The study investigated static and dynamic behavior of small, two-way reinforced concrete slabs. Two series of slabs (I and II) with different percentages of steel reinforcement were subjected to static loads and dynamic airblast overpressures. Average collapse strengths of the slabs tested statically were 23.2 (Series I) and 36.5 (Series II) psi; flexural resistances were 14.1 and 18.2 psi. Midspan deflections at peak tensile membrane action for the static slabs averaged 4.4 (Series I) and 4.1 (Series II) inches; ultimate collapse strengths of the slabs averaged 28.7 (Series I) and 45.5 (Series II) psi. Midspan deflections at collapse of the dynamic slabs averaged 7.25 (Series I) and 8.1 (Series II) inches. Increases in ultimate strengths of 23.7 (Series I) and 24.6 (Series II) percent under dynamic loading were obtained. Theoretical slab strengths were determined. Modification of the equations used allowed good predictions of tensile membrane resistance of the static slabs. The equations were used to predict peak pressures sustained by the dynamic slabs.

UNCLASSIFIED

1. Dynamic loads
2. Reinforced concrete
3. Slabs
4. Static loads

I. Brown, W. M., and Black, M. S.
II. Waterways Experiment Station, Technical Report N-73-8

U. S. Army Engineer Waterways Experiment Station, CE, Vicksburg, Miss. DYNAMIC STRENGTH STUDY OF SMALL, FIXED-EDGE, LONGITUDINALLY RESTRAINED, TWO-WAY REINFORCED CONCRETE SLABS, by W. M. Brown and M. S. Black. November 1973, 106 pp. (Technical Report N-73-8)
Unclassified report

Contract No. DAHC 20-68-W-0192
Work Unit 1127E

This study is part of an effort to develop helpful criteria for evaluating or predicting airblast load-carrying capacity of conventional floor slabs in existing DCPA approved shelters. The study investigated static and dynamic behavior of small, two-way reinforced concrete slabs. Two series of slabs (I and II) with different percentages of steel reinforcement were subjected to static loads and dynamic airblast overpressures. Average collapse strengths of the slabs tested statically were 23.2 (Series I) and 36.5 (Series II) psi; flexural resistances were 14.1 and 18.2 psi. Midspan deflections at peak tensile membrane action for the static slabs averaged 4.4 (Series I) and 4.1 (Series II) inches; ultimate collapse strengths of the slabs averaged 28.7 (Series I) and 45.5 (Series II) psi. Midspan deflections at collapse of the dynamic slabs averaged 7.25 (Series I) and 8.1 (Series II) inches. Increases in ultimate strengths of 23.7 (Series I) and 24.6 (Series II) percent under dynamic loading were obtained. Theoretical slab strengths were determined. Modification of the equations used allowed good predictions of tensile membrane resistance of the static slabs. The equations were used to predict peak pressures sustained by the dynamic slabs.

UNCLASSIFIED

1. Dynamic loads
2. Reinforced concrete
3. Slabs
4. Static loads

I. Brown, W. M., and Black, M. S.
II. Waterways Experiment Station, Technical Report N-73-8

U. S. Army Engineer Waterways Experiment Station, CE, Vicksburg, Miss. DYNAMIC STRENGTH STUDY OF SMALL, FIXED-EDGE, LONGITUDINALLY RESTRAINED, TWO-WAY REINFORCED CONCRETE SLABS, by W. M. Brown and M. S. Black. November 1973, 106 pp. (Technical Report N-73-8)
Unclassified report

Contract No. DAHC 20-68-W-0192
Work Unit 1127E

This study is part of an effort to develop helpful criteria for evaluating or predicting airblast load-carrying capacity of conventional floor slabs in existing DCPA approved shelters. The study investigated static and dynamic behavior of small, two-way reinforced concrete slabs. Two series of slabs (I and II) with different percentages of steel reinforcement were subjected to static loads and dynamic airblast overpressures. Average collapse strengths of the slabs tested statically were 23.2 (Series I) and 36.5 (Series II) psi; flexural resistances were 14.1 and 18.2 psi. Midspan deflections at peak tensile membrane action for the static slabs averaged 4.4 (Series I) and 4.1 (Series II) inches; ultimate collapse strengths of the slabs averaged 28.7 (Series I) and 45.5 (Series II) psi. Midspan deflections at collapse of the dynamic slabs averaged 7.25 (Series I) and 8.1 (Series II) inches. Increases in ultimate strengths of 23.7 (Series I) and 24.6 (Series II) percent under dynamic loading were obtained. Theoretical slab strengths were determined. Modification of the equations used allowed good predictions of tensile membrane resistance of the static slabs. The equations were used to predict peak pressures sustained by the dynamic slabs.

UNCLASSIFIED

1. Dynamic loads
2. Reinforced concrete
3. Slabs
4. Static loads

I. Brown, W. M., and Black, M. S.
II. Waterways Experiment Station, Technical Report N-73-8

U. S. Army Engineer Waterways Experiment Station, CE, Vicksburg, Miss. DYNAMIC STRENGTH STUDY OF SMALL, FIXED-EDGE, LONGITUDINALLY RESTRAINED, TWO-WAY REINFORCED CONCRETE SLABS, by W. M. Brown and M. S. Black. November 1973, 106 pp. (Technical Report N-73-8)
Unclassified report

Contract No. DAHC 20-68-W-0192
Work Unit 1127E

This study is part of an effort to develop helpful criteria for evaluating or predicting airblast load-carrying capacity of conventional floor slabs in existing DCPA approved shelters. The study investigated static and dynamic behavior of small, two-way reinforced concrete slabs. Two series of slabs (I and II) with different percentages of steel reinforcement were subjected to static loads and dynamic airblast overpressures. Average collapse strengths of the slabs tested statically were 23.2 (Series I) and 36.5 (Series II) psi; flexural resistances were 14.1 and 18.2 psi. Midspan deflections at peak tensile membrane action for the static slabs averaged 4.4 (Series I) and 4.1 (Series II) inches; ultimate collapse strengths of the slabs averaged 28.7 (Series I) and 45.5 (Series II) psi. Midspan deflections at collapse of the dynamic slabs averaged 7.25 (Series I) and 8.1 (Series II) inches. Increases in ultimate strengths of 23.7 (Series I) and 24.6 (Series II) percent under dynamic loading were obtained. Theoretical slab strengths were determined. Modification of the equations used allowed good predictions of tensile membrane resistance of the static slabs. The equations were used to predict peak pressures sustained by the dynamic slabs.

UNCLASSIFIED

1. Dynamic loads
2. Reinforced concrete
3. Slabs
4. Static loads

I. Brown, W. M., and Black, M. S.
II. Waterways Experiment Station, Technical Report N-73-8

In accordance with ER 70-2-3, paragraph 6c(1)(b), dated 15 February 1973, a facsimile catalog card in Library of Congress format is reproduced below:

Brown, Wayne M
Dynamic strength study of small, fixed-edge, longitudinally restrained, two-way reinforced concrete slabs; final report, by W. M. Brown [and] M. S. Black. Vicksburg, U. S. Army Engineer Waterways Experiment Station, 1973.
108 p. illus. 27 cm. (U. S. Waterways Experiment Station. Technical report N-73-8)
Sponsored by Defense Civil Preparedness Agency, Contract No. DAHC 20-68-W-0192, Work Unit 1127E.
References: p. 98.

1. Dynamic loads. 2. Reinforced concrete. 3. Slabs. 4. Static loads. I. Black, Michael S., joint author. II. Defense Civil Preparedness Agency. (Series: U. S. Waterways Experiment Station, Vicksburg, Miss. Technical report N-73-8)
TA7.W34 no.N-73-8